Convergent Excitatory Pathways Mediate the Zebrafish Escape Behavior

Convergent excitatory pathways mediate the zebrafish escape behavior

A dissertation presented

by

Alix Mary Bénédicte Lacoste

to

The Department of Molecular and Cellular Biology

in partial fulfillment of the requirements

for the degree of

Doctor of Philosophy

in the subject of

Biochemistry

Harvard University

Cambridge, Massachusetts

March 2015

Thesis advisor: Prof. Alexander F. Schier Alix Mary Bénédicte Lacoste

Convergent excitatory pathways mediate the zebrafish escape behavior

Abstract

Scientists have long been fascinated by how anatomical structures in the brain can generate the diversity of behaviors apparent in the animal kingdom. While the ultimate goal of neuroscience is to understand complex brain function, the detailed mechanisms of even basic operational principles remain elusive. Larval zebrafish are an ideal system to investigate how ensembles of neurons integrate sensory information to produce simple behaviors. Among the most vital behaviors for the larvae's survival is the ability to evade predators. The escape response is mediated by a specialized neural circuit, which requires exceptional speed, robustness and flexibility. At the heart of its computation is a pair of giant neurons in the fish's hindbrain, the Mauthner cells.

When faced with aversive stimuli, a single action potential in the Mauthner cell is transmitted directly to motoneurons, producing a stereotyped escape sequence. Reliable activation of the Mauthner cell is a challenge due to its unusual biophysical properties. The main source of excitation was thought to originate directly from sensory nerves. My work identifies a secondary, convergent excitatory pathway composed of spiral fiber interneurons, which is essential for the robust activation of the Mauthner-cell-mediated-escape circuit. Using functional imaging, I found that spiral fiber neurons respond to aversive sensory stimuli that can elicit escape responses. Laser-mediated ablations of the spiral fiber neurons largely eliminate Mauthner-cell-mediated escapes, suggesting that

spiral fiber neurons play a pivotal role in this behavior. Conversely, activating these interneurons using optical techniques enhances the probability of escapes.

By exciting the Mauthner cell at the axon hillock, the site of action potential generation, spiral fiber neurons solve the challenge of overcoming the Mauthner cell's activation barrier. Additionally, this anatomically indirect, slower input may help to filter noise and prevent unnecessary firing of the Mauthner cell.

My research is the first to show the central role of a convergent excitatory pathway for a startle behavior. This motif, which can enhance the controllability and flexibility of behavior, is likely to be prevalent in other neural networks.

Table of Contents

Acknowledgments

First, I would like to thank Alex Schier for his impeccable guidance over the years. Alex treated me as a peer and this gave me the confidence to own up to my ideas. He knew how to give just the right amount of advice so that I could develop as an independent scientist. His intellect and ambitious ideas, his unique combination of professionalism and engaging personality are beyond compare. Who better than Alex could set up a productive meeting with you on a Saturday afternoon and then invite the entire lab over to his house for deadly “zombie” drinks in the evening? Alex put together an exceptionally friendly environment for work and mutual aid. One of the few things I ever heard anyone in the lab complain about – aside from the hangovers – were his perfectionist standards in writing, but even that I appreciated.

I am deeply grateful to David Schoppik for making my graduate school experience ever so challenging and enriching. David accompanied me throughout the journey, taught me many skills and encouraged me to develop them even further. He also pushed me to be more daring and independent. David woke up one morning and decided to call me "Sunshine." I had to retaliate by addressing him as "Thundercloud," a moniker he insisting I preface with “Doctor.” Dr. T., his wife Kathy Nagel, and their son Joey Schnagel were good friends to me throughout the years.

Florian Engert was a great secondary advisor who was also very complementary to Alex Schier. His neuroscience expertise was valuable to the success of my projects. I always came out of his office with a clearer picture of my research and feeling encouraged about my results.

My Ph.D. committee was very supportive. Venkatesh Murthy, my committee chair, motivated me to strengthen my knowledge of neuroscience after the qualification exam. This proved to be crucial for successfully carrying out the project. Tom Scammell had perceptive comments on every aspect of my experiments and his enthusiasm was encouraging. Catherine Dulac was quick to discern the project's essential elements and served as a great role model.

The Schier and Engert labs were incredible environments in which to grow as a scientist. I would in particular like to thank Ruben Portugues for being very present from day one, for passing on many tricks and for being a good friend; Drew Robson for patiently explaining technical concepts and fixing a million things; the multi-talented Martin Haesemeyer for jumping in whenever I needed help; Jason Rihel for transmitting his positivity and endless curiosity; Owen Randlett for his resourcefulness and particularly incisive comments on the project; Constance Richter for being an enthusiastic benchmate always happy to discuss my latest results; Andrea Pauli for being an inspiration and force of nature; Steven Zimmerman without whom there would be no functional Schier lab; and the many others I exchanged with during my time around the zebrafish. These include Misha Ahrens, Laila Akhmetova, Xiuye Chen, Guo-Liang Chew, Adam Douglass, Julien Dubrulle, Tim Dunn, Jeff Farrell, Jamie Gagnon, Mehdi

Goudarzi, Drago Guggiana, Abhinav Grama, Kristian Herrera, Kuo-Hua Huang, Peng Huang, Farhad Imam, Robert Johnson, Adam Kampff, Jennifer Li, Florian Merkle, Tessa Montague, Patrick Müller, Eva Naumann, Max Nikitchenko, Megan Norris, Iris Odstrcil, Mike Orger, Pablo Oteiza, Albert Pan, Shristi Pandey, Mariela Petkova, Michal Rabani-Drier, Clemens Riegler, Katherine Rogers, Kris Severi, Summer Thyme, Eivind Valen, Andre Valente, Nadine Vastenhouw, Caroline Wee and Ian Woods.

I would also like to thank the other sources of support I was fortunate enough to receive at Harvard. The neuroengineers at the Center for Brain Science, Ed Soucy and Joel Greenwood, kindly helped with building various parts for my rigs (even when I failed to bring treats). Michael Lawrence contributed by running the smoothest graduate program in the country. The Ashford family generously provided essential funds and put together an engaging group of students across disciplines. The NSF Graduate Research Fellowship Program and the NIH Training Program in Sleep, Circadian and Respiratory Neurobiology supplied vital financial support.

My undergraduate advisor John Ngai and the post-doc Cynthia Duggan at UC Berkeley were instrumental in my pursuing a PhD. They gave me an essential jumpstart and made it seem like it was going to be such a smooth and fun ride! Neurobiology professor Ehud Isacoff instilled confidence in an unassuming undergraduate student. Mme. Longuet, my high school biology teacher, first sparked my love for experimental design.

I am eternally grateful to my family. Chloé, my sister, has always stood by me, and is the person I trust most in this world. Her rare intelligence and generosity continuously inspire me to better myself. My brother-in-law Jean-Baptiste and little Ève have brought me a lot of joy. I am fortunate to be getting to know my cool little brother Joseph. François, my father, pushed me to excel by always expecting more of me, entertained my sense of scientific wonder during long walks, tolerated my hot head and even gave me the means to fight for my aspirations. Elizabeth, my mother, inspired my fascination for the brain. Her unconventional mind and keen intellect make her the most interesting person I know. She gave me the freedom and confidence I needed to become whatever I wanted to be. My aunt Cimmer and her husband Ben generously opened their home to me, allowing me to continue my studies in the U.S. My grandmother Clare and my grandparents, Gail and David, offered much needed nurturing. Mamée and Grand-père gave me a close-knit extended family. Julia affectionately welcomed her cousin and fellow expat into a new country. My late cousin Alexandre’s courage and love for life drove me to make the most of every instant.

My friends have been another kind of true family. My classmates, in particular Abhinav Grama and Sarah Douglass, have been a great source of support. Cecile Michotey's outrageous view of life always provoked bursts of laughter followed by passionate discussions. Her loyalty and devotion have gone well above and beyond what anyone could ever hope for in a friend. I am grateful to Clemens Grassberger for his many years of love and support. I have shared

many stimulating experiences and talks with Camille Sindhu. Rodrigo Garcia – what would I know without his affectionate mansplaining? After meeting Alexis Schulman, I became exponentially happier. Charlotte Cavaillé motivated me to push my intellectual and physical boundaries. Victoria Del Campo's wit made me laugh and feel like the most positive human being. Katie Walsh was always there for me and her ambition was contagious. Choralyne Dumesnil's charismatic presence added a spiritual note to my life. Rebecca Spencer saved my life. Mauro Martino introduced me to Watson. My precious roommates Karen Kieser, Daniel Greene, Mircea Raianu and Jessi Naff never ceased to entertain me and surrounded me with affection.

Finally, I would like to invoke a few of the most important factors in keeping me sane after sunset, before sunrise or during mindless manual tasks in the lab: my bike, my running shoes, my oar, my piano, and NPR.

List of Figures

CHAPTER 1

Neural Circuits Mediating the Escape Behavior

1.1 INTRODUCTION

Animal behavior is governed by interactions with the environment. In order to understand how the nervous system processes sensory information to produce behavior, small organisms are invaluable models. Even the simplest sensory-motor transformation requires multiple steps, from stimulus processing to integration, decision and motor output. Frequently, different sources of information need to be integrated in order to reach the best behavioral decision. How ensembles of neurons interact to select and implement specific actions is a fundamental question in neuroscience. Escape behaviors present a clear advantage to understand sensorimotor processing and decision-making because of their relatively simple underlying circuits and the presence of accessible neurons identified from sensory periphery to motor control. An understanding of escape networks can provide clues into the architecture and logic of all circuits controlling behavior. A variety of sophisticated technologies such as *in vivo* functional imaging, high-speed behavioral recordings, neuronal activation with light, and neural recordings enable the field to examine escape behavior and circuitry in detail.

Escape behaviors in response to cues signaling dangers are essential to avoid predators and are ubiquitous in the animal kingdom. Diverse species of

invertebrates such as fruit flies, crabs, and locusts (Card, 2012; Herberholz, 2012), as well as vertebrate species such as fish (Korn and Faber, 2005) produce fast escapes away from aversive cues. In mammals, the startle response has its origins in the escape response of these more ancestral species (Eaton, 1984). Due to their specialized function, escape behaviors possess three main characteristics that inform the underlying network architecture. First, speed should be optimized to allow for fast reaction times and a greater chance of survival (O'Steen et al., 2002; Walker et al., 2005). Escape reactions typically occur within 5-20 milliseconds of an aversive signal. Second, the escape behavior is essential for survival and should thus be robust. Third, escapes can also be costly because they suppress other vital activities such as feeding and mating (Whitaker et al., 2011). Therefore, the escape threshold should be set according to the animal's environment and internal state.

To enable speed, robustness and flexibility, escape circuits have evolved common strategies. Speed is optimized through large neurons supporting thick fibers that carry action potentials extremely fast. Such "giant fibers", frequently the largest axons in an animal's nervous system, exist in many invertebrates such as Drosophila, cockroaches and locusts, as well as in fish (for a review, see Card, 2012; Herberholz, 2012). Another strategy to increase processing speed is to limit the number of synapses in the pathway from sensory receptors to muscle. Synaptic delay itself is minimized by the presence of electrical synapses.

Robustness and reproducibility in escape circuits is enhanced by the presence of characteristic neurons – the giant fiber neurons mentioned earlier – commonly

referred to as command neurons. For neurons to be considered command neurons, their firing must be necessary and sufficient to elicit an entire behavioral sequence, in this case an escape motor sequence. Command neurons are regarded as prototype decision-making cells: they frequently receive a convergence of sensory input from multiple sources and must integrate this information in order to reach a firing decision. As research into escape circuits advances, it becomes apparent that true command neurons are rare if they exist at all. Rather, the concept of “command-like” neuron has increased in popularity, as escape behaviors are often governed by networks of at least a few interacting and redundant cell types. Frequently, slower parallel pathways exist in conjunction with the main circuit governed by command-like neurons. These additional pathways are generally activated by weaker stimuli and ensure that appropriate reactions occur if the main circuitry was not activated.

The third major requirement of escape networks, flexibility, is critical because the escape decision should be adjusted for different environments and weighed against other important behaviors the animal may be engaged in. Although vital for survival, this behavior is also energetically costly. Feedforward and feedback interneurons allow for a precise control of escape thresholds and timing. Along with this complex interplay of excitatory and inhibitory inputs, neuromodulators can fine-tune circuit activity. Electrical synapses that enable speed are frequently present together with chemical synapses for greater plasticity. In addition, since predators can evolve to anticipate escape sequences, efficient behaviors display a certain level of unpredictability.

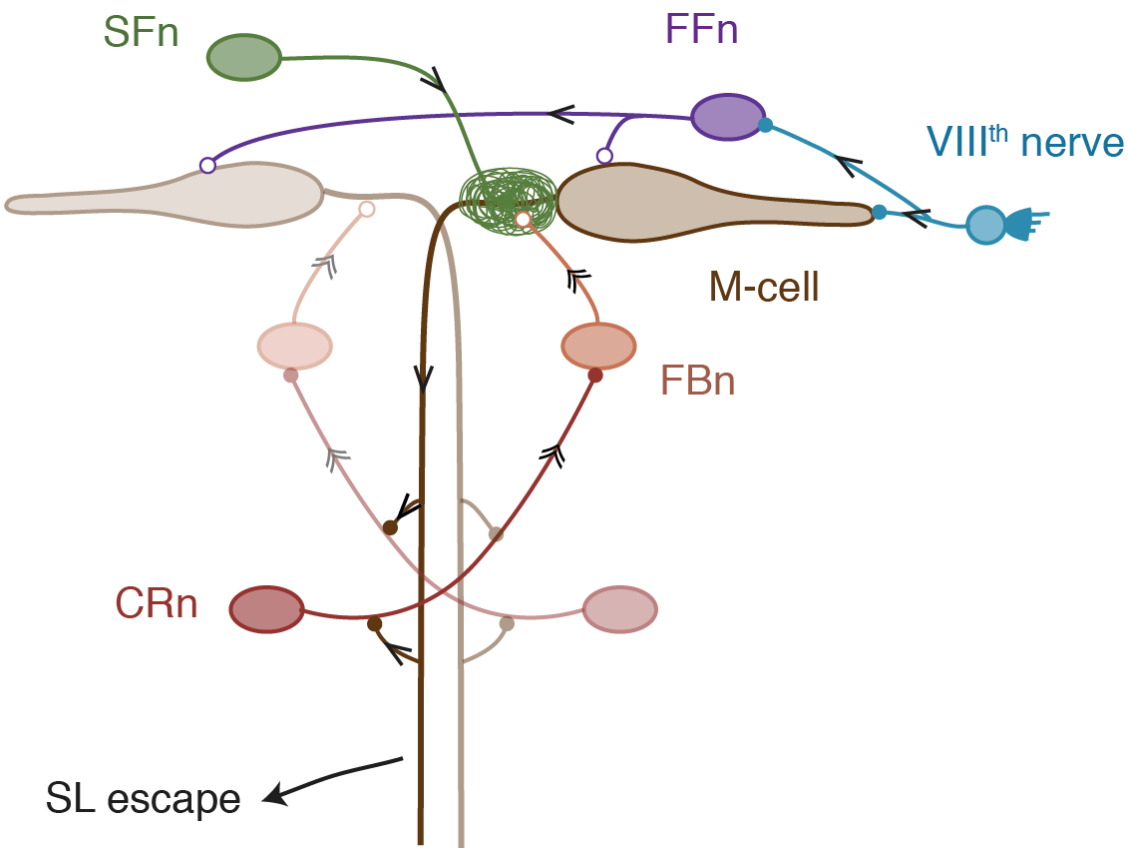

Figure 1.1. The teleost Mauthner cell escape circuit.

Aversive stimuli activate multisensory afferents that feed into the M-cell circuit. The main sensory input comes from the VIIIth nerve, which carries acoustic/vestibular information from hair cells in the inner ear. The VIIIth nerve excites the M-cell lateral dendrite where it makes mixed chemical (glutamatergic) and electrical synapses referred to as club endings. M-cells excite motor neurons on the contralateral side (not pictured) as well as other networks of neurons in the spinal cord to elicit a contralateral short-latency escape. Interneurons set the threshold and ensure that in response to directional stimuli, only one M-cell fires a single action potential. Feedforward neurons are excited by the VIIIth nerve and make inhibitory, glycinergic connections with the M-cells on both sides. This inhibition is thought to dampen sensory input to prevent innocuous sounds from activating the M-cell. Spiral fiber neurons excite the contralateral M-cell at a

Figure 1.1 (Continued) specialized structure surrounding the axon initial segment and axon hillock called the axon cap. Their axons spiral in this regions where they make both glutamatergic and electrical synapses. My findings on the role of spiral fiber neurons in the circuit are described in Chapter 2. The M-cell excites cranial relay neurons on the contralateral side, which cross and excite feedback neurons through acetylcholine signaling. Feedback glycinergic neurons inhibit the M-cell at the axon cap, preventing it from firing a second action potential. The M-cell also excites ipsilateral cranial relay neurons. This results in the activation of feedback neurons that inhibit the contralateral M-cell, ensuring that the behavior is appropriately lateralized. Single arrows indicate the feedforward pathway that leads to motoneuron activation, and double arrows indicate the feedback pathway that inhibits the M-cells. Filled circles at the end of axons indicate excitatory synapses; open circles indicate inhibitory synapses. Abbreviations: M-cell: Mauthner cell. FFn: feedforward neurons. Spiral fiber neuron: spiral fiber neurons. CRn: cranial relay neurons. FBn: feedback neurons. SL escape: short-latency escape.

1.2 THE MAUTHNER CELL ESCAPE CIRCUIT

The Mauthner cell (M-cell) mediated escape circuit, present in most fish and amphibia, is one of the best-understood escape circuits. Its name comes from the Viennese ophthalmologist Ludwig Mauthner who first identified it in teleost fish. When faced with acoustic, tactile, or visual stimuli, a single action potential in the giant command-like M-cell gives rise to motor activity that orients the animal away from the stimulus in only a few milliseconds (Eaton et al., 1977; Zottoli, 1977; Eaton and Lavender, 1981). This behavior is so vital that firing of the M-cell overrides swimming (Svoboda and Fetcho, 1996).

Studies of the M-cell circuit over the last sixty years have uncovered a wealth of important principles in neurobiology that have held true in more complex vertebrate models (Korn and Faber, 2005). Basic aspects of synaptic transmission and excitability, such as quantal release (Korn et al., 1981) and silent connections (Lin and Faber, 1988a) were first discovered in the M-cell. Current research investigates higher-order functions such as the role of synaptic plasticity in adaptive behavior (Oda et al., 1998) or health-related subjects such as regeneration after nerve damage (Zottoli et al., 1994). M-cells have been proposed to be evolutionary predecessors of reticular neurons within the nucleus gigantocellularis of the mammalian nervous system (Pfaff et al., 2012). For these reasons, M-cells are ideal models to define causal links between sensory representation, neural activity and behavior.

In this introductory chapter, I will focus on recent advances that have shed light into the architecture of the escape behavior circuitry. In particular, I will emphasize articles published since the most recent review on the M-cell circuit (Korn and Faber, 2005). A variety of technologies have made advances in understanding the M-cell circuitry possible. Early imaging and electron microscopy studies have defined the morphology of these cells, as well as the location and type of their inputs (Bartelmez, 1915; Kohno, 1970; Eaton, 1973). A detailed dissection of the electrical interactions between the M-cell and its inputs was made possible by electrophysiology (Furukawa, 1966; Koyama et al., 2011). In the past twenty years, functional imaging with calcium indicators has enabled the study of the relationship between different neuronal components in the awake

and behaving animal (O'Malley et al., 1996; Kohashi and Oda, 2008; Kohashi et al., 2012). More recently, optogenetic methods have been developed to establish the sufficiency of different components of the network (Douglass et al., 2008; Portugues et al., 2012; Monesson-Olson et al., 2014). Finally, the ability to find a signature of M-cell firing via electrical field recordings in freely swimming fish opens the door to studying the escape behavior in more natural conditions (Weiss et al., 2006; Issa et al., 2011; Monesson-Olson et al., 2014). While the majority of detailed electrophysiology studies are conducted in adult goldfish, the larval zebrafish is gaining in popularity as a model. Due to its small size, transparent brain, and genetic tractability, the larval zebrafish is an ideal model to study the escape circuit at cellular resolution in a behaving animal.

1.2.1 The escape behavior

The escape behavior is characterized by an axial movement sequence called the C-start, which is composed of three kinematic stages (Korn and Faber, 2005). Escapes are lateralized, such that stimuli on one side of the animal trigger a contralateral motor sequence away from the threat. First, the head rotates and the body bends into a “C” shape at high angular velocity and acceleration, around the center of mass. In stage 2, the animal turns in the opposite direction of the initial C-bend, moving forward and away from the aversive stimulus. The last phase of the C-start consists of a variable period of fast-burst swimming. Latency between stimulus and behavior is very short, ranging from 5-20

milliseconds, and fast reaction times increase the probability of evading predators (Walker et al., 2005).

1.2.2 The Mauthner cell

M-cells are the largest cells in the teleost brain. They consist of a pair of neurons, one on each side of the brainstem at the level of the VIIIth nerve. There are two major dendrites, the largest one extending laterally and the other ventrally. Surrounding the axon hillock and initial segment of the M-cell is a specialized structure composed of synaptic endings ensheathed by glial cells called the axon cap (Kimmel et al., 1981). This is a critical site for integration of sensory and interneuron inputs. The thick myelinated axons cross and descend along the length of the spinal cord where they excite motoneurons and interneurons.

In response to stimuli, the M-cell fires a single action potential, triggering an escape sequence in the contralateral direction. Due to its large size, unusually low input resistance, short time constant, and hyperpolarized membrane potential (~-83 mV in the goldfish), it is difficult to activate the M-cell. This implies particularly strong and long-lasting inputs are required to generate an action potential at the axon hillock.

Without the M-cell, short-latency escapes in response to acoustic/vestibular stimuli are abolished. However, kinematically comparable escapes of longer latencies still occur. M-cell segmental homologs are neurons morphologically

similar to the M-cells that are involved in these slower escapes and will be discussed in a later section.

1.2.3 Sensory inputs

The M-cell is the prototype of a sensory integrator: all systems studied project either directly or indirectly on its two major dendrites. The strongest and most well studied input originates from auditory afferents. Although many of the synapses this input makes are chemically silent, plasticity and cooperative mechanisms are thought to mediate a prolonged response that may help to efficiently depolarize the M-cell. Lateral line inputs are weaker and are involved in setting the directionality of the behavior. Tactile stimuli conveyed by the trigeminal nerve can trigger M-cell-mediated escapes at very early stages of development. At later stages, touch preferentially activates an M-cell independent escape circuit. Finally, visual information, like lateral line input, may primarily be involved in biasing the directionality of escapes.

Auditory/vestibular input

The strongest input to the M-cell originates from auditory hair cells in the ear saccular macula. The posterior cranial VIIIth nerve carries acoustic information onto the ipsilateral distal lateral dendrite where it makes mixed electrical and glutamatergic chemical synapses at structures called club endings (Nakajima,

1974; Tuttle et al., 1986; Lin and Faber, 1988b) (Figure 1.1). Whereas the M-cell can fire only once in response to sounds, auditory afferents generate bursts of action potentials (Curti et al., 2008). Electrical synapses between the auditory afferents and the M-cells encode both stimulus frequency and amplitude (Szabo et al., 2006).

Vestibular information is also conveyed to the M-cell from utricular macula hair cells in the ear and via the anterior VIIIth nerve (Szabo et al., 2007). The extent of these connections is more restricted than the saccular inputs and it is unlikely that the utricular input alone can cause firing in the M-cell.

Plasticity of auditory afferents

Primary auditory afferents in most other organisms undergo depression. However, high frequency stimulation of VIIIth afferents in the M-cell network evokes facilitation of both chemical and electrical synapses in club endings (reviewed in Curti and Pereda, 2010).

Bursts of activity in the VIIIth nerve induces long-term potentiation of the chemical synapses, increasing their conductances through NMDA-dependent mechanisms (Lin and Faber, 1988a; Pereda and Faber, 1996; Wolszon et al., 1997). Curti et al. (2008) showed that auditory afferents exhibit a persistent sodium current, endowing them with critical properties: the ability to respond to bursts of sounds with frequency matching the effective range of hearing in goldfish and the

capacity for electrical resonance with spike intervals optimized for facilitation. A majority of the club ending connections is chemically silent following a presynaptic spike (Lin and Faber, 1988a; Faber et al., 1991), but silent connections can become functional when a significant population is co-activated (Pereda et al., 2004).

Facilitation of gap junctions was first demonstrated in the M-cell network. It is due to an increase in conductance involving modifications of channels (Yang et al., 1990) through calcium-dependent postsynaptic mechanisms (Pereda et al., 1994). Rash et al. (2013) reported that electrical channels at club ending are asymmetric in their composition: connexin 35 and connexin 34.7 are found in the presynaptic and postsynaptic membranes, respectively. This asymmetry promotes bidirectionality of the electrical signals, which is normally not favored due to geometrical properties. The increase retrograde spread of M-cell responses into presynaptic endings is believed to promote lateral excitation and cooperativity between afferents (Pereda et al., 1995). This results in increased synchrony between afferents and enhanced depolarization in the M-cell dendrite (Pereda et al., 1995; Smith and Pereda, 2003).

Lateral line input

A weaker secondary input comes from lateral line afferents that project to the lateral dendrite of the M-cell (Korn and Faber, 1975). The lateral line detects movement and vibration in the water through a collection of mechanoreceptive

organs along the sides of the fish called neuromasts. These neurons originate primarily from the low threshold, high velocity neuron pool of terminal neuromasts (Pujol-Marti et al., 2012; López-Schier, 2013), which are poised to depolarize the M-cell with short latencies. In fact, stimulation of the lateral line elicits a fast depolarization of small amplitude (Mirjany and Faber, 2011). Monesson-Olson et al. (2014) demonstrated that optical activation of lateral line hair cells via channelrhodopsin was sufficient to elicit escape responses in free-swimming larvae. Electrical field recordings revealed concurrent firing in the M-cell. Flow sensing through the lateral line system may trigger an escape rapidly enough to allow successful predator evasion (McHenry et al., 2009), however it is unknown whether this response is mediated by the M-cell. Whether in natural conditions, the lateral line is sufficient to trigger M-cell-mediated behavior is therefore still unknown. A more probable role for the lateral line input may lie in the directionality of the behavior. The response to lateral line stimulation is faster in the contralateral M-cell (Mirjany and Faber, 2011), and in free-swimming adult goldfish, ablation of the anterior lateral line reduced the laterality of escapes in response to sounds (Mirjany et al., 2011).

Trigeminal input

Trigeminal axons project to the lateral dendrite of the M-cell (Kimmel et al., 1990). Douglass et al. (2008) found that photoactivation of channelrhodopsin in the somatosensory neurons of the trigeminal triggered escape behaviors in 24

hours-old zebrafish. Calcium imaging and behavioral experiments are consistent with this finding (Kohashi et al., 2012). Before 75 hours post fertilization, tactile stimuli are sufficient to induce M-cell-mediated behavior. At this stage, auditory/vestibular stimuli do not elicit escapes. After 75 hours post fertilization, auditory/vestibular stimuli activate the M-cell and ablation of the otic vesicle in the ear but not of the trigeminal ganglion eliminates short-latency M-cell-mediated escapes. Therefore, trigeminal input on the M-cell is only effective early in development.

Visual input

The optic tectum receives projections from ganglion cells in the retina (Nikolaou et al., 2012) and sends bilateral projections to the M-cell ventral dendrites (Zottoli et al., 1987). One function of visual input when it precedes other sensory stimuli may be to bias escape directionality prior to a predator's strike (Canfield, 2003). On their own, looming stimuli can evoke escapes that are correlated with M-cell activity in the adult goldfish (Preuss et al., 2006). The latency of these escapes is long, in the range of hundreds of milliseconds after the onset of the stimulus (both in adult goldfish (Preuss et al., 2006), and larval zebrafish (Dunn et al., unpublished)). Intracellular recordings show that looming stimuli evoke bursts of graded excitatory post-synaptic potentials (EPSPs) in the M-cell (Preuss et al., 2006). Dunn and colleagues (unpublished) demonstrated that ablation of the M-cell and its segmental homologs decreases the angle of the initial turn of escapes

in response to looming stimuli, but that subsequent swim kinematics are unchanged. As a result of the smaller C-bend angle, escape trajectories followed a more forwardly path. Thus, visual input may bias escape directionality when the animal is faced with multisensory inputs, and looming stimuli alone can cause escape behaviors whose effectiveness is contingent on the M-cell and its homologs.

1.2.4 Interneuron inputs

A variety of interneurons project onto the M-cell at the level of the soma and axon cap. The complex interplay between both excitatory and inhibitory interneurons affords robustness and flexibility to the M-cell circuit. These neurons are critical for setting the firing threshold and ensuring that in response to directional stimuli, only one of the two M-cells fires a single action potential.

Inhibition

Two types of inhibitory interneurons are present in the M-cell circuit. These interneurons display synchronized oscillations (Marti et al., 2008) and inhibit different parts of M-cell through several mechanisms. The first type of inhibitory interneurons are feedforward cells: they receive direct connections from the auditory/vestibular VIIIth nerve afferents and make glycinergic chemical synapses onto the soma of both M-cells (Koyama et al., 2011; Figure 1.1). In contrast to

larval zebrafish, feedforward neurons in adult goldfish also project to the M-cell axon cap. These glycinergic neurons globally dampen the effect of sensory stimuli to effectively raise the threshold for firing.

The second type of inhibition comes from feedback interneurons that make glycinergic synapses at the axon cap of both M-cells (Koyama et al., 2011; Figure 1.1). M-cells excite cholinergic interneurons in the spinal cord called cranial relay neurons (also referred as T-reticular (Kimmel et al., 1985)) that project bilaterally to the feedback inhibitory neurons (Koyama et al., 2011; Figure 1.1). This two-synapse circuit introduces a delay line that is effective after initial M-cell firing. It prevents the M-cell from firing twice, which would produce a dual C-bend and give rise to an ineffective escape. This lack of repetitive firing of M-cells is also thought to be due to the presence of DTX-sensitive K+ channels of the Kv1 family (Nakayama and Oda, 2004). Feedback inhibitory neurons may also be involved in ensuring that in the majority of cases, only one M-cell fires in response to sensory stimuli, since bilateral activation of escape networks would result in inadequate behavior. When one M-cell produces an action potential, feedback interneurons inhibit the contralateral M-cell, preventing it from firing.

Both types of inhibitory neurons were first described in detail in goldfish and have been referred to as PHP cells, for passive hyperpolarization, because of their unusual electrical inhibition effects occurring without the presence of electrical synapses. Such nonsynaptic electrical effects, called epathic or field effects, were described by electrophysiology (Furukawa and Furshpan, 1963; Korn and Faber, 1975). Electrical inhibition is due to outward currents at the axon cap

generated by inhibitory axons that flow inward across the M-cell axon hillock and hyperpolarize it. In free-swimming adult goldfish, M-cell spiking latency and the timing of electrical inhibition by feedforward neurons are similar, suggesting that these field effects can play a role in whether the M-cell fires (Weiss et al., 2008).

Excitation

A group of excitatory interneurons called spiral fiber neurons descend along the medial longitudinal fasciculus and project to the axon cap of the contralateral M-cell (Koyama et al., 2011; Figure 1.1). As they enter the axon cap, spiral fiber neurons lose their myelin and wrap around the axon hillock (Kimmel et al., 1981) where they make synaptic contacts with the M-cell axon and with one another (Nakajima, 1974). These synapses are both electrical and chemical in nature (Nakajima, 1974). Electrical stimulation of hindbrain areas near the spiral fiber neurons in adult goldfish elicited a short latency graded depolarization of the M-cell and could cause the M cell to spike (Scott et al., 1994). Through dual patch clamping experiments, Koyama et al. (2011) showed that stimulation of a single spiral fiber neuron in larval zebrafish was capable of eliciting an EPSP in the contralateral M-cell. Consistent with the anatomy of spiral fiber neuron synapses, the nature of the EPSP indicates the presence of both gap junctions and glutamatergic synapses: The EPSP had both a fast and slow component and the slow component could be eliminated by glutamatergic blockers. In addition to studies describing their effects on the M-cell, spiral fiber neurons have been

implicated in the escape behavior. Mutants for the retinoblastoma-1 gene that have defects in axon targeting, including in the spiral fiber neurons, display abnormal fast turning movements in response to touch (Lorent et al., 2001; Gyda et al. 2012).

1.2.5 Output of the Mauthner cell

The large myelinated axon of each M-cell crosses the midline and extends along the contralateral spinal cord, where it synapses onto a multitude of neurons, including primary motoneurons innervating the contralateral trunk and tail muscles (reviewed in Nissanov et al., 1990). Due to the high conduction velocity of the M-cell action potential, motoneurons along the length of the trunk and tail fire near simultaneously, ensuring a synchronous activation of muscle segments during the C-bend phase of the escape sequence. M-cells also connect to excitatory premotor interneurons that are active during swimming and may be involved in the third phase of the escape response (for a review, see Fetcho, 1991).

Of particular interest, the M-cell excites commissural interneurons in the spinal cord named CoLo (for commissural local). Satou et al. (2009) found that these neurons play an important role in initiating escapes. Their results suggest that in response to non-directional stimuli, both M-cells are capable of firing within a very short delay of each other. CoLos can silence the output of the M-cell that fires second, ensuring that the escape is appropriately lateralized.

1.2.6 Modulation of Mauthner cell circuitry

Interactions between different sensory modalities can influence M-cell firing threshold. A variety of drugs and neuromodulators are also known to affect the M-cell escape network.

Cross-modal integration

In an elegant study, Mu and colleagues (2012) found that a preceding light flash enhances auditory-evoked M-cell-mediated escapes. The underlying mechanism is an increase in the signal-to-noise ratio of spiking in the auditory afferents, as well as an increase in the transmission efficacy at club endings. Dopamine signaling in the vicinity of the M-cell lateral dendrite was found to be required for enhanced transmission of audiomotor signals and facilitated escape behavior. This is consistent with previous studies by Pereda et al. where dopamine was applied on the lateral dendrite of the M-cells in adult goldfish. Dopamine enhanced both the electrical and the chemical components of the EPSP evoked by stimulation of the auditory/vestibular nerve, through postsynaptic mechanisms (Pereda et al., 1992; 1994). Mu et al. further showed that enhancement of the auditory response by light flashes is dependent on light-responsive dopaminergic neurons in the caudal hypothalamus that project to the M-cell lateral dendrite (Mu et al., 2012).

Prepulse inhibition

Prepulse inhibition is a form of sensorimotor gating in which a weak prestimulus inhibits the startle response to a subsequent, ordinarily suprathreshold stimulus. Larval zebrafish and adult goldfish both exhibit prepulse inhibition (Burgess and Granato, 2007; Medan and Preuss, 2011). In larval zebrafish, a prepulse decreases the probability of M-cell-dependent escapes. The dopamine agonist apomorphine suppresses prepulse inhibition without affecting baseline M-cell-dependent escapes. Conversely, the antipsychotic drug haloperidol, a dopamine D2 receptor antagonist, augments prepulse inhibition (Burgess and Granato, 2007). Intracellular *in vivo* recordings of the adult goldfish M-cell showed that dopamine signaling effectively increases input resistance of the M-cell membrane during prepulse inhibition (Medan and Preuss, 2011).

Serotonin

Serotonin immunoreactivity is found surrounding the soma and the ventral dendrite of the M-cell in larval zebrafish (McLean and Fetcho, 2004). Application of serotonin in the vicinity of the M-cell axon cap in the goldfish increases both spontaneous and evoked inhibitory currents, an effect lasting tens of minutes. Serotonin appears to act on inhibitory terminals to increase the probability of glycine release. In cichlid fish, serotonin antagonists attenuate auditory-evoked EPSPs in the M-cell by reducing its input resistance (Curtin et al., 2013). Behaviorally, serotonin seems to be involved in modulating startle plasticity in

cichlid fish (Whitaker et al., 2011), however further studies are needed to establish the relevance of serotonin in escape behaviors.

Endocannabinoids

Cachope and colleagues (2007) showed that dendritic release of endocannabinoids enhances synaptic transmission at club endings in the goldfish. Repetitive stimulation of the VIIIth nerve led to the activation of metabotropic glutamate receptors and the release of endocannabinoids. Endocannabinoids promoted dopamine release and subsequent potentiation of synaptic transmission through a PKA-dependent pathway. These results were surprising given that endocannabinoids in most other contexts inhibit chemical synaptic transmission. Furthermore, this study was the first to show that endocannabinoids can increase electrical transmission at gap junctions.

Ethanol

Calcium imaging experiments performed by Ikeda et al. revealed that at doses of 300 mM and higher, ethanol decreased M-cell responses to acoustic/vibrational stimuli (Ikeda et al., 2013). Behaviorally however, ethanol did not affect the probability of short-latency escapes. Instead, long-latency escapes were diminished. This may be explained by the observation that in the M-cell homologs, which are involved in long-latency escapes, the inhibition upon

ethanol exposure was larger than in the M-cell (Ikeda et al., 2013).

Feedback from locomotion

When larval zebrafish are actively moving, the probability of them responding to acoustic/vestibular stimuli with M-cell-mediated escapes increases (Burgess and Granato, 2007). This implies that the M-cell network is modulated during swimming, as are reticulospinal neurons in lampreys (Currie and Carlsen, 1987).

1.2.7 Role of Mauthner cell homologs

Reticulospinal neurons morphologically similar to the M-cell are referred to as the segmental homologs (Metcalfe et al., 1986). M-cell homologs project to spinal motoneurons that cause contractions in the trunk musculature (Fetcho, 1991). They include paired MiD2cm and MiD3cm neurons in rhombomeres 5 and 6 respectively, and potentially the lesser known MiDi and MiV cells in rhombomeres 4-6 (Neki et al., 2014). Immunohistochemistry combined with transgenic labeling studies in zebrafish suggest that the contralateral descending MiD2cm and MiD3cm neurons are glycinergic (Barreiro-Iglesias et al., 2012; Moly et al., 2013) and that the ipsilaterally projecting MiDi cells are glutamatergic (Kinkhabwala et al., 2011; Kimura et al., 2013).

In contrast to the unique spike generated in the M-cell, MiD2cm and MiD3cm respond to VIIIth nerve stimulation with repetitive spiking (Nakayama and Oda, 2004). Their response to auditory/vestibular inputs generally requires stronger stimulation and is of longer latency compared to the response in the M-cell (Nakayama and Oda, 2004). Paired intracellular recordings in adult goldfish revealed that the M-cell either excites or inhibits different types of homologs. The connections they make are functionally unidirectional: stimulation of homologs does not elicit a response in the M-cell (Neki et al., 2014).

Lesion and calcium imaging studies revealed that M-cell homologs are involved in escapes. While ablations of the M-cell and its homologs together abolish all escapes, the relative role of these neurons varies with the type of stimulus. Different types of stimuli also give rise to diverse latency profiles in the escape response.

Tactile stimulation of the larval zebrafish head activates both the M-cell and the MiD2cm and MiD3cm homologs located ipsilateral to the stimulus (O'Malley et al., 1996; Kohashi and Oda, 2008). Typical response latencies are in the range of 4-15 ms. Newly hatched zebrafish larvae respond to head-touch with escapes that are mediated by the M-cell (Kohashi et al., 2012). After 75 hours post-fertilization however, head stimulation is no longer efficient at activating the M-cell: M-cell ablations do not affect escape latencies and probabilities (Liu and Fetcho, 1999; Kohashi et al., 2012). M-cell homolog activity during head touch is thought to mediate these persistent escape responses.

Tactile stimulation of the tail elicits escape responses with 4-15 ms latencies. Latencies are on average higher than for head stimulation, suggesting a longer and potentially multisynaptic path between touch receptors along the tail and the M-cell. In contrast to the role they play in response to head touch, the M-cells are required for responses below 6 ms (Kohashi and Oda, 2008). While tail stimuli were not found to activate MiD2cm and MiD3cm neurons by calcium imaging (O'Malley et al., 1996), array lesions of these cells and the M-cell abolish all escapes (Liu and Fetcho, 1999). Therefore, MiD2cm and MiD3cm cells are likely to mediate persistent escape responses of latencies 6 ms and above when the M-cell is ablated.

Freely swimming fish respond to acoustic/vestibular stimuli with a bimodal distribution of response latencies. Ablation of the M-cell entirely abolishes short-latency escapes (<15 ms) (Burgess and Granato, 2007). Long-latency escapes (15-40 ms) give rise to similar trajectories, however the angle of the initial C-bend and counterbend is lower, and the angular velocity is similarly reduced. These escapes are intact after M-cell ablations and may be modulated by the homologs. Long-latency escapes are more frequent in response to low-intensity stimuli, and their performance increases with stimulus strength. In contrast, the performance of M-cell-mediated short-latency escapes is not graded according to the stimulus, but their probability increases with stimulus strength. An additional difference between short- and long-latency escapes is that short-latency escapes habituate more quickly to repetitive stimuli (Burgess and Granato, 2007).

Direct activation of the otic vesicle with a puff of water in head-restrained larvae gives rise to escapes ranging from 4 to 12 ms in latency. M-cell lesions or lesion of the otic vesicles abolish responses below 6 ms (Kohashi and Oda, 2008; Kohashi et al., 2012). These fast escapes are correlated with high calcium activity in the contralateral M-cell and low activity in the MiD3cm neurons. Conversely, in long-latency escapes, the M-cell is minimally active, while the MiD3cm neuron shows large calcium transients (Kohashi and Oda, 2008), indicating that the activity of these two sets of neurons is complementary. Curiously, in goldfish, the M-cell excites contralateral MiD3cm neurons through disynaptic or polysynaptic pathways (Neki et al., 2014), raising the question of why higher activity in the M-cell is not accompanied by higher activity in MiD3cm. Consistent with electrophysiology experiments, Kohashi and Oda (2008) observed that increased activity in MiD3cm was correlated with larger initial tail bend angles during M-cell-mediated escape. Therefore, MiD3cm may both participate in initiating long-latency, M-cell independent escapes, as well as enhancing the directionality of M-cell-mediated escapes.

In summary, M-cell homologs represent a duplicate pathway for initiating escapes. This additional pathway ensures that escape responses occur in response to weaker stimuli if the main circuitry was not activated. Escapes triggered by the M-cell homologs are generally slower than those controlled by the M-cells. The high conduction velocity of the thick M-cell axon accounts for shorter latency of motor activity. Spike conduction velocities are twice as long in M-cell homologs (Eaton and Farley, 1975; Kohashi and Oda, 2008). Slower,

duplicate pathways are a common feature of escape networks in other species (Card, 2012; Herberholz, 2012). The difference between the two escape pathways, however, is more subtle than a mere difference in processing speed. M-cell circuitry is preferentially activated by auditory/vibrational stimuli, whereas M-cell homologs are more responsive to tactile stimuli directed at the head. In fact, the M-cell is not necessary for short-latency escapes to head touch, and therefore cannot be regarded strictly as a command neuron.

1.3 CONCLUSION & PERSPECTIVES

The escape response is an excellent model for understanding general mechanisms through which neural circuits control behavior from the subcellular to the system level. The underlying circuit is well adapted for its function in terms of three critical components: speed, robustness and flexibility. First, speed is achieved via a simple pathway containing few and fast electrical synapses: sensory afferents project directly on the central decision-making cell, which in turn excites motoneurons directly through its fast conducting axon. Second, due to its nature as a command-like neuron, the M-cell ensures stereotypy and robustness of behavior. In addition, an alternate, generally slower pathway can be activated in response to different or less intense stimuli, and ensures that escapes occur when the main pathway is not activated. Finally, to achieve flexibility in the face of a continuously changing environment, neuromodulators

and interneuron networks fine-tune the circuit and set appropriate thresholds for behavior.

Technological developments such as better transgenic lines (Zhu et al., 2012; Satou et al., 2013), more widespread optogenetics tools (Portugues et al., 2012) and new mutagenesis methods (Gagnon et al., 2014) will allow a better understanding of the network at a genetic and cellular level in behaving animals. In more recent year, larval zebrafish have been emerging as an important model for studying neurological disorders (Haesemeyer and Schier, 2014). Due to its role in processes such as prepulse inhibition and the identification of associated regulatory genes (Burgess and Granato, 2007), the M-cell network will certainly lead to significant discoveries into disease pathways.

One puzzle that remains in the escape circuit is that biophysical properties of the M-cell make it difficult to reach threshold, yet its sensory inputs are located on the dendrites, far from the site of action potential generation at the axon hillock. How can these inputs be effective in making the M-cell overcome its activation barrier? Electrophysiological and anatomical studies in goldfish suggest that a surprisingly strong activation of sensory synapses is required in order to trigger a spike in the M-cell.

While the input resistance of the M-cell is low, on the order of 200 kOhm, the membrane time constant is also very short, about 0.5 ms (Furukawa, 1966). As a result, the M-cell can be rapidly depolarized, but excitation also decays rapidly, diminishing the effective window for input integration. Dendritic inputs are

removed by about one space constant from the axon hillock, and since the threshold depolarization for impulse initiation in the M-cell is on the order of 15 mV, EPSPs must be at least 30 mV in amplitude at the dendrites. A single club ending produces an EPSP of approximately 140 μV (Lin and Faber, 1988b), suggesting that for the M-cell to reach firing threshold, at least 200 such afferents have to be concurrently active. The actual number of afferents needed may in reality be larger due to the feedfoward inhibitory network they also activate. Oddly, the lateral dendrite is thought to contain only approximately 100 club ending (Lin and Faber, 1988b; Faber et al., 1991), and 80% of these synapses are chemically silent (Lin and Faber, 1988b). A factor that increases the effectiveness of these synapses is facilitation between club endings as discussed previously. However, the number and physiology of club endings implies that sensory inputs need to be unusually strongly and persistently activated in order for the M-cell to reach threshold.

Electrophysiological experiments suggest that there is a secondary excitatory input from the VIIIth nerve onto the M-cell (Szabo et al., 2006) that may boost depolarization. This input appears to be located more proximal to the soma compared to club endings, and its time course implies that it is at least disynaptic. Both electrical and glutamatergic transmission contribute to its effect (Szabo et al., 2006).

In the following chapter, I report my work describing the role of spiral fiber neurons in the M-cell-mediated escape behavior. My results suggest that spiral fiber neurons are the origin of the previously unidentified multisynaptic and

proximal input onto the M-cell. I found that spiral fiber neurons are activated by sensory stimuli and are essential for the escape behavior. By providing an excitatory input directly at the M-cell spike initiation zone, spiral fiber neurons generate the drive needed to complement direct sensory input and evoke M-cell-mediated behavior.

CHAPTER 2

A Convergent and Essential Interneuron Pathway for Mauthner Cell Mediated Escapes

2.1 PREFACE

A shorter version of this chapter was published in the journal Current Biology (Lacoste et al., 2015). I designed, performed and interpreted all experiments. I conceived the study with David Schoppik, Florian Engert and Alexander F. Schier. David Schoppik helped design and interpret experiments. I built the behavioral and channelrhodopsin apparatuses with help from Drew N. Robson, David Schoppik, Martin Haesemeyer, Caroline Wee and Ruben Portugues, and wrote the software with Drew N. Robson and Martin Haesemeyer. Drew N. Robson and Jennifer M. Li built the two-photon calcium imaging apparatus. Alexander F. Schier supported the project.

2.2 ABSTRACT

The Mauthner cell (M-cell) is a command-like neuron in teleost fish whose firing in response to aversive stimuli is sufficient to produce short-latency escapes (Zottoli and Faber, 2000; Eaton et al., 2001; Korn and Faber, 2005). M-cells have

been proposed as evolutionary ancestors of startle response neurons of the mammalian reticular formation (Pfaff et al., 2012), and studies of this circuit have uncovered important principles in neurobiology that generalize to more complex vertebrate models (Korn and Faber, 2005). The main excitatory input was thought to originate from multisensory afferents synapsing directly onto the M-cell dendrites (Korn and Faber, 2005). Here, we describe an additional, convergent pathway that is essential for the M-cell-mediated startle behavior in larval zebrafish. It is composed of excitatory interneurons called spiral fiber neurons, which project to the M-cell axon hillock. By *in vivo* calcium imaging, we found that spiral fiber neurons are active in response to aversive stimuli capable of eliciting escapes. Like M-cell ablations, bilateral ablations of spiral fiber neurons largely eliminate short-latency escapes. Unilateral spiral fiber neuron ablations shift the directionality of escapes, consistent with spiral fiber neurons exciting the M-cell in a lateralized manner. Optogenetic activation of spiral fiber neurons increases the probability of M-cell-dependent escapes. These results reveal that spiral fiber neurons are essential for the function of the M-cell in response to sensory cues and suggest that parallel excitatory inputs that differ in their input location and timing ensure reliable activation of the M-cell, a feedforward excitatory motif that may extend to other neural circuits.

2.3 INTRODUCTION

Activity in the M-cells, a pair of large neurons located bilaterally in the hindbrain and projecting directly to motoneurons, is associated with escapes of short latencies (Zottoli, 1977; Liu and Fetcho, 1999; Burgess and Granato, 2007; Kohashi and Oda, 2008). Spiral fiber neurons are a group of neurons that project to the contralateral M-cell (Koyama et al., 2011) where they wrap around the axon hillock at a structure called the axon cap (Kimmel et al., 1981). Previous studies suggest that spiral fiber neurons excite the M-cell in adult goldfish (Scott et al., 1994), and stimulation of a single spiral fiber neuron in larval zebrafish is capable of eliciting an excitatory post-synaptic potential (EPSP) in the contralateral M-cell (Koyama et al., 2011). Anatomical (Kimmel et al., 1981), as well as electrophysiological and pharmacological (Koyama et al., 2011) evidence points to the presence of both glutamatergic and electrical synapses between spiral fiber neuron and M-cell. Based on these studies, spiral fiber neurons are well positioned to influence the M-cell-mediated escape behavior. In fact, mutants for the retinoblastoma-1 gene that have defects in axon targeting, including in the spiral fiber neurons, display abnormal fast turning movements in response to touch (Lorent et al., 2001; Gyda et al., 2012). However, the stimuli that drive the spiral fiber neurons have yet to be identified, and their role in the M-cell escape network remains unclear. Here, we address these questions using functional calcium imaging, ablations and detailed behavior analysis.

2.4 RESULTS

2.4.1 Spiral fiber neurons respond to aversive stimuli

We used a transgenic line, *Tg(-6.7FRhcrtR:gal4VP16)*, that labels spiral fiber neurons among other neurons in the larval zebrafish brain (Figure 2.1A). In 5 day old larval zebrafish, spiral fiber neurons are a group of ~10 neurons located bilaterally in rhombomere 3, rostro-ventral of the M-cells. These neurons all have descending projections to the contralateral M-cell axon cap and do not appear to contact other targets (Koyama et al., 2011).

We first asked whether spiral fiber neurons are capable of sensing stimuli that are classically used to elicit M-cell-dependent escapes (Figure 2.1B). In paralyzed animals embedded in agarose, we monitored calcium dynamics in the spiral fiber neurons labeled with the genetically encoded calcium indicators GCaMP-HS (Muto et al., 2011) by two-photon microscopy. We first assessed activity in the spiral fiber neuron axon terminals that wrap around the M-cell axon hillock (Figure 2.2). We observed irregular and infrequent spontaneous activity in spiral fiber neurons, at a rate of about one calcium event per minute.

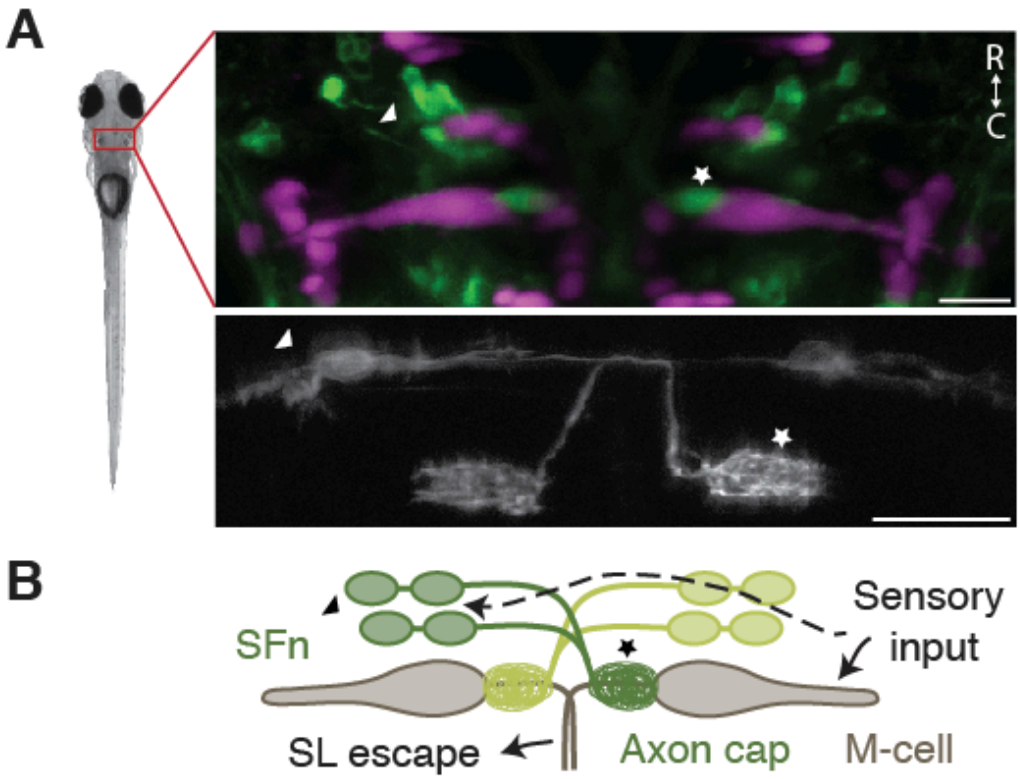

Figure 2.1. Spiral fiber neurons project to the contralateral axon cap of the Mauthner cell.

A) Left image: 5 day old zebrafish larvae. Top image: *Tg(-6.7FRhcrtR:gal4VP16)*; *Tg(UAS:GCaMP5)* labels spiral fiber neurons (arrowhead) among other neurons. The M-cell and other reticulospinal neurons are labeled with tetramethylrhodamine dextran by reticulospinal backfill. Spiral fiber neuron cell bodies are located in rhombomere 3 in two rostro-caudal clusters, approximately 25-40 μm rostral, 5-15 μm lateral, and 0-20 μm ventral of the axon cap. They all have axons descending contralaterally into the axon cap of the M-cell. Bottom image: Transient expression of membrane targeted GFP (*UAS:GAP43-GFP*) in *Tg(-6.7FRhcrtR:gal4VP16)* labels two spiral fiber neurons on the left and one spiral fiber neuron on the right that project to the contralateral M-cell axon cap (star). Pictures are oriented rostral up; scale bars: 20 μm. B) Model showing the M-cells receiving ipsilateral sensory input, which includes auditory/vestibular afferents onto the lateral dendrite. Our results suggest that spiral fiber neuron somata receive similar sensory information from the contralateral side.

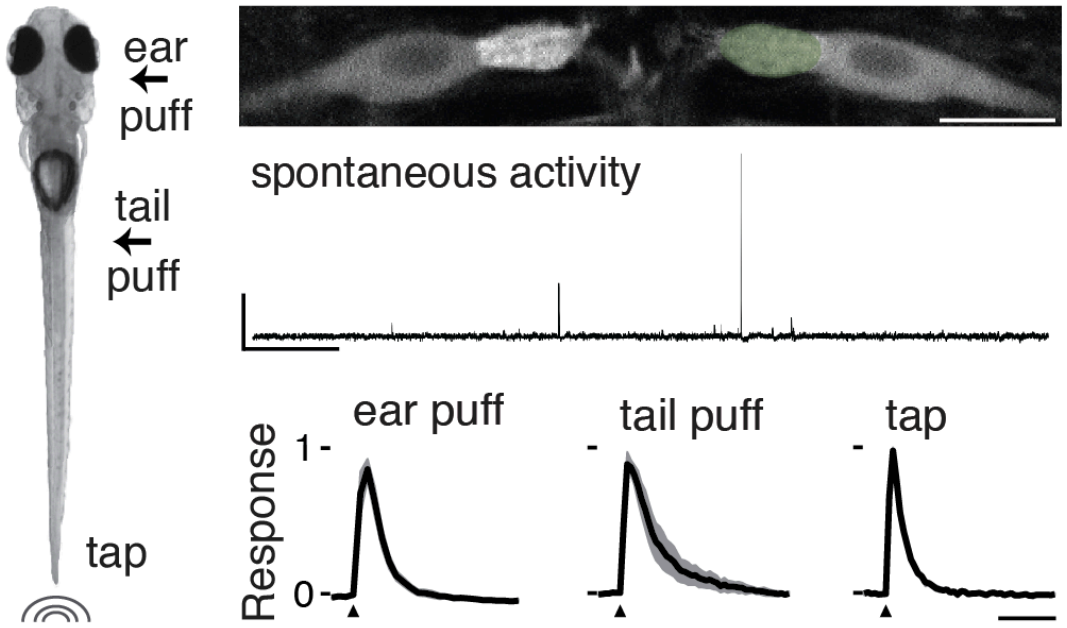

Figure 2.2. Spiral fiber neurons respond to aversive stimuli.

Left image: 3 different stimuli were delivered to paralyzed zebrafish larvae: water puffs directed at the right ear, water puffs directed at the right side of the tail, and non-directional taps delivered onto the dish holding the fish. Top image: Projection of two-photon image stack showing M-cells and spiral fiber neuron axon terminals labeled with the calcium indicator *Tg(UAS:GCaMP-HS)* driven by *Et(fos:Gal4-VP16)s1181t* and *Tg(-6.7FRhcrtR:gal4VP16)* respectively. Picture is oriented rostral up; scale bars: 20 μm. Middle panel: Typical spontaneous activity in the spiral fiber neuron axon terminals. Scale bars: 5 min horizontally, 1 Δf/f vertically. Bottom panel: Mean response amplitude in the right spiral fiber neuron axon terminals for different stimuli: ear puffs (n = 7, left panel), tail puffs (n = 5, middle panel), and taps (n = 6, right panel). For each fish, the change in fluorescence (Δf/f) from trials in which the axon cap was active was normalized to the maximum Δf/f across trials, and then averaged. The black line is the mean across fish with the standard error of the mean (SEM) shaded. Stimulus delivery is indicated by an arrowhead. Horizontal scale bar: 2 sec.

We then stimulated the animals with three different stimuli: two tactile stimuli consisting of short water pulses delivered either to the otic vesicle (which develops into the ear) (Kohashi and Oda, 2008) or delivered to the tail (O'Malley et al., 1996; Liu and Fetcho, 1999). The third stimulus we used was a primarily auditory/vibrational stimulus consisting of an abrupt tap on the dish holding the animal (similar to Burgess and Granato, 2007). We observed that all three types of stimuli elicited robust responses in the spiral fiber neuron axon terminals (Figure 2.2). Responses in the spiral fiber neurons were independent of M-cell activity: after bilateral M-cell ablations, spiral fiber neurons continued to respond to the tap stimulus with comparable amplitude (Figure 2.3). Thus, the spiral fiber neurons encode a range of sensory information.

M-cells respond to stimuli arriving ipsilaterally on their dendrites but individual spiral fiber neurons cross the midline and project to the contralateral M-cell. We thus asked whether the responses of spiral fiber neurons were lateralized accordingly. Consistent with their contralateral projections, we observed that spiral fiber neuron somata were strongly activated by ear and tail stimuli delivered on the contralateral side (Figure 2.4). Ipsilateral spiral fiber neurons also responded but more weakly (ear stimuli: $n = 10$ fish, $p < 0.05$ contralateral vs. ipsilateral; tail stimuli: $n = 10$, $p < 0.05$), an effect likely due to directional stimuli also being capable of stimulating the opposite side of the skin to a lesser extent. Responses to the non-directional tap stimulus, on the other hand, were not lateralized (Figure 2.4B, $n = 4$, $p > 0.05$).

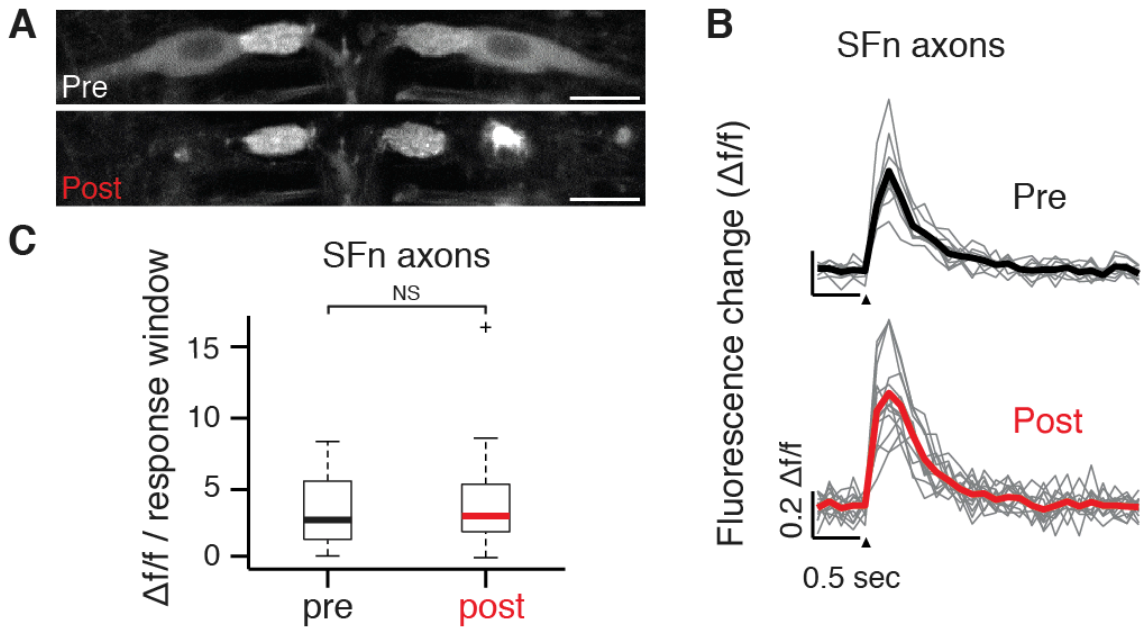

Figure 2.3. Spiral fiber neuron axons continue to respond to taps after Mauthner cell ablations.

A) Two-photon image showing M-cells and spiral fiber neuron axon terminals labeled with GCaMP-HS at the axon cap before (top image) and after (bottom image) bilateral ablation of the M-cells. Bright spots in the bottom image correspond to cell debris. Scale bar: 20 μm. Pictures are oriented rostral up. B) Representative traces of the change in spiral fiber neuron axon fluorescence at the M-cell axon cap in response to taps. Top plot: before, bottom plot: after bilateral ablation of the M-cells. Grey traces are individual trials, the black trace is the mean. Stimulus delivery is indicated by an arrowhead. C) Population fluorescence change of spiral fiber neuron axons in response to taps before (left) and after (right) ablation of the M-cells (n = 10 axon caps, y-axis is the mean fluorescence change over a 1.5 sec response window in trials where the axon cap responded). Horizontal line is the median, box edges are the 25th and 75th percentiles, whiskers extend to the most extreme data points not considered outliers and crosses are outliers. Pre and post are not significantly different (NS, p = 1, Wilcoxon signed rank sum test).

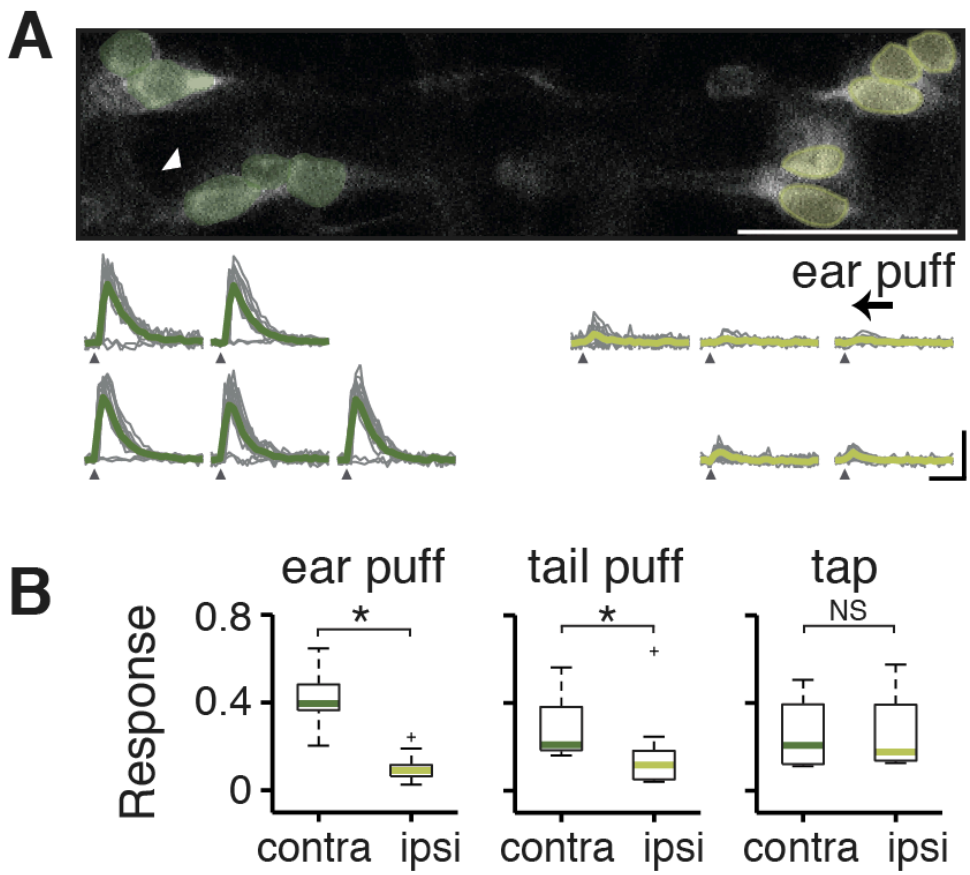

Figure 2.4. Spiral fiber neurons respond to contralateral stimuli.

A) Top panel: Single recording plane showing spiral fiber neuron somata in *Tg(-6.7FRhcrtR:gal4VP16)*; *Tg(UAS:GCaMP-HS)*. Picture is oriented rostral up; scale bar: 20 μm; the arrow points to spiral fiber neuron somata. Bottom panel: Mean Δf/f across trials in green and individual trials in grey for spiral fiber neuron somata from the top panel located on the left (dark green) and on the right (light green) responding to a water puff delivered to the right ear (arrow). Contralateral spiral fiber neurons respond to the stimulus, but ipsilateral spiral fiber neurons do not. Traces in which spiral fiber neurons on the left do not respond correspond to the same trials. Note that while caudal neurons seem to respond before rostral neurons, this is an artifact of the delay introduced by 2-photon line scanning. Scale bars: 2 sec horizontally, 2 Δf/f vertically. B) Boxplot showing the normalized response of spiral fiber neurons across fish. Response was defined

Figure 2.4 (Continued) as the area under the Δf/f curve over a 1.5 sec response window. This was normalized for each cell to the maximum response observed in a given experiment and then cells located on the contralateral (contra) and ipsilateral (ipsi) side with respect to the stimulus were averaged. Green lines are the medians across fish, box edges are the 25^{th} and 75^{th} percentiles, the whiskers extend to the most extreme data points not considered outliers, and crosses are outliers. Stimuli delivered: ear puffs (left panel, n = 10 fish, $p = 2.5*10^{-4}$), tail puffs (middle panel, n = 10, p = 0.02), and taps (right panel, n = 4, p = 0.89). * denotes $p < 0.05$, NS not significant by Wilcoxon rank sum test.

These results indicate that spiral fiber neurons receive contralateral sensory input (Figure 2.1B), and as spiral fiber neurons project to the contralateral M-cell, the laterality of sensory information is preserved across M-cell inputs.

2.4.2 Spiral fiber neuron ablations largely abolish Mauthner-cell-dependent short-latency escapes

To investigate whether spiral fiber neurons affect the escape behavior, we built an apparatus designed to elicit and quantify escapes in response to an aversive stimulus (Figure 2.5). 5-7 day old fish were embedded in agarose and their tails were freed. A mechanical tapper hit the plate onto which the fish was placed, in a similar manner to the tap stimulus used for calcium imaging experiments. By imaging at 1000 Hz, we were able to reconstruct the curvature of the tail as a function of time, and measure the direction, angle and latency of the response

(Figure 2.6A). In accordance with previous findings (Burgess and Granato, 2007; Ikeda et al., 2013), we classified escapes as either short-latency (≦12 ms) or long-latency (13 - 25 ms).

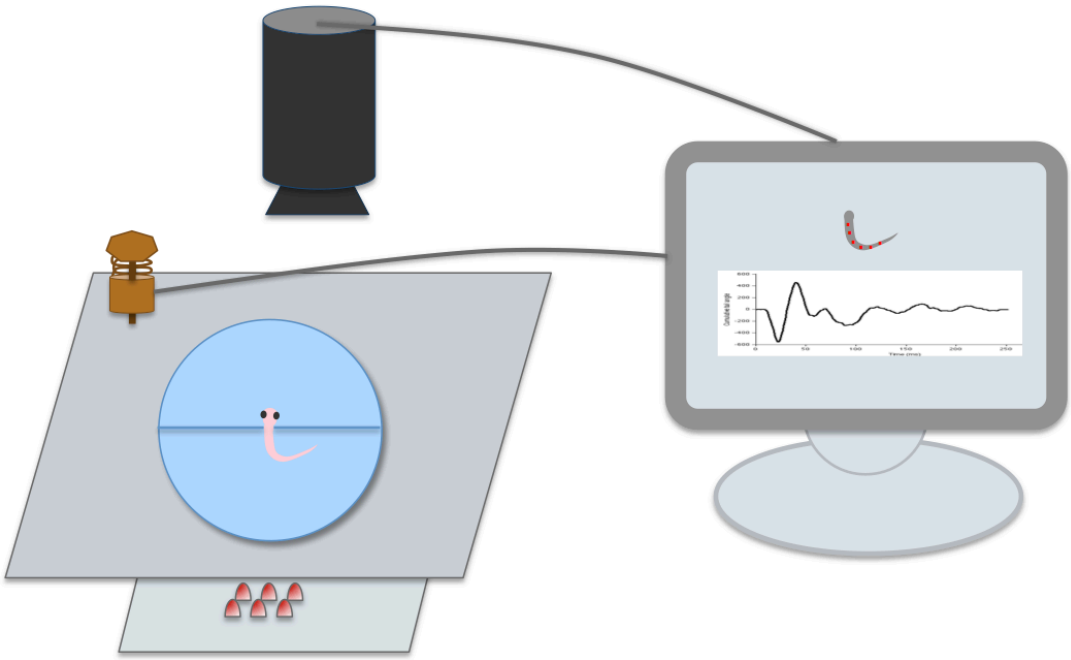

Figure 2.5. Custom-built behavioral apparatus to elicit and monitor escapes in head-restrained larvae.

A solenoid delivers impact taps while a camera records tail movement illuminated with IR lights at 1000 Hz. Tail angles are decoded by custom-written software.

The tap stimulus elicited responses with 100% probability (n = 50 larvae). The vast majority (99.7%) of these responses were escapes, with latencies ranging from 5 - 25 ms (9.9 ± 0.19 ms, mean ± standard error of the mean). Escapes

were generally stereotyped in individual larvae (Figure 2.6B). Characteristic escapes consisted of a sharp angle C-bend of the tail (>60°), followed by a counter turn in the opposite direction and subsequent swimming lasting hundreds of milliseconds (Figure 2.6C).

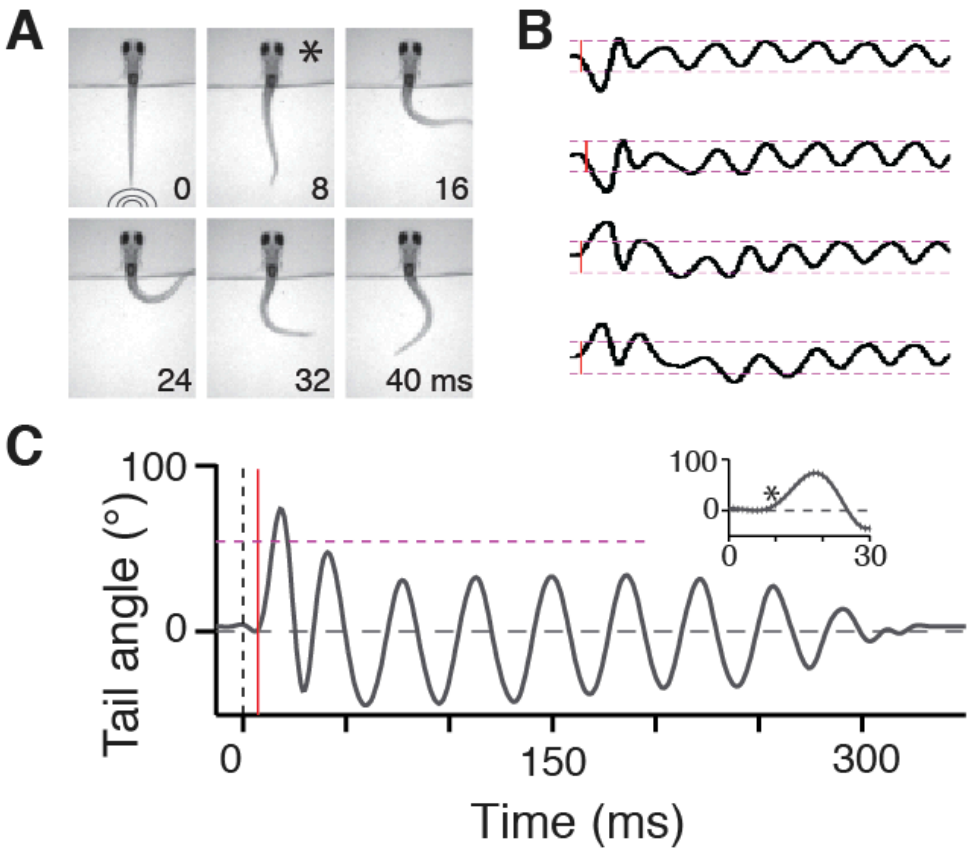

Figure 2.6. Larval zebrafish produce stereotyped escapes in response to tap stimuli.

A) Representative escape behavior of a head-embedded larval zebrafish responding to a tap stimulus. Images were recorded every millisecond and here every 8th image is shown. The first image was taken at the time the tap stimulus hit the dish holding the larvae. The image marked with a star corresponds to the beginning of the escape response (8 ms latency). B) Tail traces in response to

Figure 2.6 (Continued) taps in four trials in the same larva. Escapes can occur in both direction and are stereotyped within an animal. C) Representative smoothed tail trace showing the angle of the last tail segment with respect to the vertical in response to a tap. The escape behavior consists of a sharp angle C-bend, followed by a counter turn in the opposite direction and subsequent swimming lasting hundreds of milliseconds. The grey dotted line indicates the start of the stimulus; the red solid line shows the automatically identified latency, and the magenta dotted line indicates the angle threshold above which a tail trace is considered a C-bend. The inset shows the first 30 ms after stimulus onset and a star indicates the start of the C-bend.

Larvae produced short-latency escapes with a high probability (92 ± 1.4%) whereas long-latency escapes were observed infrequently (8.2 ± 1.4%). Responses with latencies above 25 ms (0.26 ± 0.19%) corresponded to other types of movements such as swims and turns.

To uncover the types of receptors activated by the tap stimulus, we measured tap responses in fish with non-functional hair cells (*mariner* mutants, Ernest et al., 2000) and in fish in which the lateral line was ablated by neomycin treatment (Harris et al., 2003). Our results indicate that short-latency escapes, but not long-latency escapes, are primarily mediated by the ear, while the lateral line does not play a role (Figure 2.7). Thus, tap stimuli engage several sensory systems, including the ear, and likely touch receptors.

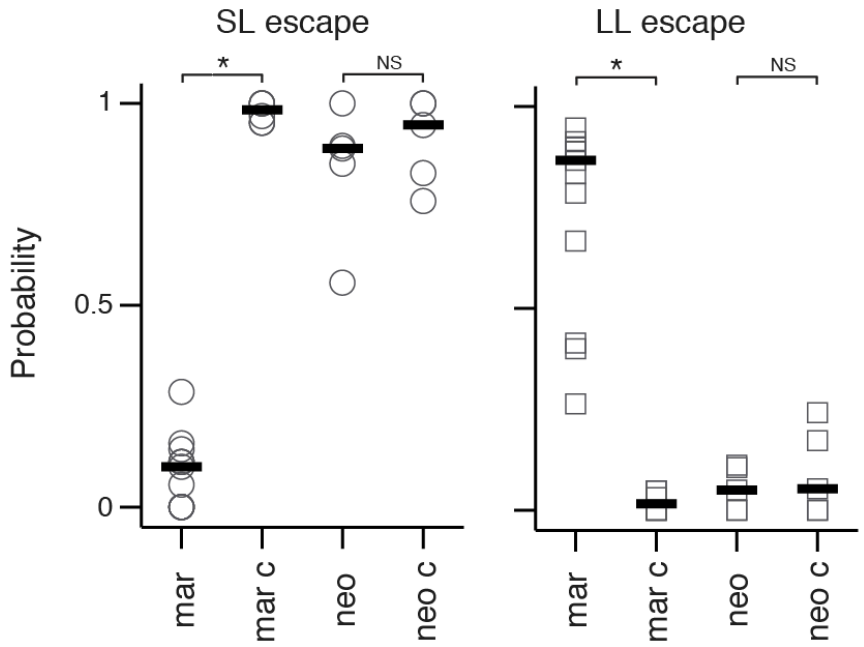

Figure 2.7. Short-latency escapes in response to taps are primarily mediated by the inner ear.

Probability of generating escapes in response to taps in the tail-free behavioral apparatus. Fish tested are homozygote mariner mutant fish lacking mechanosensory transduction in hair cells (mar, n = 13) and wild-type or heterozygote siblings (mar c, n = 6); neomycin-treated fish with ablated lateral lines (neo, n = 5) and control siblings (neo c, n = 5). Left panel: short-latency (SL) escapes. Right panel: long-latency (LL) escapes. Mariner mutants are significantly different from their controls ($p = 7.4*10^{-5}$ and $7.4*10^{-5}$ for SL and LL escapes respectively) whereas neomycin treated fish and their controls are not ($p = 0.69$ and 0.65). * denotes $p < 0.05$ by Wilcoxon rank sum test.

To analyze the respective contributions of the M-cell and spiral fiber neurons to the escape behavior, we compared the response to taps of larvae before and after three ablation conditions: M-cells (Figure 2.10A), spiral fiber neurons (Figure 2.10D) or ablation of other neurons in the area as a control (Figure

2.10G). Targeted ablations were carried out using a pulsed infrared laser as described previously (Bianco et al., 2012). To ensure that ablations did not induce damage elsewhere in the nervous system, we stained larvae brains from experiments in which spiral fiber neurons had been unilaterally ablated. There was no noticeable difference in the appearance of nuclei between the ablated and intact side (Figure 2.8). At the ablated axon cap, glycinergic receptors were preserved, while synaptic terminals were reduced in size, as expected (Figure 2.9).

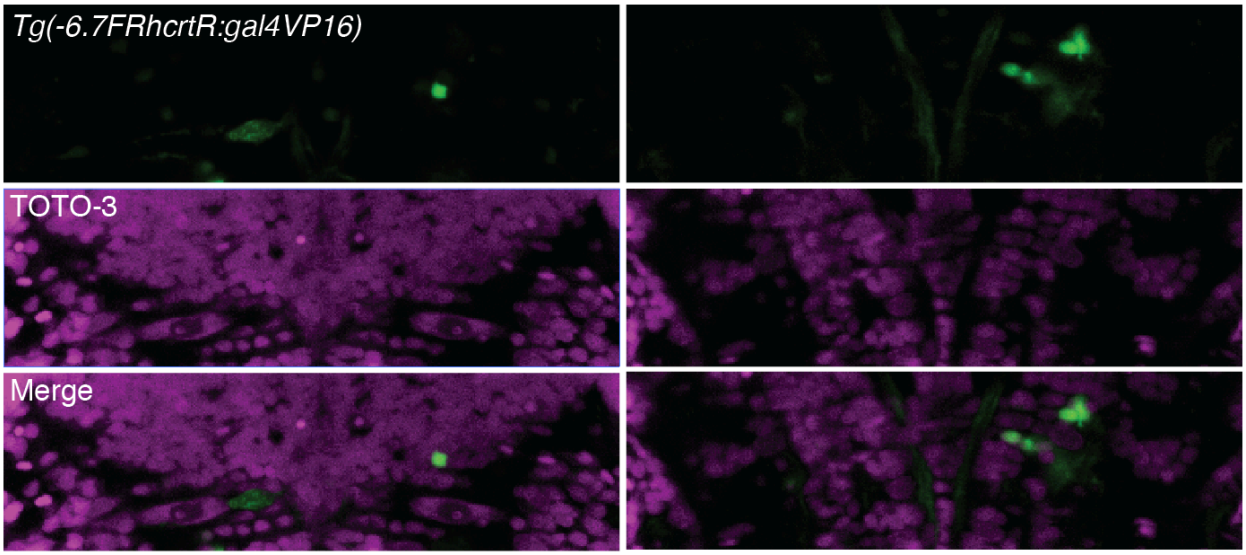

Figure 2.8. Nuclear staining in unilateral spiral fiber neuron ablated larva.

Spiral fiber neuron somata were ablated on the left. Top row: *Tg(-6.7FRhcrtR:gal4VP16); Tg(UAS:GCaMP-HS)* labels spiral fiber neurons in green. Middle row: TOTO-3 labels nuclei in purple. Bottom row: Top and middle rows merged. Left column: Plane of the M-cell and spiral fiber neuron axons at the cap. The axon cap is visible on the left only. Right column: Plane of the spiral fiber neuron somata. Ablated spiral fiber neurons on the left are no longer visible and nuclei in that region appear normal.

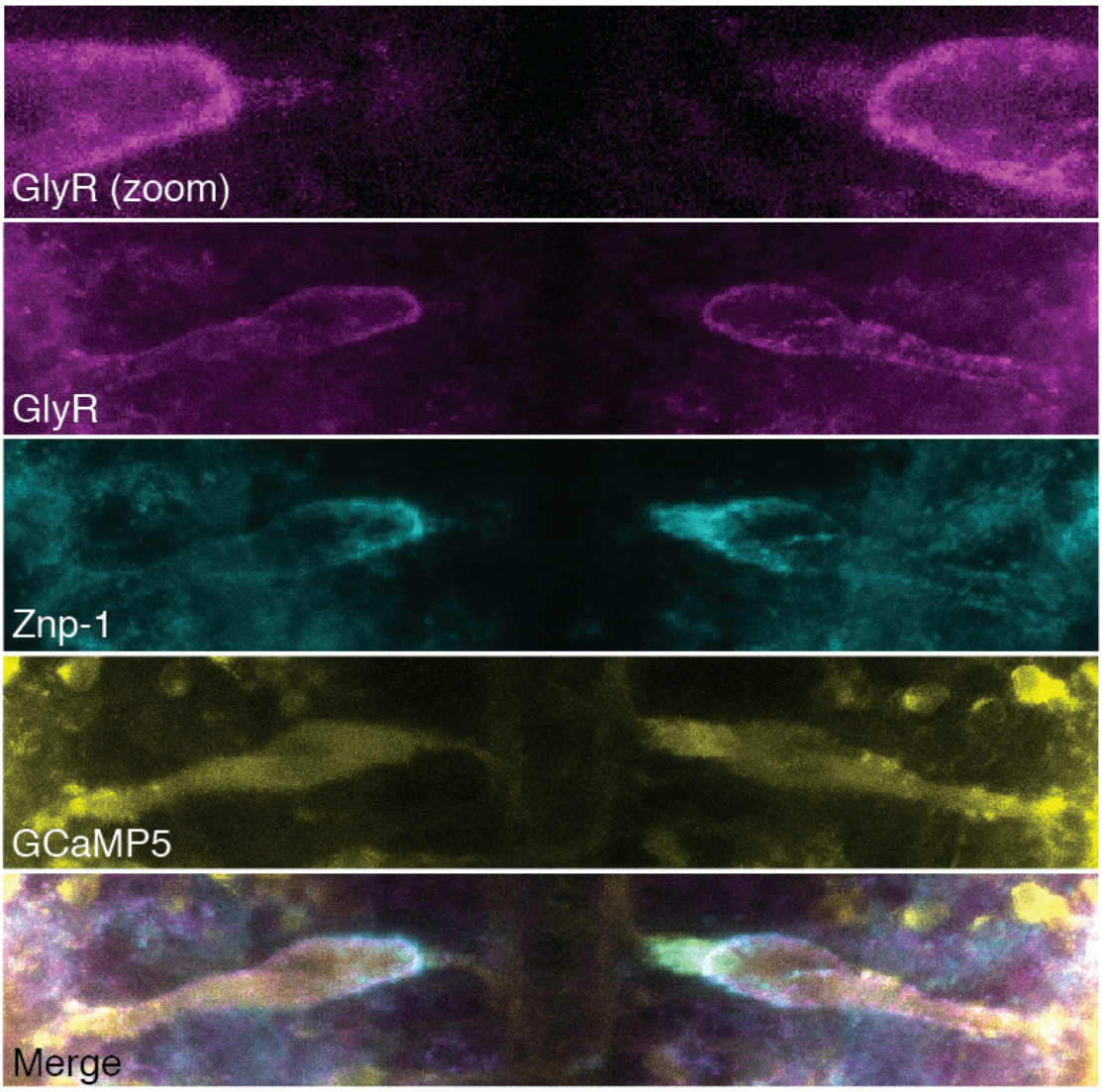

Figure 2.9. Labeling of the Mauthner cell and axon cap after unilateral spiral fiber neuron ablations.

Spiral fiber neuron somata were ablated on the right. GlyR: glycine receptor antibody shows a haze at the axon cap. Znp-1: synaptotagmin antibody, which marks presynaptic terminals, is reduced at the ablated axon cap, presumably due to the absence of spiral fiber neuron-M-cell axon synapses, and the preservation of inhibitory glycinergic neurons that synapse in this region. GCaMP5: fluorescence in *Tg(-6.7FRhcrtR:gal4VP16); Et(fos:Gal4-VP16)s1181t; Tg(UAS:GCaMP-HS)* larvae labels the M-cells, the spiral fiber neuron axons at the cap, and other neurons in the region.

Previous studies have shown that short-latency escapes in response to auditory stimuli require the M-cells but tactile stimuli only partially depend on the M-cells (O'Malley et al., 1996; Liu and Fetcho, 1999; Kohashi and Oda, 2008; Kohashi et al., 2012). Two sets of segmental homologs are thought to elicit escapes of longer latency when the M-cell does not fire (Liu and Fetcho, 1999; Kohashi and Oda, 2008; Issa et al., 2011). Thus, due to the multisensory nature of our stimulus, we expected the M-cells to be partially required for short-latency escapes. Indeed, we found that after M-cell ablations, the number of short-latency escapes performed decreased in favor of long-latency escapes (n = 14 fish, Figure 2.10B). The mean probability of short-latency escapes decreased on average 1.8-fold and long-latency escapes increased 3-fold ($p < 0.05$, Figure 2.10C). Spiral fiber neuron ablations had a similar effect: after ablations, the majority of escapes observed were long-latency (Figure 2.10E). Short-latency escapes were reduced by 6-fold and long-latency escapes increased 8.1-fold (n = 13, $p < 0.05$, Figure 2.10G). Control ablations did not induce a change in the escape latency profile (Figure 2H) or probability of escapes (n = 23, $p > 0.05$, Figure 2.10I). The overall probability of response was not affected by any of the ablation procedures ($p > 0.05$, Figures 2.10C, 2.10F and 2.10I).

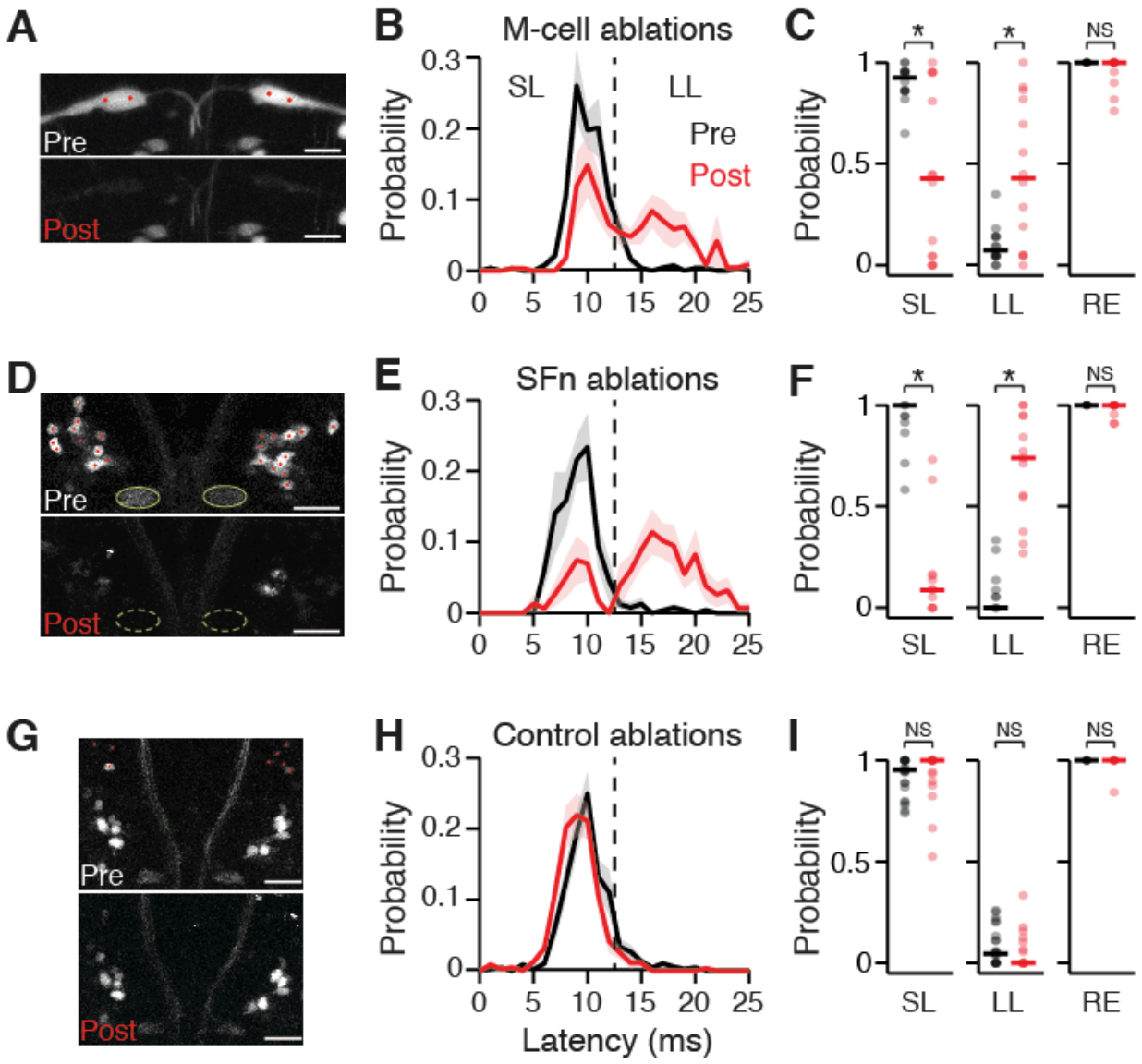

Figure 2.10. Loss of Mauthner cells or spiral fiber neurons largely abolish short-latency escapes.

Results of M-cell ablations (A-C, n = 14 fish), spiral fiber neuron ablations (D-F, n = 13) and control ablations (G-I, n = 23) on the escape behavior in response to taps. A, D, G. Stack projections showing before (top image) and immediately after (A) or 24 hours after (D, G) two-photon laser-mediated bilateral ablations (bottom image). A) *Et(fos:Gal4-VP16)s1181t; Tg(UAS:GCaMP-HS)*. D, G. *Tg(-6.7FRhcrtR:gal4VP16); Tg(UAS:Kaede)*. Red dots mark the cells or location within the M-cell that were targeted for ablation. Green ovals in D mark the axon

Figure 2.10 (Continued) caps, which are no longer apparent 24 hours after ablations. High fluorescence cell debris can be observed in the post images. B), E), H). Escape probability as a function of latency of all escapes performed, mean +/- SEM, before ablations (black) and after (red). The dotted line at 13 ms demarcates short- (SL, ≦12 ms) and long latency (LL, 13-25 ms) escapes. C), F), I). Probabilities of different types of responses as a function of all trials before (black) and after (red) ablations. Individual fish are displayed as semi-transparent dots and horizontal bars are the medians. Left: SL escapes; middle: LL escapes; right: overall responses (RE). M-cell: $p = 0.013$ (SL), 0.016 (LL) and 0.075 (RE); spiral fiber neuron: $p = 2.4*10^{-4}$, $2.4*10^{-4}$, and 0.10; Control: $p = 0.28$, 0.20 and 0.33; Wilcoxon signed rank test (SL, LL) or paired t-test (RE). * denotes $p < 0.05$; NS not significant. Pictures are oriented rostral up; scale bars: 20 μm.

To compare the effect of ablation across groups, we evaluated the change in short-latency escape probability after ablations. The effects of M-cell and spiral fiber neuron ablations were significantly different from controls ($p < 0.05$). A fraction of M-cell ablations did not produce a strong effect, likely due to compensatory escape pathways. Nevertheless, the effects of M-cell and spiral fiber neuron ablations were not statistically distinguishable from each other ($p > 0.05$, Figure 2.11). Taken together, these experiments show that the phenotype of ablating the spiral fiber neurons is similar to that of ablating the M-cells, indicating that spiral fiber neurons play an essential role in M-cell-mediated escapes.

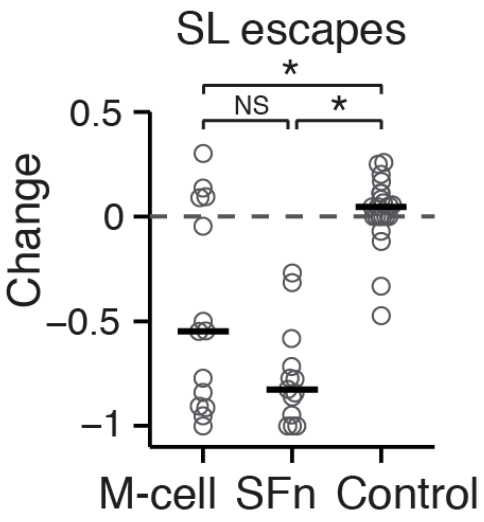

Figure 2.11. Mauthner cell and spiral fiber neuron ablation phenotypes are comparable.

Change in SL escape probability as a function of all trials (post - pre) based on the SL data plotted in Figure 2.10. Individual fish (grey circles), median (black line). M-cell vs. Spiral fiber neuron: $p = 0.11$; M-cell vs. Control: $p = 0.011$; spiral fiber neuron vs. Control: $p = 1.6*10^{-6}$, Wilcoxon rank sum test.

2.4.3 Spiral fiber neurons bias the laterality of Mauthner-cell-mediated escapes

M-cells provide excitation to the contralateral side of the spinal network, resulting in contralateral tail bends. Due to inhibition (Takahashi et al., 2002; Korn and Faber, 2005; Satou et al., 2009), only one of the two M-cells elicits an escape response at any one time. In accordance with this circuit design, previous studies have shown that after unilateral M-cell ablation, the probability of contralateral short-latency escape is decreased, with a concomitant increase in ipsilateral short-latency escapes (Zottoli, 1977; Liu and Fetcho, 1999; Burgess and Granato, 2007; Kohashi and Oda, 2008). Since spiral fiber neurons project to one M-cell only, we asked whether they also affect the escape behavior in a lateralized manner. To test this, we compared the effect of unilateral M-cell

(Figure 2.12B) and spiral fiber neuron (Figure 2.12C) ablations on the directionality of the escape behavior in response to non-directional tap stimuli (Figure 2.12A). We expected that following the anatomy of the circuit, ablation of one M-cell or its contralateral spiral fiber neurons would bias escapes towards the ipsilateral and contralateral side with respect to the ablated somata, respectively (Figure 2.12E). We found that the overall frequency of short-latency escapes did not change following M-cell ablations (Figure 2.12D). However, as expected, unilateral M-cell ablations biased escapes towards one side (Figure 2.12F). Regardless of the original direction preference of individual fish before ablations, in all cases short-latency escapes contralateral to the ablated M-cell were virtually eliminated (n = 11, 35 ± 9.0% pre to 7.0 ± 3.6% post, Figure 2.12G). The directionality of the other, infrequent types of responses, such as long-latency escapes and swims, was not affected by the ablations (data not shown). Spiral fiber neuron unilateral ablations had a similar effect as ablation of the M-cell they project to (Figure 2.12F). The percentage of short-latency escapes contralateral to the ablated spiral fiber neuron somata increased from 44 ± 6.4% to 91 ± 4.1% (n = 17, Figure 2.12G), while the overall fast-escape escape probability remained unchanged (Figure 2.12D). The laterality bias following M-cell or spiral fiber neuron ablation was not statistically distinguishable ($p > 0.05$). These experiments support the requirement of spiral fiber neurons for the normal functioning of their target M-cell.

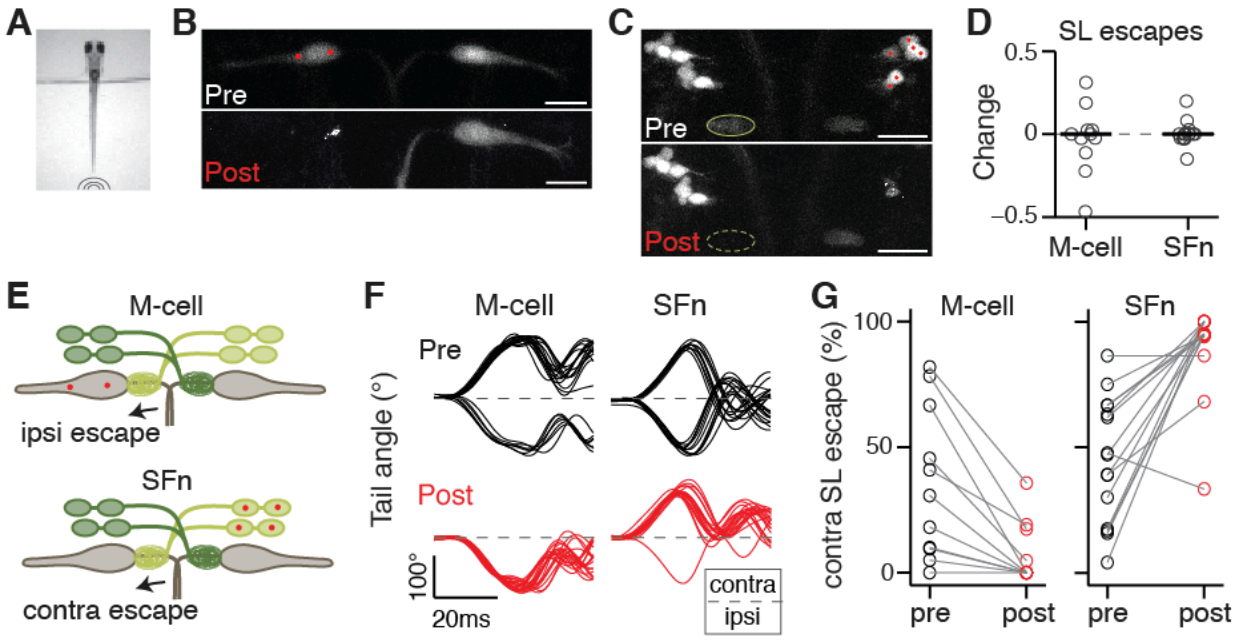

Figure 2.12. Spiral fiber neurons are necessary for lateralized Mauthner-cell-mediated escapes.

A) Tail free larvae are presented with a non-directional tap stimulus as in Figure 2.10. B) Projection of two-photon image stack showing M-cells before (top image) and 24 hours after (bottom image) ablation of the M-cell on the left in *Et(fos:Gal4-VP16)s1181t; Tg(UAS:Kaede)*. C) Projection of two-photon image stack showing spiral fiber neurons before (top image) and 24 hours after (bottom image) ablation of spiral fiber neuron somata located on the right in *Tg(-6.7FRhcrtR:gal4VP16); Tg(UAS:Kaede)*. The axon cap (green oval) contralateral to the targeted spiral fiber neurons is no longer apparent 24 hours after ablations. D) Normalized change in short-latency (SL) escape probability as a function of all trials (post-pre / post+pre). Individual fish (grey circles) and median (black line). Left: M-cell ablation (n = 11). Right: spiral fiber neuron ablations (n = 17). The probability change is not significantly different from 0 in either condition (p = 0.67 and 0.98 respectively, Wilcoxon signed rank test). E) Model showing that when M-cells or spiral fiber neurons are ablated unilaterally, escapes in response to taps become strongly biased towards one direction: ipsilateral to the ablated M-cell or contralateral to the ablated spiral fiber neurons. F) Example tail traces for a fish before (top plots, black) and after (bottom plots, red) ablation of the left M-

Figure 2.12 (Continued) cell (left plots) and a fish before and after ablations of spiral fiber neuron somata on the right (right plots). The directionality of the initial tail bend is expressed as ipsilateral (ipsi) or contralateral (contra) with respect to the ablated soma(ta). Traces begin at the time of tap delivery. G) Probability of contralateral SL escapes as a function of all SL escapes of either direction. Left panel: M-cell ablation. Right panel: spiral fiber neuron ablations. Escapes shift toward the ipsilateral side for M-cell ablation, and to the contralateral side for spiral fiber neuron ablations. The laterality bias following M-cell or spiral fiber neuron ablation was not statistically distinguishable ($p = 0.76$, t-test). Scale bars: 20 μm. Pictures are oriented rostral up.

2.4.4 Spiral fiber neuron ablations do not change calcium dynamics in the Mauthner cell soma in response to taps

In response to auditory/vibrational stimuli, the M-cell receives two spatially segregated inputs, sensory afferents synapsing onto its dendrites, and spiral fiber neurons projecting to its axon hillock. An interesting question is where on the subcellular structure of the M-cell these two pathways converge. To test the effect of spiral fiber neuron input onto the M-cell, we analyzed M-cell calcium dynamics in response to taps before and after unilateral ablations of spiral fiber neurons in larvae embedded in agarose and paralyzed with alpha-bungarotoxin (Figure 2.13A). Calcium signals could only be observed in the M-cell soma and not at the axon or axon hillock when spiral fiber neurons were not labeled. Therefore, unilateral spiral fiber neuron ablations allowed us to compare the M-cell soma lacking spiral fiber neuron projections with the other M-cell that retained spiral fiber neuron input, in the same animal.

Figure 2.13. Calcium dynamics in the Mauthner cell soma are not affected by spiral fiber neuron ablations.

A) Projection of two-photon image stack showing M-cells and spiral fiber neurons in *Tg(-6.7FRhcrtR:gal4VP16); Et(fos:Gal4-VP16)s1181t; UAS:GCaMP5* (projection). Top: before ablation of spiral fiber neurons on the right (red dots). Bottom: immediately after ablations. The left axon cap (green oval) fluoresces strongly due to calcium release upon ablations. Scale bar: 20 μm. Pictures are oriented rostral up. B) Change in fluorescence (Δf/f) in response to taps (arrowheads) before and after unilateral spiral fiber neuron ablations for one representative fish paralyzed with α-bungarotoxin and embedded in agarose. Contra M-cell: M-cell located contralateral to the ablated spiral fiber neuron somata; Contra AC: contralateral axon cap corresponding to axon terminals of the ablated spiral fiber neurons; Ipsi M-cell: ipsilateral M-cell with preserved spiral fiber neuron input; Ipsi AC: axon cap corresponding to axon terminals of the intact spiral fiber neurons. The mean across trials is plotted in black and individual trials in grey. Top panels: before unilateral spiral fiber neuron ablations; bottom panels: after spiral fiber neuron ablations. Stimulus delivery is indicated by an arrowhead. C) Mean response amplitude in individual larvae (circles), before and after unilateral spiral fiber neuron ablations. First row: values represent the mean Δf/f / sec, which was computed over a 1.5 sec response window across trials with a non-zero Δf/f. The median difference pre versus post was statistically significant only in the contralateral axon cap (Contra M-cell, $p = 0.90$; Contra AC, $p = 9.8*10^{-4}$; Ipsi M-cell, $p = 0.067$; Ipsi AC, $p = 0.46$, Wilcoxon signed rank test, n = 11 fish). Second row: values represent the mean peak Δf/f across all trials. The median difference pre versus post was statistically significant only in the contralateral axon cap (Contra M-cell, $p = 0.90$; Contra AC, $p = 9.8*10^{-4}$; Ipsi M-cell, $p = 0.083$; Ipsi AC, $p = 0.46$). The identity line is in black and the red circle represents the fish exemplified in B). D) Histograms showing the distribution of activity ratios between the ipsilateral and the contralateral M-cell before and after unilateral spiral fiber neuron ablations (ratio of response amplitudes normalized from -1 to 1: (contra - ipsi) / (contra + ipsi), Δf/f / sec, discarding trials in which both M-cell responses were flat, n = 130 trials pre and 139 trials post, across 11 larvae). Third panel: Histogram mean and 95% confidence interval (0.12, [0.010, 0.22], pre; 0, [-0.11, 0.11], post; $p = 0.18$, Wilcoxon rank sum test).

Figure 2.13 (Continued)

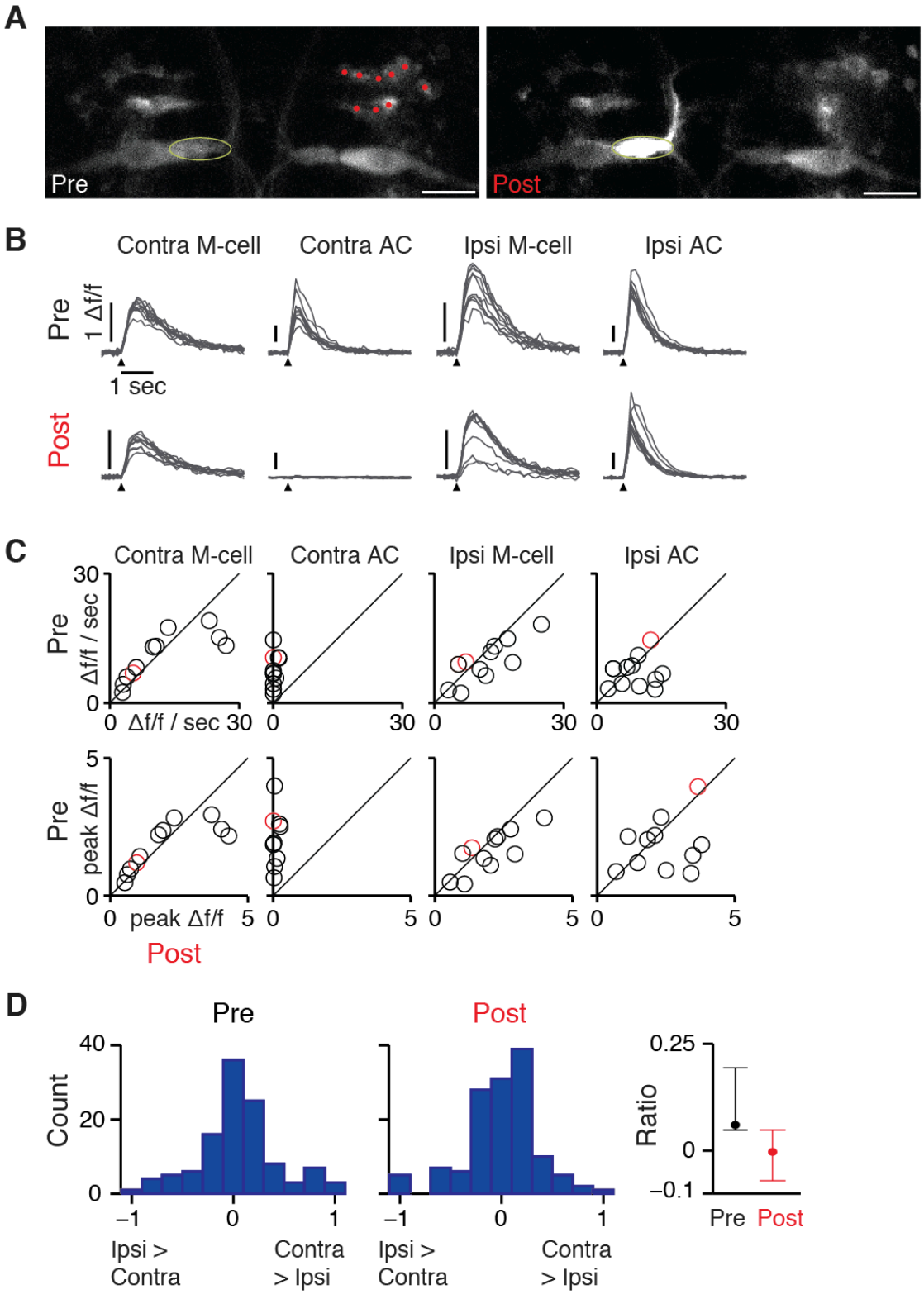

We found that after unilateral spiral fiber neuron ablation, contralateral axon terminals failed to respond to taps, confirming the death of their associated somata (Figures 2.13B, C). M-cell and spiral fiber neuron axons ipsilateral to the ablated spiral fiber neuron somata continued to respond to stimuli with comparable fluorescence changes ($p > 0.05$, Figures 2.13B, C). Contralateral M-cells that had lost spiral fiber neuron input also continued to respond to stimuli, and response amplitudes were comparable to the levels before spiral fiber neuron ablations ($p > 0.05$, Figure 2.13B). Comparing the relative amplitude of responses in the contralateral vs. ipsilateral M-cell, we found that this ratio did not change significantly after spiral fiber neuron ablations (Figure 2.13D). To eliminate potential defects in the normal functioning of the M-cell circuit due to the drug alpha-bungarotoxin, we repeated these experiments in non-paralyzed fish. Our results were comparable (see Figure A.1 of the Appendix). These results indicate that dendritic inputs are responsible for the bulk of calcium signals in the M-cell soma. Since spiral fiber neurons play a necessary role in M-cell-mediated motor output, these experiments argue that spiral fiber neuron and direct sensory inputs are integrated at the level of the M-cell axon hillock to elicit an escape response.

2.4.5 Spiral fiber neuron activation enhances the probability of Mauthner-cell-mediated escapes

Our results demonstrate that spiral fiber neurons are an essential excitatory input in the M-cell circuit. We next asked whether activating the spiral fiber neurons could decrease the threshold for M-cell-mediated escapes. To test this hypothesis, we expressed channelrhodopsin2 (ChR2) in neurons labeled in *Tg(-6.7FRhcrtR:gal4VP16)* by crossing with *Tg(UAS:ChR2(H134R)-EYFP)* and tested larvae responsiveness to low-intensity taps alone or the same weak taps paired with blue light. ChR2 excitation light was delivered via a blue laser beam focused on the fish's head 20-60 ms before the tap occurred and for a total of 100 ms (Figure 2.14A). We observed a strong enhancement of short-latency, M-cell-mediated escapes in ChR2 positive fish when the weak taps were paired with blue light (4.4 fold enhancement, $p < 0.05$), but not in controls lacking ChR2 (Figure 2.14B). In addition to modulating the probability of short-latency escapes, we reasoned that the excitatory effect of spiral fiber neurons on the M-cell might decrease escape latency. As postulated, short-latency escapes in response to taps paired with light occurred on average 0.95 ms earlier than those in response to taps alone in ChR2 positive fish ($p < 0.05$). Latency was not affected in ChR2 negative controls (Figure 2.14C). The probability of long-latency escapes was also moderately enhanced by pairing taps with blue light in ChR2 positive fish only (2.1 fold mean increase), likely due to unspecific effects of blue light (Figure 2.14D). The latency of these escapes was not affected (Figure 2.14E).

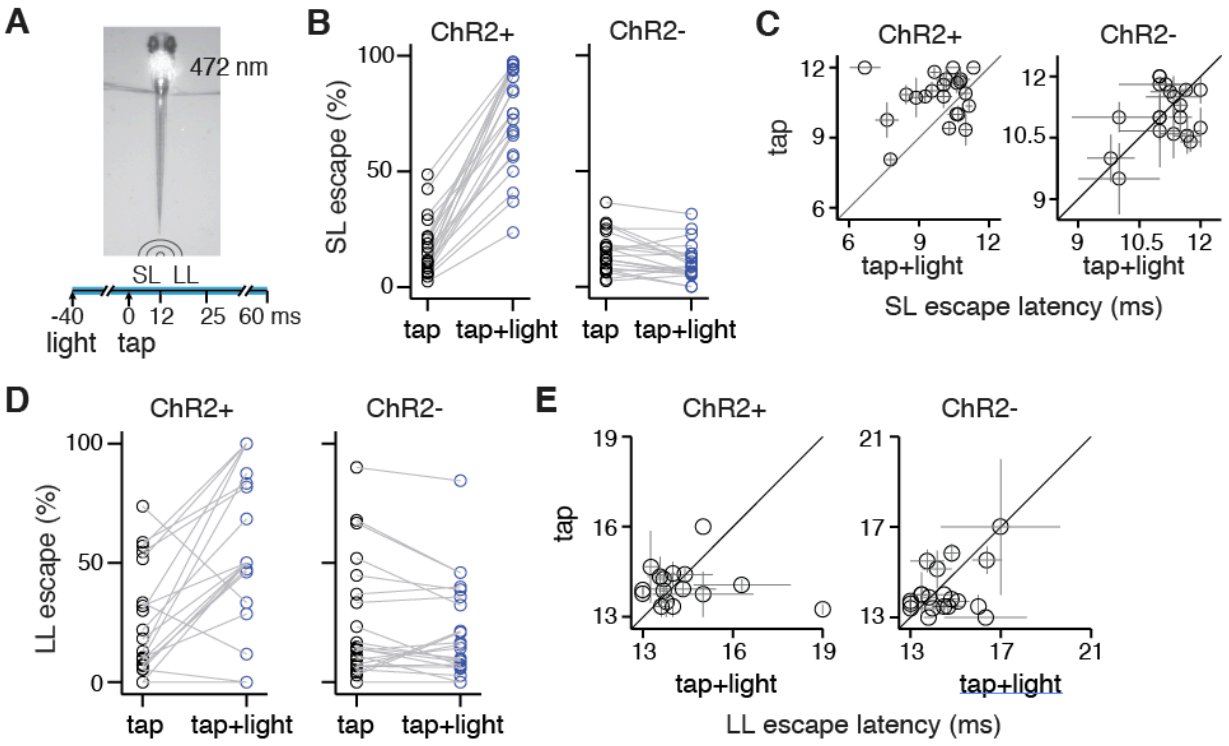

Figure 2.14. Spiral fiber neuron activation enhances the probability and decreases the latency of Mauthner-cell-mediated escapes.

A) 473 nm blue light is shone on the hindbrain of *Tg(-6.7FRhcrtR:gal4VP16); Tg(UAS:ChR2(H134R)-EYFP)* larvae using a focused laser beam for a total of 100 ms. 20-60 ms after the onset of the light, a low-intensity tap is delivered and tail movements are scored for short-latency (SL) or long-latency (LL) escapes. B) % SL escapes for individual fish in response to taps alone (black circles) and taps paired with blue light (blue circles). Left panel: ChR2+ fish (n = 22, 17% ± 4.9% tap, 73.4% ± 4.7% tap + light, mean ± SEM, corresponding to a 4.4 fold enhancement of SL escapes with blue light, $p = 5.6*10^{-12}$). Right panel: ChR2- controls (n = 22, 15% ± 1.9% tap, 11% ± 1.7% tap + light, corresponding to a 1.4 fold decrease of SL escapes with blue light, $p = 6.3*10^{-3}$). C) % LL escapes for individual fish in response to taps alone (black circles) and taps paired with blue light (blue circles). Left panel: ChR2+ fish (n = 22, 23% ± 4.9% tap, 54% ± 7.1% tap + light, mean ± SEM, corresponding to a 2.4 fold enhancement of LL escapes with blue light, $p = 1.1*10^{-4}$). Part of this enhancement could be due to the blue

Figure 2.14 (Continued) light alone eliciting escapes. Right panel: ChR2-controls (n = 22, 25% ± 5.3% tap, 21% ± 4.4% tap + light, p = 0.79). D) LL escape latency in ms in response to taps (y-axis) or taps paired with blue light (x-axis). Left panel: ChR2+ fish (n = 22, 14.2 ± 0.41 tap, 14.3 ± 0.30 ms tap + light, mean ± SEM, p = 0.79). Right panel: ChR2- fish (n = 22, 14.1 ± 0.23 tap, 14.5 ± 0.25 ms tap + light, p = 0.24).

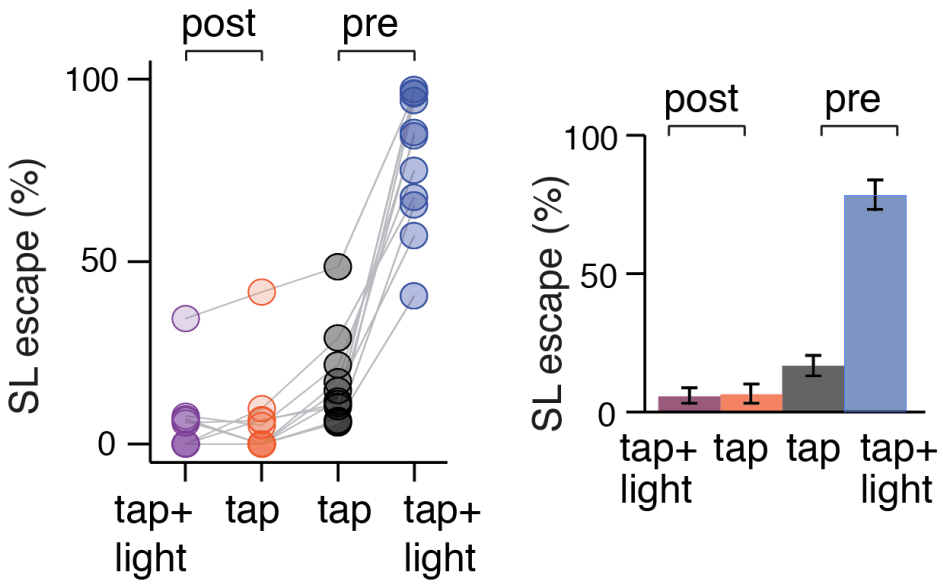

Figure 2.15. Enhancement of short-latency escapes with blue light is abolished after spiral fiber neuron ablations.

% SL escapes in response to taps or taps paired with light before (pre) or after (post) bilateral spiral fiber neuron ablations (n = 11 ChR+ larvae, pre: 17% ± 3.7% tap, 78 ± 5.4% tap + light, mean ± SEM, corresponding to a 4.7-fold enhancement, p = 1.2*10-6; post: 6.3% ± 3.5% tap, 5.6 ± 2.9% tap + light, p = 0.65). The first panel shows individual fish as circles. The second panel shows mean ± SEM of the data in the first panel. Data in the pre condition are a subset of the data in Figure 2.14B.

To determine whether the ChR2-mediated enhancement of short-latency escapes was dependent on spiral fiber neurons, we tested behavior after spiral fiber neuron ablations. Short-latency escapes in response to taps alone were nearly abolished after spiral fiber neuron ablations, confirming our earlier ablation results. Crucially, pairing taps with blue light did not increase the probability of these escapes (Figure 2.15).

Our results suggest that the observed enhancement in M-cell-mediated escapes is caused specifically by activation of spiral fiber neurons with ChR2, although we cannot rule out that the blue excites labeled neurons that connect to the M-cell through spiral fiber neurons.

We next asked whether excitation of spiral fiber neurons alone could evoke escape behaviors. In half of the larvae (11/22), a 100 ms blue light pulse gave rise to escapes with a probability above 10% (Figure 2.16A). Spiral fiber neuron ablations eliminated these escapes in all but one larva where lesions may have been incomplete. The latency from onset of blue light to behavior was long and variable (70 ± 30 ms, mean ± standard deviation, Figure 2.16B), which is not unusual for ChR2-mediated behavior (Douglass et al., 2008; Kubo et al., 2014; Thiele et al., 2014; but see Monesson-Olson et al., 2014). Escape directionality in response to taps paired with blue light and light alone was not correlated, suggesting that spiral fiber neuron excitation was bilateral (Figure 2.16C). Optically induced escapes were kinematically similar to those induced by taps, but the angle of the initial C-bend was lower (Figures 2.16D, E), in agreement

with reports that electrical stimulation of the M-cell alone gives rise to less effective escapes (Nissanov et al., 1990).

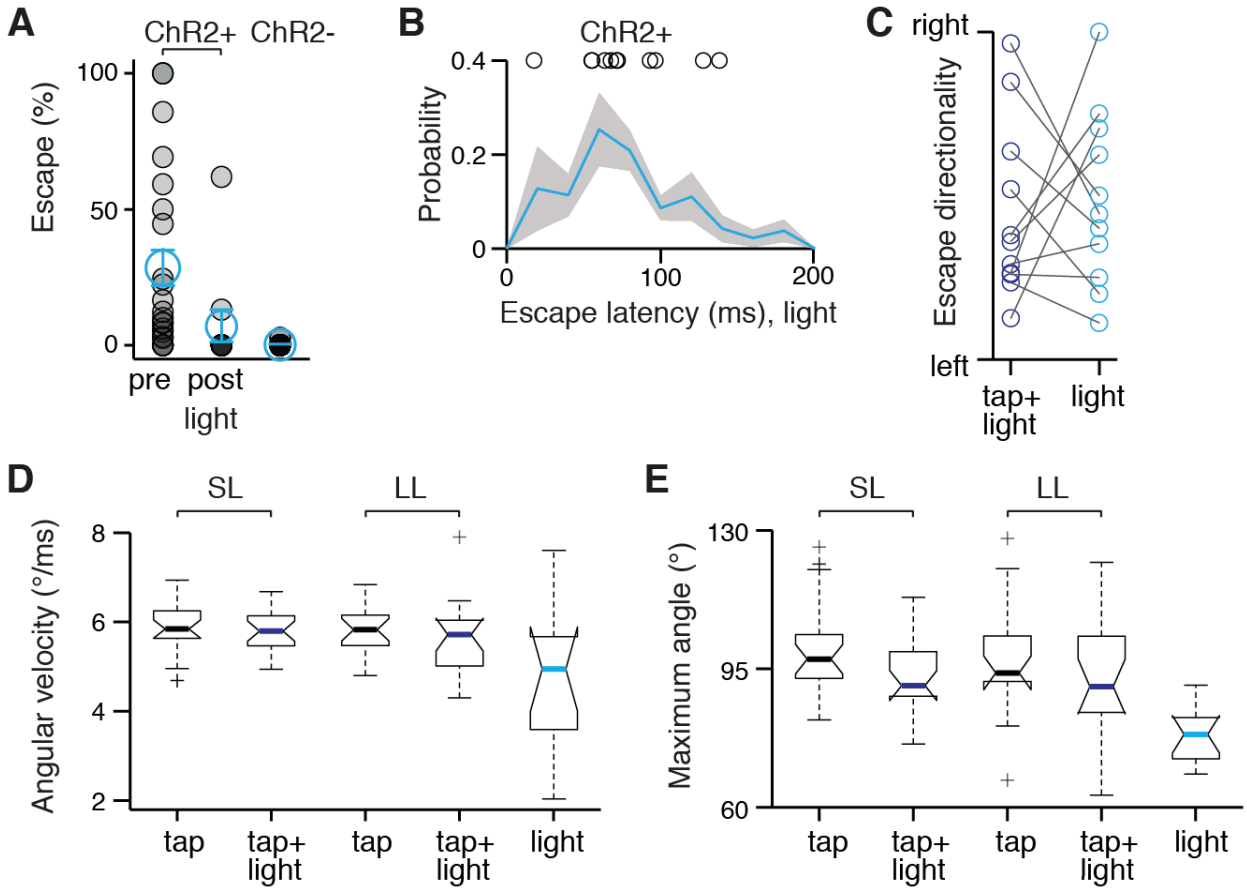

Figure 2.16. Excitation of spiral fiber neurons with ChR2 can elicit escapes.

A) % Escapes for individual fish (black circles, mean ± SEM in blue) in response to blue light alone. ChR2+ fish before (pre) and after (post) spiral fiber neuron ablations (n = 11); ChR2- fish (n = 22). B) Distribution of escape latencies in ChR2+ responding to blue light alone (blue line ± shaded SEM, n = 197 escapes). Circles represent the mean of escape latencies for larvae displaying >10 % probability of escapes (n = 11). C) Escape directionality in response to taps paired with blue light or blue light alone in ChR2+ larvae displaying >10 % probability of escapes to light alone (n = 11). D) Mean angular velocity of the

Figure 2.16 (Continued) initial C-bend in SL or LL escapes in response to taps, taps paired with blue light in ChR2+ larvae (n = 22), or blue light alone in ChR2+ larvae whose response probability to light alone exceeded 10% (n = 11). Horizontal lines are the medians across fish, box edges are the 25th and 75th percentiles, whiskers extend to the most extreme data points not considered outliers, box plots whose notches do not overlap have different medians at the 5% significance level, and crosses are outliers. The light condition is significantly different from the other 4 conditions. Other comparisons are not significant (multiple comparisons test after ANOVA, $\alpha = 0.05$). E) Mean maximum angle of the initial C-bend in SL or LL escapes in response to taps, taps paired with blue light in ChR2+ larvae (n = 22), or blue light alone in ChR2+ larvae whose response probability to light alone exceeded 10% (n = 11). The light condition is significantly different from the other 4 conditions. Other comparisons are not significant.

Due to variable sensitivities, individual larvae were tested with different tap strengths to elicit 5-50% short-latency escapes at baseline. An interesting possibility is that the effectiveness of ChR2-mediated excitation might be related to the inherent excitability of the M-cell circuit. This was not the case: sensitivity to taps did not correlate with enhancement of short-latency escapes (Figure 2.17). In contrast, the effectiveness of blue light correlated with escape latency across fish (Figure 2.17) and likely reflects ChR2 expression level. Together, our optogenetic results demonstrate that exciting the spiral fiber neurons strongly potentiates M-cell-mediated behavior.

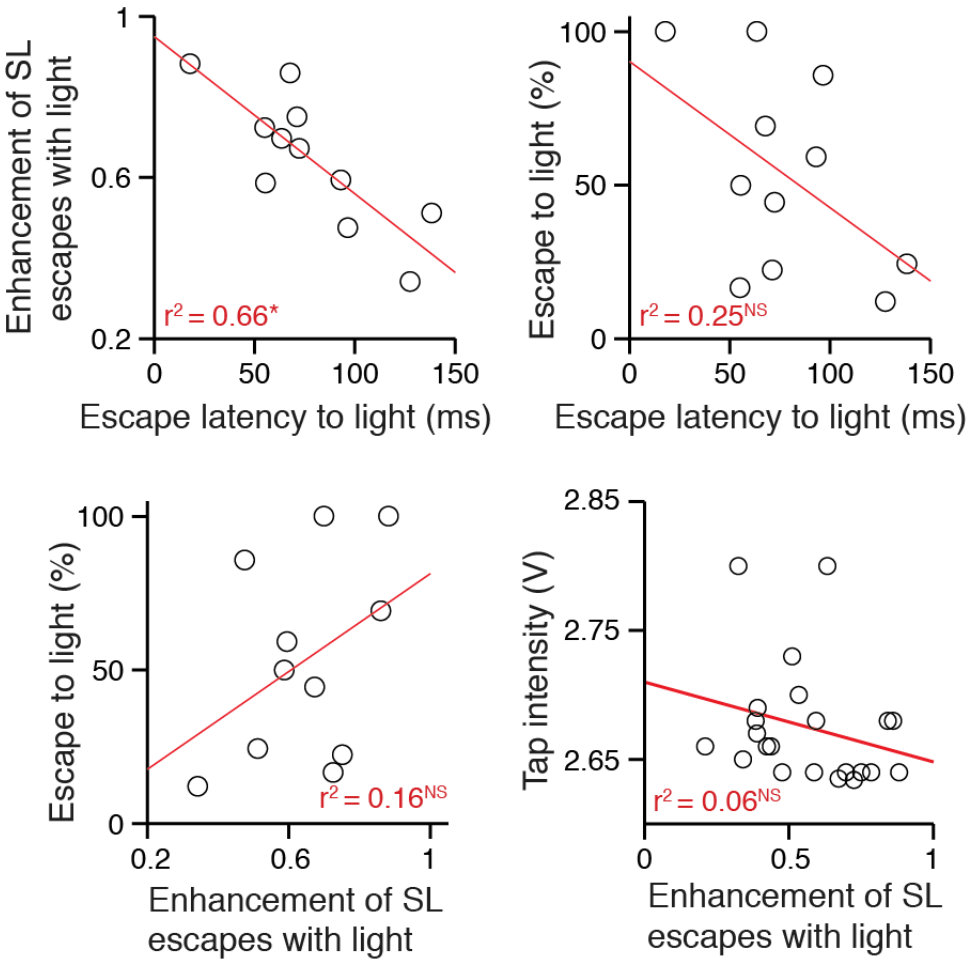

Figure 2.17. ChR2 effectiveness correlates with escape latency. Correlation between escape latency in response to blue light, enhancement in the probability of SL escapes when taps are paired with blue light (probability of SL escapes to tap+light - probability of SL escapes to tap), probability of escapes to blue light, and the tap intensity used to elicit escapes. ChR2+ larvae that showed >10% probability of escapes to blue light are represented as circles (11/22 tested) for the first 3 plots; all 22 larvae are represented on the last plot. A caveat of the tap intensity measure is that the voltage used to drive the solenoid tapper is not linearly proportional to the intensity of the disturbance caused by the tap. r^2 values represent the goodness of fit from linear regression (red line). * denotes $p < 0.05$; NS: $p > 0.05$ comparing F-statistics and constant model.

2.5 DISCUSSION

Our study unveils a functional pathway by which sensory information is indirectly conveyed to the escape circuit: spiral fiber neurons respond to aversive cues and excite the M-cell at the axon cap. We provide three lines of evidence that support the notion that spiral fiber neurons are essential for M-cell-mediated escapes: (1) like M-cell ablations, bilateral spiral fiber neuron ablations nearly abolish short-latency escapes; (2) ablating spiral fiber neurons unilaterally shift the directionality of escapes, suggesting that without spiral fiber neuron input, M-cell activity is compromised; (3) optically activating the spiral fiber neurons strongly enhances M-cell-mediated escapes in response to subthreshold stimuli. In the following sections, we relate our data to previous electrophysiological studies of the M-cell, discuss the utility of a spatially and temporally distinct convergent pathway, and describe how convergent pathways may be a widespread motif in neural circuits.

2.5.1 Two spatially and temporally distinct sources of excitation converge on the Mauthner cell

Previous electrophysiological recordings in the goldfish have identified an input of unknown origin onto the M-cell. Our findings suggest that this input has the characteristics of spiral fiber neuron excitation. In response to natural sounds, M-cell activity is composed of spatially and temporally distinct components: fast

repetitive EPSPs are superimposed on an underlying slower depolarization (Szabo et al., 2006). Auditory/vestibular afferents making mixed electrical and chemical synapses on the M-cell lateral dendrites (Nakajima, 1974; Tuttle et al., 1986; Lin and Faber, 1988b) are responsible for the fast component of the M-cell response and for part of the slower component (Szabo et al., 2006). The slower component also relies on electrical and glutamatergic input near the soma (Szabo et al., 2006), but the origin of this input is unknown. Spiral fiber neurons make both electrical and glutamatergic synapses close to the M-cell soma (Koyama et al., 2011) and we find that they are active in response to sensory stimuli. This suggest that they are the origin of the secondary, slower component of the M-cell response, which was observed approximately 3 ms after the onset of the fast component. A 3 ms delay places this slower input within the M-cell's integration window: in response to auditory stimuli, initial depolarization in the goldfish M-cell occurs within 1 ms, but firing occurs from 3-12 ms (Zottoli, 1977; Eaton and Lavender, 1981; Weiss et al., 2006). Thus, in response to auditory/vibrational stimuli, excitatory inputs to the M-cell converge from two temporally and spatially distinct sources: distal sensory afferents provide rapid electrical and slower chemical input, and spiral fiber neurons provide a slow proximal input.

2.5.2 Spiral fiber neuron input is integrated with dendritic afferents at the Mauthner cell axon hillock

The combined anatomical, electrophysiological, ablation, and calcium imaging data support a model wherein spiral fiber neuron and afferent inputs are integrated at the level of the M-cell axon hillock. Others have found that large amplitude calcium activity in the M-cell is correlated with short-latency escapes, and similar to calcium activity elicited by antidromic action potentials (Kohashi and Oda, 2008). Our results suggest that without spiral fiber neuron input, the M-cell's ability to fire is compromised. One might ask, then, why the loss of spiral fiber neuron input did not decrease calcium levels in the M-cell soma. Differences between our study and published reports may explain this apparent inconsistency. First, while others mainly observe all or none calcium events in the M-cells that are thought to indicate firing events (O'Malley et al., 1996; Kohashi and Oda, 2008; Satou et al., 2009; Kohashi et al., 2012), our recordings show graded responses (see Figure A.2 of the Appendix). This difference may be due to the type of calcium indicator or the type of stimulus used. Second, studies using unilateral stimuli report that only one M-cell is active at a time (O'Malley et al., 1996; Kohashi and Oda, 2008; Kohashi et al., 2012). In contrast, we observe concurrent activity in the M-cells (Figure 2.13D). This is consistent with a study by Satou and colleagues (2009) where the M-cells were coactive 55% of the time in response to non-directional stimuli. Their data suggest that in these cases, both M-cells fire, but with a delay, and that the excitatory effects of the trailing spikes are shunted by commissural inhibitory neurons in the spinal cord.

However, the authors observe a higher probability of co-activity in the M-cells by calcium imaging compared to what was inferred from behavioral analysis (55% vs. 30%). Therefore, the calcium transients observed may not be accurate predictors of action potentials. Instead, they may primarily reflect sensory input rather than output. It is conceivable that the strong excitatory drive generated by auditory/vestibular afferents can saturate the slow-kinetic calcium indicator in the M-cell soma, and mask the potential effect of backpropagating depolarization. In our ablation experiments, direct sensory input is intact and may dominate measurable somatic calcium entry in the M-cell. Thus, our results imply that dendritic afferents elicit the bulk of calcium entry into the M-cell soma and that spiral fiber neuron actions are primarily restricted to the axon hillock. Since M-cell-mediated behavior is impaired in the absence of spiral fiber neurons, it suggests that spiral fiber neuron and dendritic inputs are integrated not in the M-cell soma but rather at the level of the M-cell axon hillock, the site of action potential initiation (Furshpan and Furukawa, 1962).

2.5.3 Spiral fiber neurons represent a convergent input that enhances circuit robustness

Short-latency escapes, which are triggered by a single firing event in the M-cell, are vital to avoid predation but should be restricted to legitimate threats. Therefore, the M-cell must be reliably activated when necessary and otherwise appropriately gated. The robust activation of the M-cell is faced with three

hurdles: first, due to a low input resistance, short time constant, and hyperpolarized membrane potential, the M-cell requires strong currents to reach firing threshold (Curti and Pereda, 2010); second, feedforward interneurons inhibit the M-cell (Zottoli and Faber, 1980; Faber et al., 1989), and third, dendritic excitation is strongly attenuated by the time it reaches the soma due to passive cable properties (up to 4-fold in the adult goldfish M-cell (Szabo et al., 2006)). By providing an excitatory drive directly at the axon hillock, the site of action potential generation (Furshpan and Furukawa, 1962), spiral fiber neurons solve the challenge of overcoming the M-cell's high activation barrier. An additional challenge in the circuit is to ensure that the M-cell is not activated by innocuous short-lived sounds. Spiral fiber neurons introduce a delay line that may prevent unnecessary firing of the M-cell: transient depolarization of the M-cell by dendritic afferents would end before the necessary spiral fiber neuron input arrives at the axon hillock, precluding integration of the two pathways and rendering brief sensory input ineffective. Thus, in the M-cell escape circuit, indirect proximal input provides a necessary excitatory drive undiminished by distance and can serve as a mechanism to filter noise. Experiments combining stimulation of the two pathways and recordings in the M-cell are needed to directly test these scenarios.

2.5.4 Indirect excitatory pathways as a circuit motif

The spiral fiber neuron input is the first example of a necessary indirect pathway in a startle circuit. A diverse set of other circuits present anatomical similarities, where multiple, sometimes temporally and spatially segregated excitatory pathways converge. The interaction of inputs in these networks is poised to enhance the controllability and flexibility of the system. A first example is the crayfish escape network, in which tactile afferents project to command neurons and also to excitatory interneurons that then feed forward to the command neurons. The amplitude of excitation elicited by the interneurons is larger than the excitation coming from direct tactile afferents (Zucker, 1972), suggesting that like spiral fiber neurons in the M-cell circuit, these crayfish interneurons might be essential for producing escapes. Another example is the mammalian hippocampus where CA1 pyramidal neurons receive sensory information via a direct and an indirect pathway. One path inputs monosynaptically onto the neurons' distal dendrites, but has a weak influence over somatic voltage. A slower trisynaptic pathway projecting to the proximal dendrites provides a stronger input (Dudman et al., 2007). Thus, similarly to spiral fiber neuron inputs in the M-cell circuit, the indirect pathway to CA1 introduces a powerful delay line that is more proximal. These examples of comparable circuitry in invertebrates and mammals suggest that the necessity of convergent excitatory pathways might be a general motif of neural circuits.

2.6 EXPERIMENTAL PROCEDURES

Zebrafish care and strains

All protocols and procedures involving zebrafish were approved by the Harvard University/Faculty of Arts & Sciences Standing Committee on the Use of Animals in Research and Teaching (IACUC). Larvae were raised at 28.5°C on a standard 14/10 hour light/dark cycle at a density of 20-50 fish in 10 cm diameter petri dishes filled with 25-40 mL buffered E3 (1mM HEPES added). *Mitfa-/-* mutants that lack melanophores were used for all ablation and calcium imaging experiments.

Generation of transgenic fish

Tg(-6.7FRhcrtR:gal4VP16): -6.7FRhcrtR was amplified using a nested PCR strategy. First, a 6775bp DNA fragment immediately upstream of the *Fugu rubripes hcrtr2* start site was amplified from genomic DNA, using a high-fidelity polymerase (PfuUltra II Fusion, Stratagene) with primers

5'-AATCCAAATTCCCAGTGACG-3' and 5'- CCAGATACTCGGCAAACAAA-3', 56° C annealing temperature, 1:45 elongation time. The PCR product was TOPO cloned into a TA vector (Life Technologies). Using the resulting plasmid as a template, a 6732bp fragment was amplified using primers 5'-AATCCAAATTCCCAGTGACG-3' and 5'-CCAGATACTCGGCAAACAAA-3', 55°C annealing temperature, 1:45 elongation and similarly TOPO cloned into a

GATEWAY-compatible vector (PCR8/GW, Life Technologies). The resulting entry vector was recombined into a destination vector upstream of gal4-VP16, between Tol2 integration arms [S9]. *Tg(UAS-E1b:Kaede)s1999t* embryos were injected at the one-cell stage with 0.5nL of 50ng/uL plasmid and 35ng/uL *Tol2 transposase* mRNA in water, and their progeny screened for fluorescence. One founder produced three fluorescent progeny; one survived. To identify transgenic fish without using a UAS reporter, potential carriers were genotyped using the following primers to generate a 592bp product spanning the upstream Tol2 arm and the start of the *Fugu* sequence: 5'- CAATCCTGCAGTGCTGAAAA-3' and 5'-TGATTCATCGTGGCACAAAT-3' 57°C annealing temperature, 0:30 elongation time.

Tg(-6.7FRhcrtR:gal4VP16) labels distributed cells in rhomomeres 2-7 of the hindbrain, including neurons in the tangential and medial vestibular nuclei, and other octavolateral nuclei. There are distributed cells in the spinal cord including the commissural primary ascending (CoPA) neurons. Dispersed cells are visible in the anterior and posterior lateral line, statoacoustic and trigeminal ganglia. In the hypothalamus, the line labels a cluster of cells that do not overlap with oxytocin, hypocretin or QRFP positive cells. Sparse labeling is detected in the habenula and midbrain tegmentum. Skin and notochord cells are also labeled.

Tg(14xUAS-E1b:hChR2(H134R)-EYFP): hChR2(H134R)-EYFP was subcloned downstream of 14 copies of a UAS element and an E1b minimal promoter in a vector containing an SV40 polyA sequence and Tol2 recognition arms. This vector was co-injected with *tol2 transposase* mRNA into TLAB embryos at the

single cell stage. Potential founders were screened by crossing to *Tg(isl1:Gal4-VP16,14xUAS:Kaede)* and monitoring tail movements in response to blue light from an arc lamp on a stereomicroscope (Leica MZ16) at 30 hours post-fertilization.

Tg(UAS:GCaMP5) was generated by LR recombination of a 14xUAS fragment upstream of *GCaMP5G* and between Tol2 recognition arms, using custom Gateway-compatible entry and destination vectors (Life Technologies). 30 ng/uL of this vector was injected with Tol2 RNA into WIK embryos at the one-cell stage. Potential founders were screened by crossing to *Tg(-6.7FRhcrtR:gal4VP16)*.

The following transgenic lines were used: *Tg(UAS:Kaede)* (Hatta et al., 2006), *Tg(UAS:GCaMP-HS)* (Muto et al., 2011), and *Et(fos:Gal4-VP16)s1181t* (Scott and Baier, 2009).

Monitoring neural activity by calcium imaging

Calcium imaging was performed with a custom two-photon microscope equipped with a 0.95 NA 20X (Olympus) controlled by custom software written in C# (Microsoft). Z drift was actively compensated by comparing each scanned image to an anatomical reference stack collected immediately prior to imaging. Each newly scanned image was cross correlated in three dimensions with the reference stack using Intel Performance Primitives (IPP) and C#. The lateral search size was ±10 μm and the axial search size was ±5 μm (11 image slices of

the reference stack). The depth of the best z slice was low pass filtered and kept within 1 µm of the original focal plane by adjusting the objective height in 1 µm increments. Images were acquired at either 4 or 8 frames a second.

For imaging, 5-6 days post-fertilization (dpf) larvae were paralyzed by soaking in a ~50 µL droplet of 125 mM alpha-bungarotoxin (VWR, 89138-082) for 2 minutes. Fish were then rinsed in E3 and embedded in 2% low-melting point agarose (AquaPor LM, EC-204, National Diagnostics) in E3 for imaging. Neurons were labeled with the genetically-encoded calcium indicators GCaMP-HS (*Tg(UAS:GCaMP-HS*)) for experiments described in Figures 2.2, 2.3 and 2.4 and with GCaMP5 (*Tg(UAS:GCaMP5*)) for experiments in Figure 2.13.

Three different types of stimuli were used. Water puffs were delivered through a pipette (either a custom pulled glass pipette of ~0.3 mm inner diameter (IB120F-4, World Precision Instrument) or a blunt tip needle 25G 1½" (Jorgensen Laboratories) delivered ~0.5 mm away from the otic vesicle or the middle of the tail, where a small area was freed of agarose. The strength of the pulse varied from 10 to 40 PSI, with 5-15 ms duration, and was adjusted to obtain a high probability of reliable response without damaging the tissue. Tap stimuli were delivered to the dish holding the larva via a push type solenoid (28-I-12D, Allied Electronics) working with a spring system. Fish whose probability of response was low or sharply decreased as the experiment progressed were excluded from the analysis (~15%).

Analysis of calcium signals was done in Matlab (Mathworks, Natick MA). Individual images were first registered in x-y with reference to the first image of an experiment. Regions of interest (ROIs) corresponding to individual neurons or the axon cap were manually drawn. Calcium imaging data is reported as Δf/f = (fluorescence over a selected ROI - baseline fluorescence of ROI) / (baseline fluorescence - background fluorescence). Trials for which an ROI showed activity above baseline after the stimulus were scored automatically by the analysis code as response trials and then manually verified.

For experiments combining calcium imaging in the M-cell with laser ablations of spiral fiber neurons, larvae were paralyzed with alpha-bungarotoxin. To ensure that the toxin did not influence our experimental outcomes, non-paralyzed fish were also tested. No differences in calcium dynamics were observed, and the outcome of the ablations was similar. Post imaging was done starting 10-20 minutes after ablations. Pilot experiments indicated that there was no difference in our results if this interval was prolonged.

High-speed behavioral analysis

A custom-built high-speed video tracking apparatus and custom software written in C# was used to monitor and quantify escape responses to tap stimuli. It consisted of a camera (Pike F-032, Allied Vision Technologies) and variable lens (1:3.9 75 mm, 25.5 mm, Tamron) run at 1000 frames/second by binning pixels, resulting in 104 x 56 images. Larval zebrafish tails were illuminated with IR light.

Taps of three different intensities were delivered to the dish holder on which the larva was placed in the same manner as in the calcium imaging experiments. A stimulus interval of 20 seconds was used, with which no habituation was observed. The software sent a 250 ms pulse of varying voltage to the solenoid to deliver taps. Because different voltages gave rise to varying stimulus timing, actual tap timing was monitored using a small piezo element (Sparkfun Electronics SEN-10293) mounted close to the solenoid. Due to the non-directional nature of the stimulus, escapes occurred in either direction. The software tracked tail position online using five equidistant points positioned on the tail. Analysis of tail segment angles was done offline with custom-written scripts in Matlab. Tail angles reported correspond to the angle of the last tail segment with respect to the vertical. Response latency was defined as the interval between the tap and the first frame at which a tail movement was detected. Tail traces were smoothed using a Butterworth filter (4^{th} order, cutoff = 0.15 Hz). Scripts automatically detected responses and classified them as escapes or non-escapes and detected escape latency. All classifications were then manually verified. Escapes were defined as responses beginning with a turn exceeding 60 degrees in amplitude in the first 25 ms after the stimulus.

To test behavior, 5-7 dpf fish were embedded in 2% low-melting point agarose on a 35 mm diameter petri dish lid, and a scalpel was used to free the tail. A glass cover slip (Gold Seal cover glass, 48x60 mm No.1) was secured with high vacuum grease (Dow Corning) on top of the dish to make a tight water seal and prevent shadows caused by water vibrations. Larvae were allowed to acclimate

for at least 30 minutes and then tested individually in the behavioral apparatus for 20 minutes in the dark. Fish were stimulated with alternating tap intensities and only the strongest tap stimulus was used for the analysis because it elicited the greatest number of escapes. Individual fish whose initial probability of fast escapes averaged over all tap intensities was below 50% were unhealthy and discarded from the analysis (~10% of fish).

Homozygous *mariner* mutants (Nicolson et al., 1998) deficient in hair cell mechanotransduction (Ernest et al., 2000) were screened based on their lack of a swim bladder, their lying on their side, and their circling movements in response to touch at 4 dpf. Neomycin (neomycin sulfate, Invitrogen 21810-031) treatment was used to kill lateral line neuromasts (Harris et al., 2003). A 50 mM stock solution in E3 was stored at 4°C and diluted 1:100 to use at a final concentration of 500 μM. Larvae were allowed to swim in this solution for 20 minutes and then washed 3 times in E3. Behavioral tests were done no later than 2 hours after treatment to avoid regeneration of neuromasts. Loss of neuromasts was verified on non-tested fish by staining with 2.6 mM DASPEI (2-(4-(dimethylamino)styryl)-N-Ethylpyridinium Iodide, Invitrogen D-426) for 20 minutes (Harris et al., 2003).

Experiments involving neuron ablations were done in one day. Baseline responses were recorded in the morning. Larvae were subsequently anesthetized (0.016% w/v tricaine methane sulfonate, Sigma A5040) and placed under a two-photon microscope for neuronal ablations. After the ablation procedure lasting 5-20 minutes, the anesthetic solution was replaced with E3 and

larvae were allowed to recover for at least 4 hours and no more than 10 hours before testing their behavior post-ablation.

Laser ablation of neurons

A pulsed two-photon laser was used to ablate specific cells in the M-cell circuit. Laser pulses were focused with a 0.95 NA 20X objective (Olympus) and generated from a Ti:Sapphire system (Spectra Physics MaiTai HP) operating at a 80 MHz repetition-rate with a 80 fs pulse duration. Two methods were used alternatively to achieve neuronal ablation. In one method, the laser was scanned in a spiral pattern over a small area of a selected cell with increasing power (Orger et al., 2008). When brief flashes of high intensity were detected by the software, scanning was automatically stopped. These flashes are thought to arise from absorption of multi-photon energy by water molecules, creating plasma and killing the cell (Vogel and Venugopalan, 2003). An alternative method consisted in sending a single high-power and brief (20-100 ms) pulse. We used a maximum power at sample of 200 mW (820 nm) measured with a power meter (ThorLabs S130C). In most cases, brief flashes of high intensity were observed at the PMT, suggesting plasma formation.

We used different indicators in neurons for ablations: UAS driving *ChR2*, *GCaMP-HS*, *GCaMP5* or *Kaede*. Neurons were targeted based on anatomy and were ablated starting with the ventral-most neurons. For M-cell ablations, two locations on the soma were targeted to prevent the cell from recovering. The

number of labeled spiral fiber neurons varied by fish between 6-10 cells on each side. All labeled neurons were targeted, however, it is possible that some ablations were unsuccessful, given the tight packing of cells. Deeper spiral fiber neurons were more challenging to ablate, and sometimes required several attempts with increasing laser pulse lengths. For control ablations, we ablated neurons labeled in the *Tg(-6.7FRhcrtR:gal4VP16)* with no apparent connections to the escape circuit and located 20-40 μm rostral and no more than 10 μm away dorsally or ventrally from spiral fiber neuron somata, consisting of 2-6 neurons on each side. Brains were imaged immediately and usually 24 hours after ablation to evaluate the specificity and extent of lesions.

ChR2 stimulation

A 473 nm diode pumped solid state blue laser (DPSSL-473-10, Roithner LaserTechnik) was used to excite ChR2 in heterozygote *Tg(-6.7FRhcrtR:gal4VP16); Tg(UAS:ChR2(H134R)-EYFP)* larvae. The laser beam was focused with a lens on the larva's head to a spot size of approximately 250 μm in diameter with 13 mW power over the sample. 5-7 dpf larvae were embedded in agarose and their tail freed. Escape behavior was then tested in the behavioral apparatus described above, and the tap intensity was optimized for each fish in order to obtain a 5-50% probability of short-latency escapes. Approximately 30 trials were used for each of the following three conditions: 1) low-intensity taps delivered on their own, 2) the same taps paired with a 100 ms

blue light pulse delivered 20-60 ms before the taps, and 3) 100 ms light pulses delivered alone. Latency was computed as the time between the onset of the tap and the first movement of the tail, or in the case of the blue light only, from the onset of the light pulse. The delay used between the light and tap in condition 2) was increased if a 20 ms delay did not result in an enhancement of short-latency escapes. For 10/22 ChR2+ larvae, the delay was 20 ms. The mean latency of escapes to blue light only across these fish was 63 ms (± 25 ms standard deviation). For 11/22 fish, the delay was 60 ms and the mean latency of escapes to blue light only across the 7 fish that responded was 92 ms ± 35 ms. One fish was tested with a 40 ms delay and produced escapes with an average latency of 72 ms. Since short-latency escapes occur within 12 ms of the tap, this implies that the escapes assigned as short-latency in condition 2) were generally not caused by the blue alone but by the combination of light and tap. It is possible that a subset of long-latency escapes, however, are an effect of the light only stimulus, which could account for the higher probability of long-latency escapes in condition 2). The delays used for condition 2) in control ChR2- siblings matched in number those used for ChR2+ larvae.

Ablations of spiral fiber neurons were carried out as described above. Larvae were allowed 4-6 hours to recover from the anesthetic before testing post ablation behavior.

Sparse neuron labeling

To label a small number of spiral fiber neurons, 0.5 nL of 30 ng/μL of plasmid encoding GFP with an N-terminal GAP43 membrane localization sequence (Bianco et al., 2012) dissolved in water was injected at the one-cell stage into *Tg(-6.7FRhcrtR:gal4VP16)* fish. Embryos were screened under a fluorescent stereoscope (Leica MZ16) with a GFP emission filter. ~10% of embryos had sparse labeling of neurons in the nervous system. The other ~90% either showed no expression or broad expression. Individual spiral fiber neurons were identified by florescence at 72 hours post fertilization.

Retrograde labeling of reticulospinal neurons

To label the reticulospinal system including the M-cells, we backfilled neurons from the spinal cord. 5 dpf larvae were anesthetized and placed on a dish filled with solidified 5% agarose. Excess water surrounding the fish was removed with a paper wipe, so that the fish was stable. A scalpel was used to sever the spinal cord just caudal of the swim bladder. A sharpened tungsten needle was dipped in a drop of ~40 mM tetramethylrhodamine dextran (Life Technologies, D-3308) whose consistency was adjusted with water to make a gel-like substance. The needle was then placed onto the cut in the spinal cord. Larvae were immediately transferred to E3 and allowed to recover for two hours, while the die filled the reticulospinal system. Their brains were then imaged with a Zeiss LSM 780 NLO microscope used as a confocal.

Statistics

The Jarque-Bera test was first performed to examine the normality assumption of data. For normal data, a Student's t-test was used to compare samples. For non-normal data, significance was determined using the Wilcoxon signed rank test for paired data and Wilcoxon rank sum test for independent samples. All data are reported as mean ± standard error of the mean.

2.7 ACKNOWLEDGMENTS

We thank Adam Douglass and Jared Wortzman for generating the *Tg(UAS:GCaMP5)* fish, Koichi Kawakami for the *Tg(UAS:GCaMP-HS)* line, Herwig Baier for the *Et(fos:Gal4-VP16)s1181t* line, Joel Greenwood and Edward Soucy for technical support with the behavioral apparatus, Steve Zimmerman, Karen Hurley, and Jessica Miller for fish care, Misha Ahrens, Timothy Dunn, Joseph Fetcho, Minoru Koyama, Florian Merkle, Iris Odstril, Yuchin Pan, Carlos Pantoja, Constance Richter, Kristen Severi, and additional members of the Engert and Schier labs for many helpful discussions.

CHAPTER 3.

Conclusions And Prospects

I discovered that in the Mauthner cell (M-cell) circuit, spiral fiber interneurons form a convergent pathway that is crucial for eliciting escapes. Such a feedfoward excitatory motif may be present in other circuits controlling behavior in a diversity of species. In the specialized M-cell escape network, I propose that there may be two functions for an essential feedforward input: First, due to biophysical properties of the M-cell and of its distal primary sensory afferents, direct dendritic input may not be sufficient on its own to elicit M-cell firing. By synapsing at the axon hillock, the site of action potential initiation, spiral fiber neurons complement dendritic input to produce M-cell-mediated escapes reliability. Second, spiral fiber neurons form an indirect pathway that may help to filter innocuous stimuli. This pathway relays sensory input via multiple synapses, slowing down the signal. Short-lived sounds might reach the M-cell axon hillock through the dendritic pathway first, and then through the indirect pathway. This timing delay would preclude the integration of short-lived inputs, effectively preventing the M-cell to produce escapes in response to harmless stimuli.

These findings raise interesting questions and open the path for future studies: What are the sensory inputs to spiral fiber neurons? How are spiral fiber neurons modulated to affect M-cell activity and behavior? Do spiral fiber neurons play a role in multisensory integration?

3.1 Spiral fiber neuron inputs

My work establishes that spiral fiber neurons are sensitive to a variety of sensory stimuli that can elicit the escape response. How do spiral fiber neurons receive sensory information? Which sensory receptors contribute to their response? To answer these questions, we can use viral tracing studies to determine anatomy, and optogenetic or electrical stimulation experiments to understand the nature of functional connections.

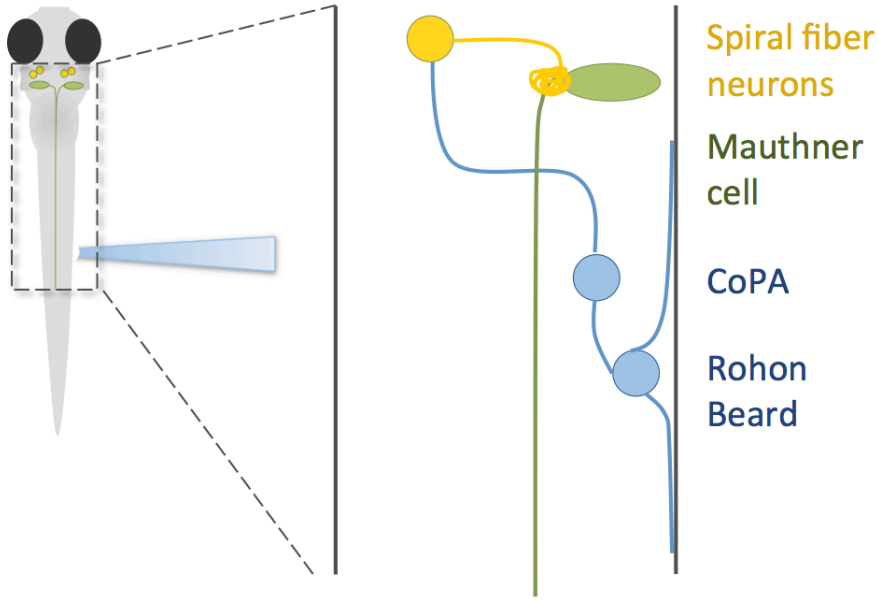

Figure 3.1. Putative pathway for tactile information to be transmitted from the tail to the Mauthner cells.

Rohon-Beard neurons are depolarized in response to touch on the tail. They project to commissural primary ascending interneurons (CoPAs), which cross the midline and synapse on the spiral fiber neurons. Sensory information crosses the midline again through the spiral fiber neuron axons to reach the M-cell and preserve the correct laterality of the escape behavior.

Spiral fiber neuron axons cross the midline to project to the contralateral M-cell. I found that they respond to sensory information originating from the contralateral side, consistent with the laterality of the escapes they modulate (Chapter 2). The design of this circuit is peculiar: sensory information in the spiral fiber neuron pathway crosses the midline twice. Is there a functional significance to this double crossing? One possibility is that sensory information of certain modalities thought to cross the midline reaches the M-cell through ipsilateral projections to the spiral fiber neurons. Tactile stimuli directed at the fish's tail activate ipsilateral Rohon-Beard neurons. Paired patch clamp recordings in the Fetcho lab (Minoru Koyama, personal communication) indicate that these sensory neurons project to commissural primary ascending interneurons (CoPAs), which cross the midline and ascend to excite spiral fiber neurons (Figure 3.1). This putative multisynaptic input may explain why escape responses to tail touch occur at a longer latency compared to responses to head touch and auditory/vestibular stimuli. In this pathway, the spiral fiber neurons' contralateral projections preserve the laterality of the circuit so that animals escape away from threats. Similarly, it is conceivable that visual input from the retina, which is known to cross the midline through the optic nerve, may project to spiral fiber neurons.

To map sensory input to the spiral fiber neurons, viral tracing studies are ideal (Luo et al., 2008). Viral methods are actively being developed in the zebrafish. Zhu and colleagues (2009) successfully used a modified Rabies virus as a retrograde neuronal tracer. By injecting the virus into the dorsal posterior telencephalon, a target of the olfactory bulb, they observed labeled cells in the

olfactory bulb. To label neurons that project to the spiral fiber neurons, one could use modified viruses that pass synapses in the retrograde direction (Figure 3.2).

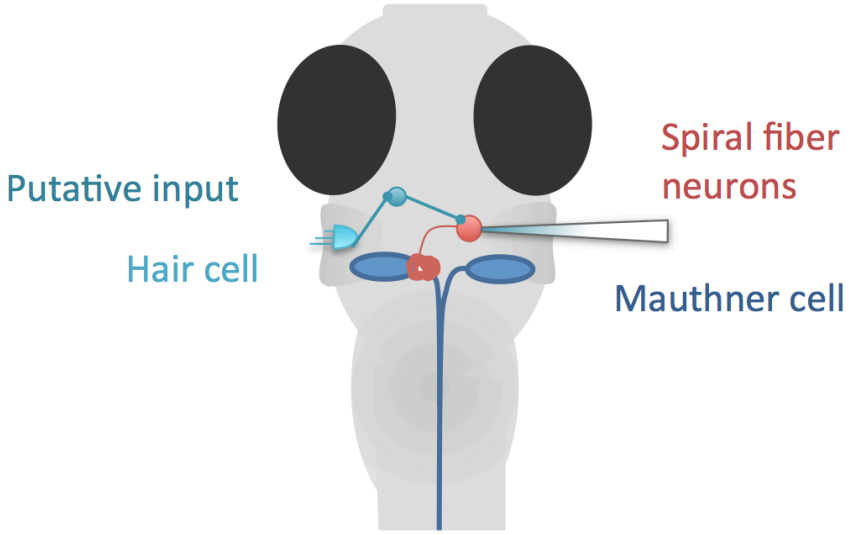

Figure 3.2. Viral tracing strategy to label spiral fiber neuron inputs.

Injecting retrograde viruses containing genes for fluorescent proteins such as modified Rabies or VSV viruses (blue pipette) near the spiral fiber neuron dendrites (red cell) can label spiral fiber neuron afferents (blue cell). If polysynaptic viruses are used, one may label sensory afferents such as the hair cells of the ear (blue cell on the left). The placement of the putative spiral fiber neuron afferent cell is for illustration purposes only.

Rabies and VSV viruses can be made to pass through one or multiple synapses. Using these techniques, it would be interesting to find out how many synapses exist between sensory neurons and the spiral fiber neurons. Alternatively or in conjunction with viral tracing techniques, electron microscopy could be used to find upstream inputs.

Spiral fiber neurons may also receive a variety of non-sensory inputs that modulate their excitability. As I will discuss in the next section and in Appendix A2.2, they may receive information about the arousal state of the animal through neurons producing the neuropeptide hypocretin. Neuropeptide signaling, however, does not require synapses, and spiral fiber neurons may be sensitive to neuromodulators without direct connections.

3.2 Convergent pathways can enhance circuit flexibility

Neural circuits that modulate behavior benefit from flexibility. Rarely is it advantageous for behaviors to be fully fixed. Rather, environmental and internal states have been shown to play a role. For example, in a visuo-motor pathway in *Drosophila*, a group of neurons shows amplified responses to visual motion when flies are walking rather than at rest (Chiappe et al., 2010). Such modulation of visual acuity may aid in processing image speed depending on the motor state of the animal.

Few studies have investigated how escape circuits are modulated by behavioral or internal states. It has been shown that zebrafish are more likely to escape to an aversive stimulus when the animal is in motion (Burgess and Granato, 2007), but the physiological basis of this modulation is not known. Presumably, there is

a feedback pathway from motor neurons or proprioceptive neurons in the spinal cord. Exactly where this modulation takes place is an interesting question.

In the case of the M-cell circuit, if one considers the sensory dendritic pathway on its own, the possibility for modulation is limited. Sensory receptors such as hair cells project to the VIIIth nerve, which synapses directly onto the M-cell lateral dendrite. In this monosynaptic circuit scenario, changing the sensitivity of the system requires modulating either the activity of the primary sensory neurons, or the synapses between the VIIIth nerve and the M-cell. Modifying the excitability of hair cells is not optimal because it would influence other neurons that are sensitive to sounds. To modulate the M-cell circuit specifically, it is preferable to change the excitability of neurons that project solely to the circuit. Since spiral fiber neurons' only apparent target is the M-cell, the indirect and convergent pathway they constitute is well placed to be a site of modulation for the M-cell-mediated escape behavior.

Generally, parallel pathways have the advantage of increasing the capacity for modulation in a network. Whenever a neuron receives separate inputs that originate from at least partially overlapping sources, as is the case for feedforward pathways like the spiral fiber neuron pathway, the flexibility and controllability of the system is enhanced. Indirect pathways by definition are comprised of more than one layer of synaptic connections. At each layer, there is a possibility for differential processing of the signal and modulation from other inputs. Environmental and internal factors can regulate individual pathways to fine-tune behavioral outcome.

I became interested in the question of whether the M-cell system could be modulated by environmental and internal influences and whether spiral fiber neurons play a role. I conducted preliminary work in which I found that overexpression of a small neuropeptide called hypocretin that is involved in arousal states in mammals and fish increases the probability of M-cell-mediated escapes. Evidence suggests that spiral fiber neurons may be sensitive to this peptide. If this hypothesis is correct, the spiral fiber neuron parallel pathway may be a gateway for arousal states to modulate the threshold for escape initiation (see Appendix A2.1).

Spiral fiber neurons may also receive modulatory influences from other sources, such as upstream and downstream inputs, or other neuropeptides. To investigate these possibilities, it will be necessary to identify the inputs to spiral fiber neurons as discussed in the previous section. Additionally, one may isolate what neuropeptide or neurotransmitter receptors spiral fiber neurons express using immunohistochemistry, *in situ* hybridization, single-cell transcriptomics, electrical recordings or calcium imaging recordings. Studying the mechanisms of modulation by spiral fiber neurons would be an important step towards understanding how feedforward pathways enhance the flexibility of neural circuits.

3.3 Multisensory integration

Multisensory integration can enhance the detection of events in the environment (Lovelace et al., 2003; Bell et al., 2005; Stein and Stanford, 2008). When zebrafish encounter predators, sensory modalities such as sound, vision and touch are likely to be activated at the same time. Hence, activating these senses together may increase the probability of fast escapes. The M-cell network is an ideal system to study how multisensory information modulates behavior given its sensitivity to stimuli of various modalities and its defined control of motor output. For example, a brief flash of light delivered before a sound cue was found to enhance the probability of M-cell-mediated fast escape (Mu et al., 2012).

Within the topic of multisensory integration, an interesting line of investigation is how stimuli of different modalities are represented in neuronal populations. Are the population dynamics fundamentally different for multiple stimuli and single stimuli? Studies addressing these questions at the cellular level are lacking. I found that spiral fiber neurons respond to a range of sensory stimuli (Chapter 2), making them an excellent model to investigate these questions across a complete and behaviorally relevant neuronal population. The nature of the multisensory representation in spiral fiber neurons can be inferred from their calcium dynamics in response to stimuli. Preliminary experiments suggest that the response amplitude of M-cells and spiral fiber neurons is larger when two stimuli are presented concurrently as opposed to separately (see Appendix

A2.2). This raises the question of how spiral fiber neurons combine inputs from different modalities to affect M-cell activity and the escape behavior.

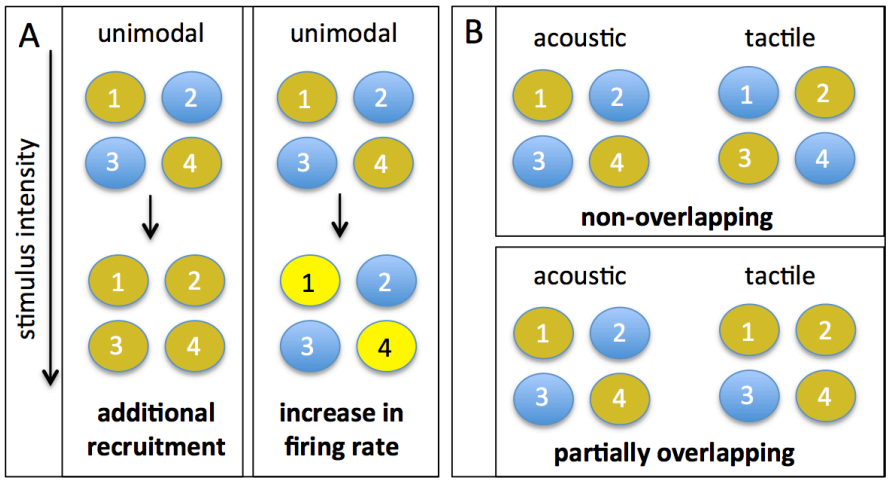

Figure 3.3. Possible models for how spiral fiber neurons represent different unimodal stimuli.

Individual spiral fiber neuron cell bodies are symbolized by circles. A blue filling represents an inactive neuron while lighter shades of yellow reflect stronger responses to the stimulus. A) spiral fiber neurons could code for stimulus intensity by recruiting additional neurons (#3 & #2) or/and increasing the firing rate of neurons already in the active pool (#1 & #4). B) Two stimuli could give rise either to a non-overlapping or an overlapping active neuron pool.

One interesting line of inquiry is how spiral fiber neurons represent stimulus strength. A first possibility is that the firing rate, evaluated by the level of calcium activity, increases with stimulus strength. An alternative is that as the stimulus becomes stronger, more spiral fiber neurons are recruited to the active pool (Figure 3.3). Acoustic and tactile stimuli could lead to different modes of recruitment. In addition, the population could be homogenous or heterogeneous

in terms of the relative sensitivity of each neuron to a specific modality. Single spiral fiber neurons could respond to multiple stimulus modalities or different neurons in the spiral fiber neuron population could respond to different types of stimuli (Figure 3.3). Preliminary experiments suggest that the spiral fiber neuron population is heterogeneous in its sensory representation (see Appendix A.2.2).

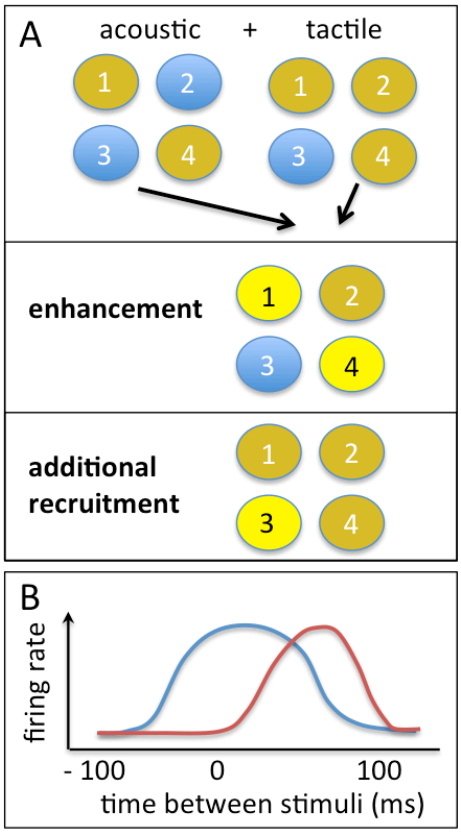

Figure 3.4: Possible models for the integration of multisensory stimuli within spiral fiber neurons.

A blue filling represents an inactive neuron while lighter shades of yellow reflect stronger responses. A) In this case, cells responding to acoustic and tactile stimulation are partially overlapping (#1 & #4 respond to acoustic stimulation, while #1, #2 & #4 respond to tactile stimulation). Most commonly, population responses to co-stimulation result in enhancement of the response in multisensory cells (#1 & #4) and/or recruitment of additional neurons (#3). B) If we consider that two simultaneous stimuli enhance a neuron's response, then the optimal enhancement could either occur when the two stimuli are presented simultaneously (blue trace) or with a time delay (red trace).

Another interesting question is how spiral fiber neurons integrate multimodal stimuli. Models of multisensory integration most commonly predict enhancement of individual neuronal responses and/or recruitment of additional neurons from

the population in the active pool (Stanford and Stein, 2007; Driver and Noesselt, 2008). If there are individual spiral fiber neurons that respond to both acoustic and tactile stimuli, then these neurons may enhance their activity when both stimuli are delivered together. Additionally, there may be recruitment of neurons that are not sensitive to individual unimodal stimuli but require co-stimulation to become active (Figure 3.4A).

One may ask whether the temporal distance between two stimuli influences their integration. Modulation of neural activity is often maximal when two stimuli are delivered simultaneously; Figure 3.4B). It will be interesting to uncover how this is represented at the cellular level.

Given its sensitivity to stimuli of various modalities and its defined control of motor output, the spiral fiber neuron-M-cell network is an ideal system to study how multisensory information is represented in neuronal populations to control behavior.

APPENDIX

A.1 Supplementary materials for Chapter 2: A convergent and essential interneuron pathway for Mauthner-cell-mediated escapes

To eliminate potential defects in the normal functioning of the M-cell circuit due to the paralytic drug alpha-bungarotoxin, we repeated the calcium imaging experiments of Figure 2.13 in non-paralyzed fish. Although on average, the ablation of spiral fiber neurons were less successful than in our experiments with paralyzed fish, the results were comparable (Figure A.1).

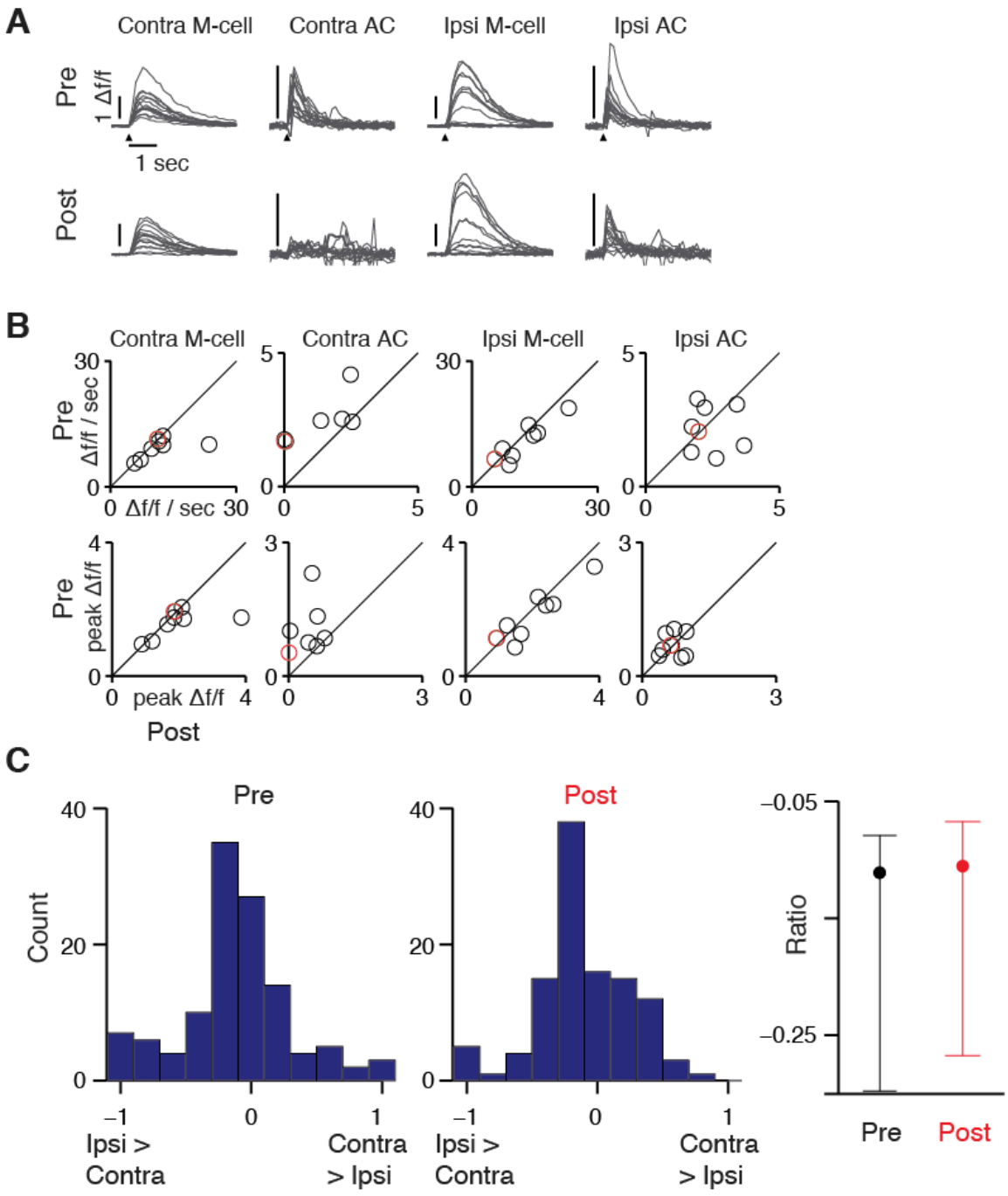

Figure A1. Calcium dynamics in the Mauthner cell soma are not affected by spiral fiber neuron ablations in non-paralyzed larvae.

A) Change in fluorescence (Δf/f) in response to taps (arrowheads) before and after unilateral spiral fiber neuron ablations for one representative fish embedded in agarose. Contra M-cell: M-cell located contralateral to the ablated spiral fiber

Figure A.1 (Continued) neuron somata; Contra AC: contralateral axon cap corresponding to axon terminals of the ablated spiral fiber neurons; Ipsi M-cell: ipsilateral M-cell with preserved spiral fiber neuron input; Ipsi AC: axon cap corresponding to axon terminals of the intact spiral fiber neurons. The mean across trials is plotted in black and individual trials in grey. Top panels: before unilateral spiral fiber neuron ablations; bottom panels: after spiral fiber neuron ablations. Stimulus delivery is indicated by an arrowhead. B) Mean response amplitude in individual larvae (circles), before and after unilateral spiral fiber neuron ablations. First row: values represent the mean Δf/f / sec, which was computed over a 1.5 sec response window across trials with a non-zero Δf/f. The median difference pre versus post was statistically significant only in the contralateral M-cell and contralateral axon cap (Contra M-cell, $p = 0.023$; Contra AC, $p = 0.016$; Ipsi M-cell, $p = 0.11$; Ipsi AC, $p = 0.74$, Wilcoxon signed rank test, $n = 8$ fish). Second row: values represent the mean peak Δf/f across all trials. The median difference pre versus post was statistically significant only in the contralateral axon cap (Contra M-cell, $p = 0.078$; Contra AC, $p = 0.0078$; Ipsi M-cell, $p = 0.46$; Ipsi AC, $p = 0.74$). The identity line is in black and the red circle represents the fish exemplified in A). C) Histograms showing the distribution of activity ratios between the ipsilateral and the contralateral M-cell before and after unilateral spiral fiber neuron ablations (ratio of response amplitudes normalized from -1 to 1: (contra - ipsi) / (contra + ipsi), Δf/f / sec, discarding trials in which both M-cell responses were flat, $n = 130$ trials pre and 139 trials post, across 11 larvae). Third panel: Histogram mean and 95% confidence interval (-0.11, [-0.19, -0.031, pre; -0.10, [-0.17, -0.040], post; $p = 0.83$, Wilcoxon rank sum test).

Others mainly observe all or none calcium events in the M-cells that are thought to indicate firing events (O'Malley et al., 1996; Kohashi and Oda, 2008; Satou et al., 2009; Kohashi et al., 2012). However, our recordings show graded responses (Figure A.2).

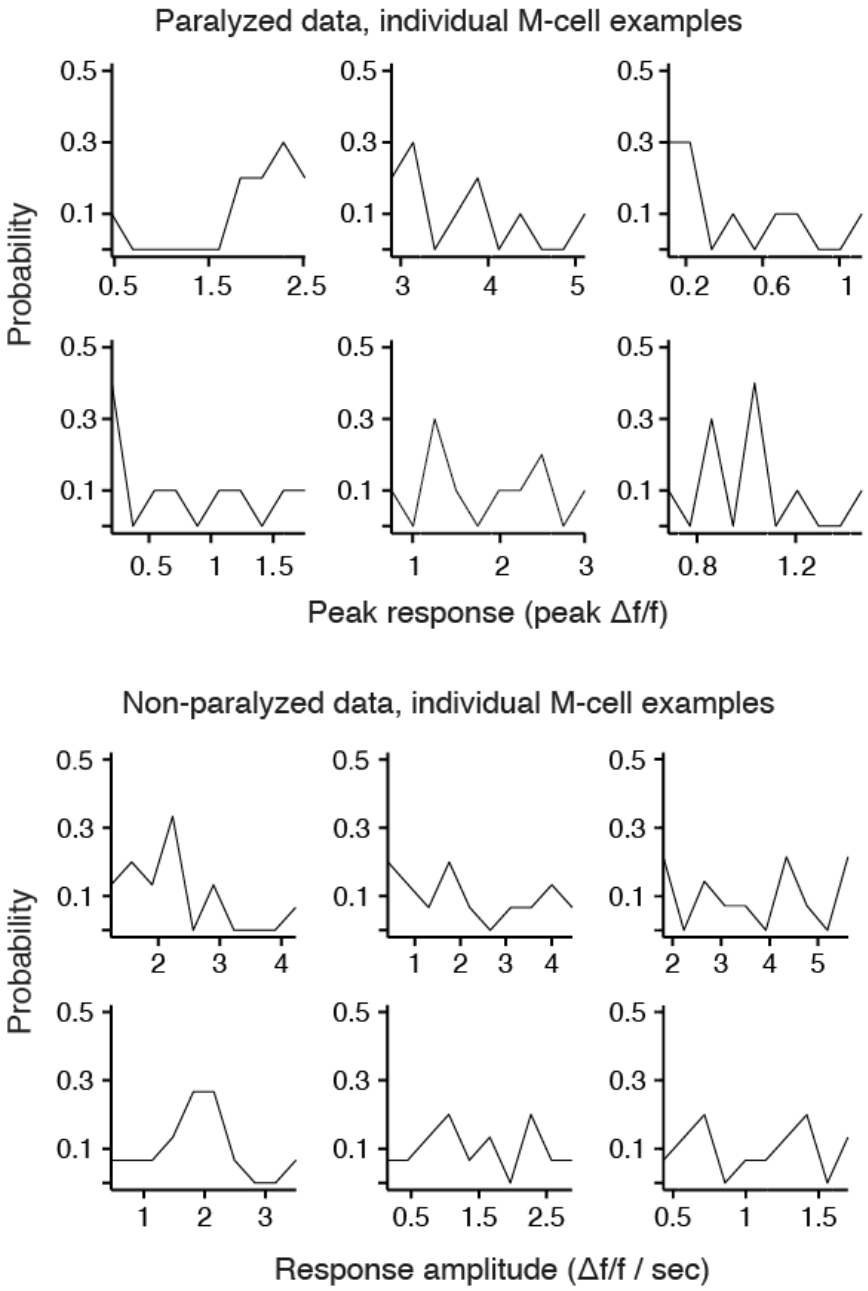

Figure A.2. Calcium dynamics in the Mauthner cell soma are graded.

Distribution of changes in fluorescence in the M-cells of fish embedded in agarose and stimulated with taps. Each plot corresponds to an example M-cell (n = 20 trials each distributed into 10 bins that vary across M-cells). Plotting peak response or response amplitude leads to similar results in individual cells.

A.2 Supplementary materials for Chapter 3: Conclusions and prospects

A.2.1 Neuropeptide modulation of arousal in the Mauthner cell circuit

Arousal states govern behavior and set the adequate response to external stimuli. Low levels of arousal during sleep lead to dramatically reduced responses to external cues (Mullin, 1938). In contrast, heightened arousal in the face of threat promotes fast and large responses (Löw et al., 2008). These observations raise the question of whether arousal signals can modulate the escape behavior.

I became interested in this question and in particular, in the arousal effects of the neuropeptide hypocretin. Since the discovery that the disease narcolepsy is correlated with the loss of hypocretin (also called orexin) neurons in humans (Chemelli et al., 1999; Lin et al., 1999), hypocretin has been implicated in the consolidation of sleep and wake states. Patients with narcolepsy, a disease affecting approximately 1 in 2,000 Americans, suffer from increased daytime sleepiness and unconsolidated periods of sleep and wake. In addition, severe narcoleptics suffer from cataplexy, a sudden loss of muscle tone usually triggered by strong emotions. In spite of the prevalence and the severity of the symptoms of this disease, existing treatments are poor. A major reason for this is that the complex effects of the peptide hypocretin on brain circuitry are largely mysterious. Hypocretin is produced and secreted by neurons in the posterior hypothalamus, which project broadly to the major arousing systems in the central

nervous system. Hypocretin neuron activity correlates with periods of wakefulness and arousal (Estabrooke et al., 2001; Mileykovskiy et al., 2005), and optogenetic stimulation of hypocretin-producing neurons with channelrhodopsin in sleeping mice increases the probability of waking (Adamantidis et al., 2007). In the larval zebrafish, studies in the Schier lab demonstrated that overexpressing hypocretin promotes locomotor activity and inhibits rest during the night (Prober et al., 2006).

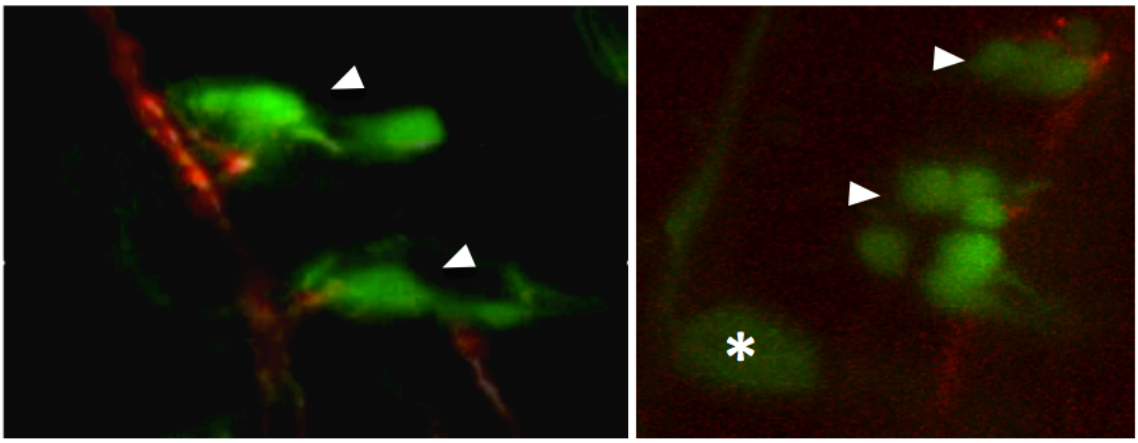

Figure A.3. Spiral fiber neurons are apposed to hypocretin axons.

spiral fiber neurons (arrowhead) are labeled in green in the *Tg(-6.7FRhcrtR:gal4VP16); Tg(UAS:GFP)* line. The M-cell axon cap (asterisk) is visible. Hypocretin axons are labeled in red with the *Tg(hcrt:Kaede)* line and project near spiral fiber neuron cell bodies. Pictures: David Schoppik.

We hypothesized a connection between hypocretin and the M-cell network because two lines of evidence suggest that spiral fiber neurons are sensitive to this neuropeptide. First, my colleague David Schoppik generated a putative

zebrafish hypocretin receptor gal4 driver line by taking 6.8kb upstream of the Fugu hypocretin receptor gene.

This line, *Tg(-6.7FRhcrtR:gal4VP16),* which I discussed in Chapter 2, labels the spiral fiber neurons. Second, using fluorescence imaging, we observed that axons of hypocretin producing neurons seem to appose spiral fiber neuron cell bodies (Figure A.3). Therefore, spiral fiber neurons represent an attractive candidate site of modulation by hypocretin. The hypothesis is that hypocretin may act as an arousing signal to modify the probability or efficiency of the M-cell-mediated escape response, through modulation of the spiral fiber neurons.

To begin to test this hypothesis, I sought to determine whether abnormal levels of hypocretin change the M-cell-mediated escape response. I overexpressed hypocretin in all cells of the zebrafish larvae using a transgenic line where the hypocretin gene is expressed downstream of a heat- promoter (HS-Hcrt, Prober et al., 2006). After placing the larvae carrying this transgene in a hot water bath for one hour, hypocretin is produced and secreted throughout the embryo. Using this HS-Hcrt line, I compared the behavior of fish responding to taps before and after overexpression of hypocretin (see Chapter 2 for a description of the methods). Ablation experiments in Chapter 2 reveal that short-latency escapes depend on the M-cell and the spiral fiber neurons. Therefore, I asked whether hypocretin modulates short-latency escapes. I used three tap intensities to test responsiveness: weak, medium and strong. I found that in response to weak and medium taps, there was a selective increase in the probability of M-cell-dependent, short-latency escapes after heat shock in the HS-Hcrt+ larvae (weak

taps: 1.8-fold increase: 0.32 ± 0.090 pre, 0.58 ± 0.082 post, mean ± standard error of the mean, $p = 9.8*10^{-3}$, medium taps: 1.3-fold increase: 0.67 ± 0.082 pre; 0.87 ± 0.038, p = 0.014, Wilcoxon signed rank test, n = 12 fish). There was also a moderate increase in the probability of short-latency escapes in response to weak taps in the HS-Hcrt- control siblings (1.3-fold increase: 0.32 ± 0.095 pre, 0.42 ± 0.082 post, p = 0.016, n = 8 fish), likely due to the non-specific arousing effects of the heat shock (Figure A.4). These results suggest that hypocretin signaling enhances the excitability of the M-cell escape circuit.

The second hypothesis was that spiral fiber neurons express the hypocretin receptor, making them sensitive to hypocretin. Since hypocretin has an excitatory effect on its targets, applying it to the zebrafish brain should depolarize the spiral fiber neurons. I piloted these experiments with calcium imaging: Using the methods introduced in Chapter 2, I recorded calcium dynamics in the spiral fiber neurons after application of the human form of the peptide hypocretin. I could not observe activity in spiral fiber neurons or other neurons labeled in *Tg(-6.7FRhcrtR:gal4VP16)*. However, this experiment presented several caveats: It is unclear 1) whether the human form of hypocretin can signal through the zebrafish hypocretin receptor, 2) whether the peptide we used was functional at room temperature, and 3) whether it could penetrate the brain of the larvae. In addition, hypocretin may depolarize spiral fiber neurons, but not cause spikes. Subthreshold activity cannot be detected by calcium imaging. An alternative approach would be to record the response of spiral fiber neurons to the

hypocretin peptide by electrophysiology. Thus, experiments to test the sensitivity of spiral fiber neurons to hypocretin need to be expanded upon.

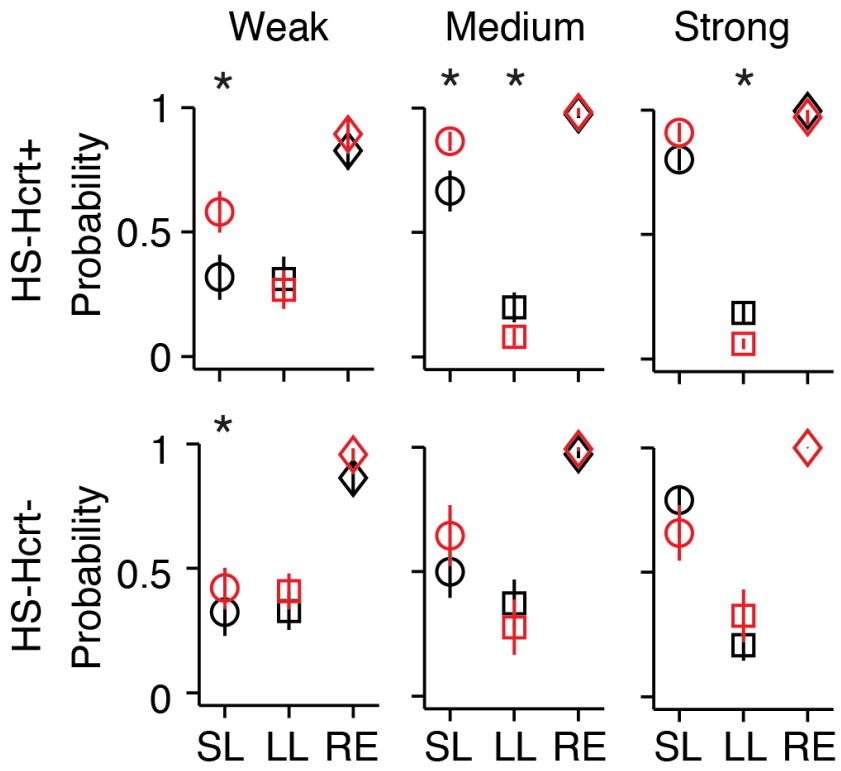

Figure A.4. Hypocretin overexpression enhances the probability of Mauthner-cell-dependent, short-latency escape.

Response probability to weak, medium and strong taps in HS-Hcrt+ larvae (n = 12) and their control HS-Hcrt- siblings (n = 8). SL: short-latency escapes, LL: long-latency escapes, RE: overall response probability, including escapes, turns and swims. * indicates $p < 0.05$, Student's paired t-test for normal data and Wilcoxon signed rank test for non-normal data.

In summary, I found that hypocretin overexpression selectively increases the probability of M-cell-dependent escapes. Further experiments are needed to

determine whether this effect is mediated by the spiral fiber neurons. Studying the effects of hypocretin in the M-cell circuit will be a step forward to understanding neuropeptide modulation of behavior, particularly in the context of arousal.

A.2.2 Multimodal integration in the Mauthner-cell-mediated escape circuit

I found that spiral fiber neurons respond to different types of stimuli (Chapter 2), including touch and sounds. The three stimuli I tested are a combination of different sensory modalities: they are detected by different types of sensory receptors or processed by different neural pathways. Using mutants that lack mechanosensory transduction in hair cells (*mariner* mutants), I found that M-cell escapes in response to taps are primarily mediated by the inner ear. Water puffs directed at the ear stimulate the trigeminal ganglion, a group of neurons that respond to tactile inputs on the larva's head. This stimulus may also activate auditory hair cells weakly. Water puffs directed at the tail activate Rohon-Beard neurons, mechanosensory cells along the fish's tail and trunk. This stimulus may also depolarize lateral line neuromasts to a lesser extent.

To begin to study how multiple modalities interact in the M-cell circuit, I piloted calcium imaging experiments where I delivered the touch and sound stimuli separately or simultaneously. I first asked whether touch and sound enhance activity in the network. Figure A.5 shows preliminary results where the M-cell and the spiral fiber neuron axons labeled at the axon cap respond to taps and tail

puffs of low intensity. When the two stimuli are delivered together, the amplitude of the response increases. As my results from Chapter 2 suggest, M-cell somatic activity does not reliably predict firing probability, at least when the spiral fiber neuron input at the axon hillock is removed. Therefore, to answer the question of whether the M-cell is more likely to fire when the two stimuli are presented together, concurrent extracellular recordings or monitoring of escape behavior is needed.

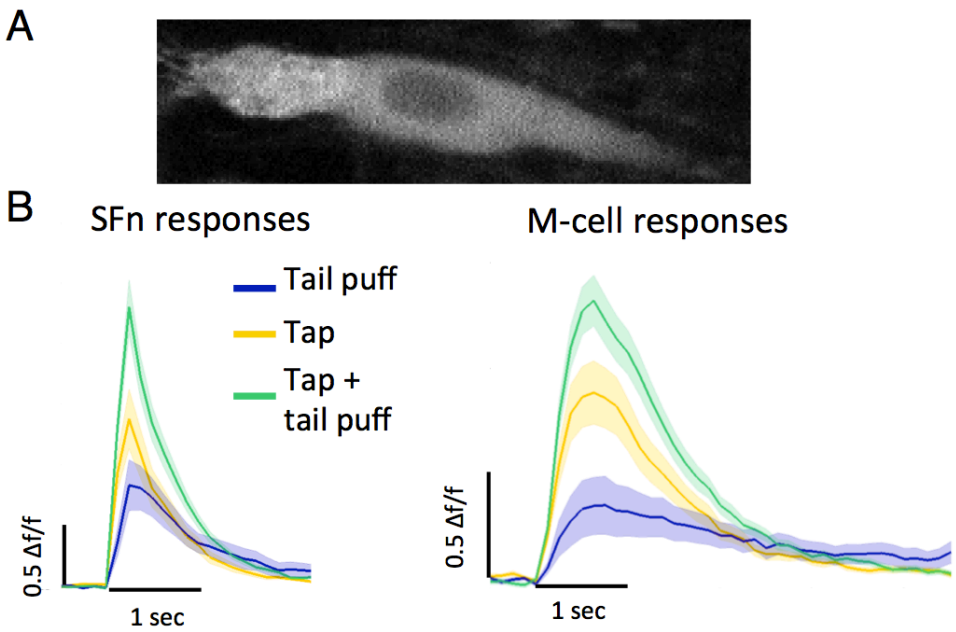

Figure A.5. Two stimuli delivered concurrently increase responses in the Mauthner cell and spiral fiber neurons.

A) The M-cell and spiral fiber neuron terminals at the axon cap are labeled with the calcium indicator GCaMP5. B) Mean ± standard error across trials of changes in fluorescence in one experiment plotted for the spiral fiber neuron axon terminals and the M-cell soma. Blue trace: puffs of water delivered to the right side of the larvae's tail (ipsilateral to the M-cell and spiral fiber neurons that are plotted). Yellow trace: taps delivered onto the dish holding the fish. Green trace: Taps and tail puffs delivered at the same time.

The response amplitude of spiral fiber neuron terminals also increases when taps and tail puffs are delivered together (Figure A.5). Calcium events in the spiral fiber neurons are likely to signal firing, as they do in most neuronal populations. The observed increase in amplitude suggests that as a population, the spiral fiber neurons fire more and are a larger source of excitation for the M-cells when stimuli are co-delivered.

Preliminary experiments suggest that the spiral fiber neuron population is heterogeneous in its sensory representation. Many neurons are multisensory, that is, they respond to tail puffs as well as taps. However, some neurons seem to prefer one stimulus while others respond more strongly to the other. In addition, clusters of neurons may be correlated in their response profile (Figure A.6).

Figure A.6. Heterogeneity in the spiral fiber neuron population in response to multisensory stimuli.

A) In this experiment, 13 spiral fiber neuron somata are visible in the recording plane. B) Amplitude of the change in fluorescence in response to stimuli in the 13 cells shown in A. Traces represent mean ± standard error across non-zero trials. C) Response probability in the 13 cells. Legend: Blue: puffs of water delivered to the right side of the larvae's tail. Yellow: taps delivered onto the dish holding the fish. Green: Taps and tail puffs delivered simultaneously.

Figure A.6 (Continued)

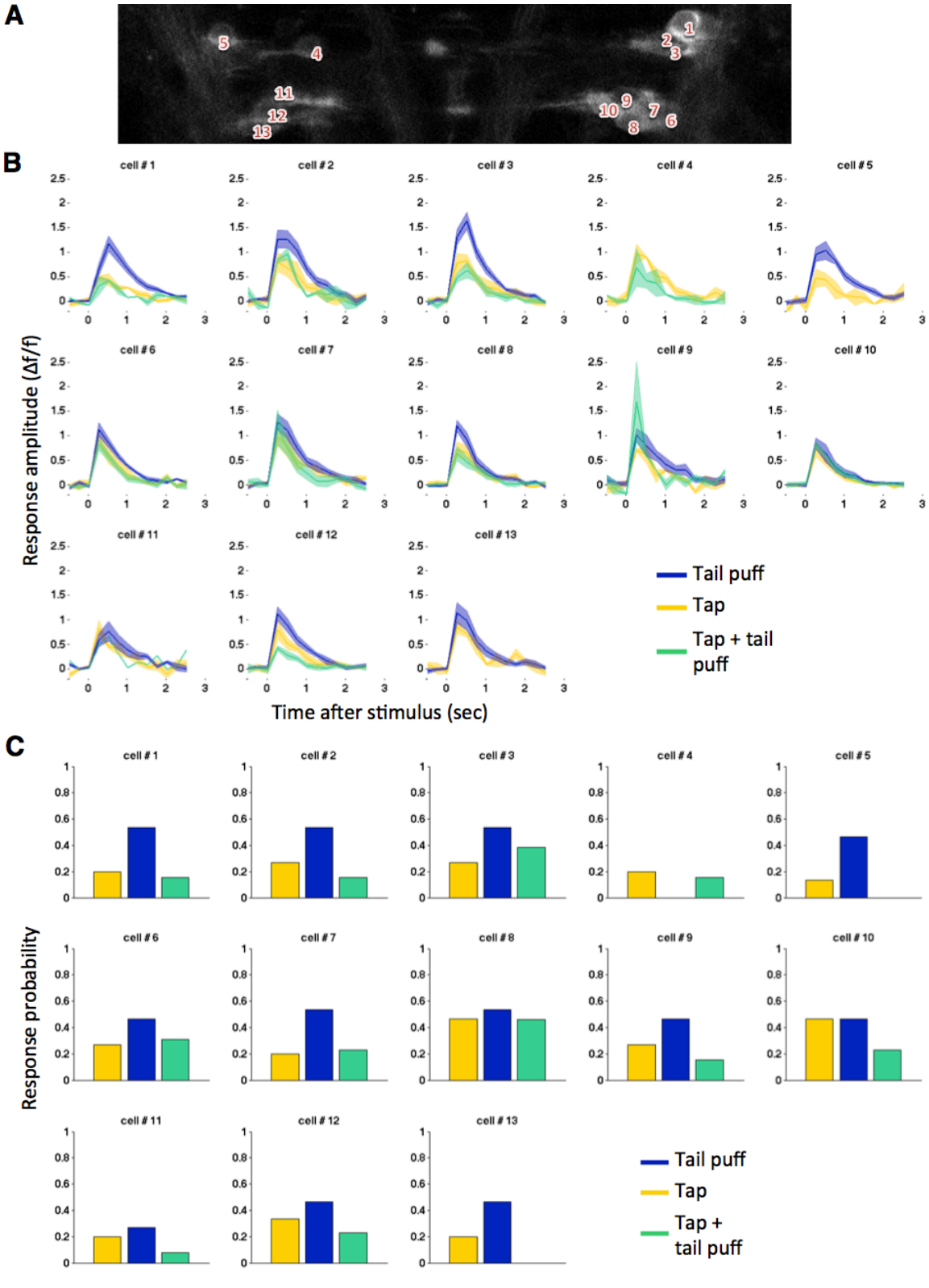

REFERENCES

Adamantidis AR, Zhang F, Aravanis AM, Deisseroth K, de Lecea L (2007) Neural substrates of awakening probed with optogenetic control of hypocretin neurons. Nature 450:420–424.

Barreiro-Iglesias A, Mysiak KS, Adrio F, Rodicio MC, Becker CG, Becker T, Anadón R (2012) Distribution of glycinergic neurons in the brain of glycine transporter-2 transgenic Tg(glyt2:Gfp) adult zebrafish: Relationship to brain-spinal descending systems. J Comp Neurol 521:389–425.

Bartelmez G (1915) Mauthner's cell and the nucleus motorius tegmenti. J Comp Neurol 25:87–128.

Bell AH, Meredith MA, Van Opstal AJ, Munoz DP (2005) Crossmodal integration in the primate superior colliculus underlying the preparation and initiation of saccadic eye movements. J Neurophysiol 93:3659–3673.

Bianco IH, Ma L-H, Schoppik D, Robson DN, Orger MB, Beck JC, Li JM, Schier AF, Engert F, Baker R (2012) The tangential nucleus controls a gravito-inertial vestibulo-ocular reflex. Curr Biol 22:1285–1295.

Burgess HA, Granato M (2007) Sensorimotor Gating in Larval Zebrafish. J Neurosci 27:4984–4994.

Cachope R, Mackie K, Triller A, O'Brien J, Pereda AE (2007) Potentiation of electrical and chemical synaptic transmission mediated by endocannabinoids. Neuron 56:1034–1047.

Canfield JG (2003) Temporal constraints on visually directed C-start responses: behavioral and physiological correlates. Brain Behav Evol 61:148–158.

Card GM (2012) Escape behaviors in insects. Curr Opin Neurobiol 22:180–186.

Casagrand JL, Guzik AL, Eaton RC (1999) Mauthner and reticulospinal responses to the onset of acoustic pressure and acceleration stimuli. J Neurophysiol 82:1422–1437.

Chemelli RM, Willie JT, Sinton CM, Elmquist JK, Scammell T, Lee C, Richardson JA, Williams SC, Xiong Y, Kisanuki Y, Fitch TE, Nakazato M, Hammer RE, Saper CB, Yanagisawa M (1999) Narcolepsy in orexin knockout mice: molecular genetics of sleep regulation. Cell 98:437–451.

Chiappe ME, Seelig JD, Reiser MB, Jayaraman V (2010) Walking modulates speed sensitivity in Drosophila motion vision. Curr Biol 20:1470–1475.

Currie SN, Carlsen RC (1987) Modulated vibration-sensitivity of lamprey Mauthner neurones. J Exp Biol 129:41–51.

Curti S, Gomez L, Budelli R, Pereda AE (2008) Subthreshold Sodium Current Underlies Essential Functional Specializations at Primary Auditory Afferents. J Neurophysiol 99:1683–1699.

Curti S, Pereda AE (2010) Functional specializations of primary auditory afferents on the Mauthner cells: interactions between membrane and synaptic properties. J Physiol Paris 104:203–214.

Curtin PCP, Medan V, Neumeister H, Bronson DR, Preuss T (2013) The 5-HT5A Receptor Regulates Excitability in the Auditory Startle Circuit: Functional Implications for Sensorimotor Gating. J Neurosci 33:10011–10020.

Douglass AD, Kraves S, Deisseroth K, Schier AF, Engert F (2008) Escape Behavior Elicited by Single, Channelrhodopsin-2-Evoked Spikes in Zebrafish Somatosensory Neurons. Current Biology 18:1133–1137.

Driver J, Noesselt T (2008) Multisensory interplay reveals crossmodal influences on “sensory-specific” brain regions, neural responses, and judgments. Neuron 57:11–23.

Dudman JT, Tsay D, Siegelbaum SA (2007) A novel role for synaptic inputs at distal dendrites: instructive signals for hippocampal long-term plasticity. Neuron 56:866–879.

Eaton R (1973) Development of the Mauthner neurons in embryos and larvae of the zebrafish, Brachydanio rerio. Copeia.

Eaton R, Lavender W (1981) Identification of Mauthner-initiated response patterns in goldfish: evidence from simultaneous cinematography and electrophysiology. J Comp Physiol 144:521–531.

Eaton RC (1984) Neural Mechanisms of Startle Behavior. Springer Science & Business Media.

Eaton RC, Bombardieri RA, Meyer DL (1977) The Mauthner-initiated startle response in teleost fish. J Exp Biol 66:65–81.

Eaton RC, Farley RD (1975) Mauthner neuron field potential in newly hatched larvae of the zebra fish. J Neurophysiol 38:502–512.

Eaton RC, Lee RK, Foreman MB (2001) The Mauthner cell and other identified neurons of the brainstem escape network of fish. Prog Neurobiol 63:467–485.

Ernest S, Rauch GJ, Haffter P, Geisler R, Petit C, Nicolson T (2000) Mariner is defective in myosin VIIA: a zebrafish model for human hereditary deafness. Hum Mol Genet 9:2189–2196.

Estabrooke IV, McCarthy MT, Ko E, Chou TC, Chemelli RM, Yanagisawa M, Saper CB, Scammell TE (2001) Fos expression in orexin neurons varies with behavioral state. J Neurosci 21:1656–1662.

Faber DS, Fetcho JR, Korn H (1989) Neuronal networks underlying the escape response in goldfish. General implications for motor control. Ann N Y Acad Sci 563:11–33.

Faber DS, Korn H, Lin JW (1991) Role of medullary networks and postsynaptic membrane properties in regulating Mauthner cell responsiveness to sensory excitation. Brain Behav Evol 37:286–297.

Fetcho JR (1991) Spinal network of the Mauthner cell. Brain Behav Evol 37:298–316.

Furshpan EJ, Furukawa T (1962) Intracellular and extracellular responses of the several regions of the Mauthner cell of the goldfish. J Neurophysiol 25:732–771.

Furukawa T (1966) Synaptic interaction at the mauthner cell of goldfish. Prog Brain Res 21:44–70.

Furukawa T, Furshpan EJ (1963) Two inhibitory mechanisms in the Mauthner neurons of goldfish. J Neurophysiol 26:140–176.

Gagnon JA, Valen E, Thyme SB, Huang P, Ahkmetova L, Pauli A, Montague TG, Zimmerman S, Richter C, Schier AF (2014) Efficient Mutagenesis by Cas9 Protein-Mediated Oligonucleotide Insertion and Large-Scale Assessment of Single-Guide RNAs. PLoS ONE 9:e98186.

Gyda M, Wolman M, Lorent K, Granato M (2012) The Tumor Suppressor Gene Retinoblastoma-1 Is Required for Retinotectal Development and Visual Function in Zebrafish Link BA, ed. PLoS Genet 8:e1003106.

Haesemeyer M, Schier AF (2014) The study of psychiatric disease genes and drugs in zebrafish. Curr Opin Neurobiol 30C:122–130.

Harris JA, Cheng AG, Cunningham LL, MacDonald G, Raible DW, Rubel EW (2003) Neomycin-Induced Hair Cell Death and Rapid Regeneration in the Lateral Line of Zebrafish (Danio rerio). JARO - Journal of the Association for Research in Otolaryngology 4:219–234.

Hatta K, Tsujii H, Omura T (2006) Cell tracking using a photoconvertible

fluorescent protein. Nat Protoc 1:960–967.

Herberholz J (2012) Decision making and behavioral choice during predator avoidance. Frontiers in Neuroscience:1–15.

Holmes NP, Spence C (2005) Multisensory integration: space, time and superadditivity. Current Biology 15:R762–R764.

Ikeda H, Delargy AH, Yokogawa T, Urban JM, Burgess HA, Ono F (2013) Intrinsic properties of larval zebrafish neurons in ethanol. PLoS ONE 8:e63318.

Issa FA, O'Brien G, Kettunen P, Sagasti A, Glanzman DL, Papazian DM (2011) Neural circuit activity in freely behaving zebrafish (Danio rerio). J Exp Biol 214:1028–1038.

Kimmel CB, Hatta K, Metcalfe WK (1990) Early axonal contacts during development of an identified dendrite in the brain of the zebrafish. Neuron 4:535–545.

Kimmel CB, Metcalfe WK, Schabtach E (1985) T reticular interneurons: a class of serially repeating cells in the zebrafish hindbrain. J Comp Neurol 233:365–376.

Kimmel CB, Sessions SK, Kimmel RJ (1981) Morphogenesis and synaptogenesis of the zebrafish Mauthner neuron. J Comp Neurol 198:101–120.

Kimura Y, Satou C, Fujioka S, Shoji W, Umeda K, Ishizuka T, Yawo H, Higashijima S-I (2013) Hindbrain V2a Neurons in the Excitation of Spinal Locomotor Circuits during Zebrafish Swimming. Current Biology 23:843–849.

Kinkhabwala A, Riley M, Koyama M, Monen J, Satou C, Kimura Y, Higashijima S-I, Fetcho J (2011) A structural and functional ground plan for neurons in the hindbrain of zebrafish. Proc Natl Acad Sci USA 108:1164–1169.

Kohashi T, Nakata N, Oda Y (2012) Effective Sensory Modality Activating an Escape Triggering Neuron Switches during Early Development in Zebrafish. J Neurosci 32:5810–5820.

Kohashi T, Oda Y (2008) Initiation of Mauthner- or non-Mauthner-mediated fast escape evoked by different modes of sensory input. J Neurosci 28:10641–10653.

Kohno K (1970) Symmetrical Axo-Axonic Synapses in Axon Cap of Goldfish Mauthner Cell. Brain Res 23:255–&.

Korn H, Faber DS (1975) An electrically mediated inhibition in goldfish medulla. J Neurophysiol 38:452–471.

Korn H, Faber DS (2005) The Mauthner cell half a century later: a neurobiological model for decision-making? Neuron 47:13–28.

Korn H, Triller A, Mallet A, Faber DS (1981) Fluctuating responses at a central synapse: n of binomial fit predicts number of stained presynaptic boutons. Science 213:898–901.

Koyama M, Kinkhabwala A, Satou C, Higashijima S-I, Fetcho J (2011) Mapping a sensory-motor network onto a structural and functional ground plan in the hindbrain. Proc Natl Acad Sci USA 108:1170–1175.

Kubo F, Hablitzel B, Dal Maschio M, Driever W, Baier H, Arrenberg AB (2014) Functional Architecture of an Optic Flow-Responsive Area that Drives Horizontal Eye Movements in Zebrafish. Neuron 81:1344–1359.

Lacoste AMB, Schoppik D, Robson D, Haesemeyer M, Portugues R, Li JM, Randlett O, Wee CL, Engert F, Schier AF (2015) A convergent and essential interneuron pathway for Mauthner-cell-mediated escapes. Current Biology 25. http://dx.doi.org/10.1016/j.cub.2015.04.025.

Lin JW, Faber DS (1988a) Synaptic transmission mediated by single club

endings on the goldfish Mauthner cell. II. Plasticity of excitatory postsynaptic potentials. J Neurosci 8:1313–1325.

Lin JW, Faber DS (1988b) Synaptic transmission mediated by single club endings on the goldfish Mauthner cell. I. Characteristics of electrotonic and chemical postsynaptic potentials. J Neurosci 8:1302–1312.

Lin L, Faraco J, Li R, Kadotani H, Rogers W, Lin X, Qiu X, de Jong PJ, Nishino S, Mignot E (1999) The sleep disorder canine narcolepsy is caused by a mutation in the hypocretin (orexin) receptor 2 gene. Cell 98:365–376.

Liu KS, Fetcho JR (1999) Laser ablations reveal functional relationships of segmental hindbrain neurons in zebrafish. Neuron 23:325–335.

Lorent K, Liu KS, Fetcho JR, Granato M (2001) The zebrafish space cadet gene controls axonal pathfinding of neurons that modulate fast turning movements. Development 128:2131–2142.

Lovelace CT, Stein BE, Wallace MT (2003) An irrelevant light enhances auditory detection in humans: a psychophysical analysis of multisensory integration in stimulus detection. Brain Res Cogn Brain Res 17:447–453.

López-Schier H (2013) Developmental and architectural principles of the lateral-line neural map. Frontiers in Neural Circuits:1–9.

Löw A, Lang PJ, Smith JC, Bradley MM (2008) Both predator and prey: emotional arousal in threat and reward. Psychol Sci 19:865–873.

Luo L, Callaway EM, Svoboda K (2008) Genetic dissection of neural circuits. Neuron 57:634–660.

Marti F, Korn H, Faure P (2008) Interplay between subthreshold potentials and gamma oscillations in Mauthner cells' presynaptic inhibitory interneurons. NSC 151:983–994.

McHenry MJ, Feitl KE, Strother JA, Van Trump WJ (2009) Larval zebrafish rapidly sense the water flow of a predator's strike. Biol Lett 5:477–479.

McLean DL, Fetcho JR (2004) Relationship of tyrosine hydroxylase and serotonin immunoreactivity to sensorimotor circuitry in larval zebrafish. J Comp Neurol 480:57–71.

Medan V, Preuss T (2011) Dopaminergic-induced changes in Mauthner cell excitability disrupt prepulse inhibition in the startle circuit of goldfish. J Neurophysiol 106:3195–3204.

Metcalfe WK, Mendelson B, Kimmel CB (1986) Segmental homologies among reticulospinal neurons in the hindbrain of the zebrafish larva. J Comp Neurol 251:147–159.

Mileykovskiy BY, Kiyashchenko LI, Siegel JM (2005) Behavioral Correlates of Activity in Identified Hypocretin/Orexin Neurons. Neuron 46:787–798.

Mirjany M, Faber DS (2011) Characteristics of the anterior lateral line nerve input to the Mauthner cell. J Exp Biol 214:3368–3377.

Mirjany M, Preuss T, Faber DS (2011) Role of the lateral line mechanosensory system in directionality of goldfish auditory evoked escape response. J Exp Biol 214:3358–3367.

Moly PK, Ikenaga T, Kamihagi C, Islam AFMT, Hatta K (2013) Identification of initially appearing glycine-immunoreactive neurons in the embryonic zebrafish brain. Dev Neurobiol: 6:616–632.

Monesson-Olson BD, Browning-Kamins J, Aziz-Bose R, Kreines F, Trapani JG (2014) Optical stimulation of zebrafish hair cells expressing channelrhodopsin-2. PLoS ONE 9:e96641.

Mu Y, Li X-Q, Zhang B, Du J-L (2012) Visual Input Modulates Audiomotor Function via Hypothalamic Dopaminergic Neurons through a Cooperative

Mechanism. Neuron 75:688–699.

Mullin F (1938) Variations in threshold of auditory stimuli necessary to awaken the sleeper. American Journal of Physiology 123:477–481.

Muto A, Ohkura M, Kotani T, Higashijima S-I, Nakai J, Kawakami K (2011) Genetic visualization with an improved GCaMP calcium indicator reveals spatiotemporal activation of the spinal motor neurons in zebrafish. Proc Natl Acad Sci USA 108:5425–5430.

Nakajima Y (1974) Fine structure of the synaptic endings on the Mauthner cell of the goldfish. J Comp Neurol 156:379–402.

Nakayama H, Oda Y (2004) Common sensory inputs and differential excitability of segmentally homologous reticulospinal neurons in the hindbrain. J Neurosci 24:3199–3209.

Neki D, Nakayama H, Fujii T, Matsui-Furusho H, Oda Y (2014) Functional Motifs Composed of Morphologically Homologous Neurons Repeated in the Hindbrain Segments. J Neurosci 34:3291–3302.

Nicolson T, Rüsch A, Friedrich RW, Granato M, Ruppersberg JP, Nüsslein-Volhard C (1998) Genetic analysis of vertebrate sensory hair cell mechanosensation: the zebrafish circler mutants. Neuron 20:271–283.

Nikolaou N, Lowe AS, Walker AS, Abbas F, Hunter PR, Thompson ID, Meyer MP (2012) Parametric Functional Maps of Visual Inputs to the Tectum. Neuron 76:317–324.

Nissanov J, Eaton RC, DiDomenico R (1990) The motor output of the Mauthner cell, a reticulospinal command neuron. Brain Res 517:88–98.

O'Malley DM, Kao Y-H, Fetcho JR (1996) Imaging the functional organization of zebrafish hindbrain segments during escape behaviors. Neuron 17:1145–1155

O'Steen S, Cullum AJ, Bennett AF (2002) Rapid evolution of escape ability in Trinidadian guppies (Poecilia reticulata). Evolution 56:776–784.

Oda Y, Kawasaki K, Morita M, Korn H, Matsui H (1998) Inhibitory long-term potentiation underlies auditory conditioning of goldfish escape behaviour. Nature 394:182–185.

Orger MB, Kampff AR, Severi KE, Bollmann JH, Engert F (2008) Control of visually guided behavior by distinct populations of spinal projection neurons. Nat Neurosci 11:327–333.

Pereda A, Triller A, Korn H, Faber DS (1992) Dopamine enhances both electrotonic coupling and chemical excitatory postsynaptic potentials at mixed synapses. Proc Natl Acad Sci USA 89:12088–12092.

Pereda AE, Bell TD, Faber DS (1995) Retrograde synaptic communication via gap junctions coupling auditory afferents to the Mauthner cell. J Neurosci 15:5943–5955.

Pereda AE, Faber DS (1996) Activity-dependent short-term enhancement of intercellular coupling. J Neurosci 16:983–992.

Pereda AE, Nairn AC, Wolszon LR, Faber DS (1994) Postsynaptic modulation of synaptic efficacy at mixed synapses on the Mauthner cell. J Neurosci 14:3704–3712.

Pereda AE, Rash JE, Nagy JI, Bennett MVL (2004) Dynamics of electrical transmission at club endings on the Mauthner cells. Brain Res Brain Res Rev 47:227–244.

Pfaff DW, Martin EM, Faber D (2012) Origins of arousal: roles for medullary reticular neurons. Trends Neurosci:1–9.

Portugues R, Severi KE, Wyart C, Ahrens MB (2012) Optogenetics in a transparent animal: circuit function in the larval zebrafish. Curr Opin

Neurobiol 23:119–126.

Preuss T, Osei-Bonsu PE, Weiss SA, Wang C, Faber DS (2006) Neural representation of object approach in a decision-making motor circuit. J Neurosci 26:3454–3464.

Prober DA, Rihel J, Onah AA, Sung R-J, Schier AF (2006) Hypocretin/orexin overexpression induces an insomnia-like phenotype in zebrafish. J Neurosci 26:13400–13410.

Pujol-Marti J, Zecca A, Baudoin JP, Faucherre A, Asakawa K, Kawakami K, Lopez-Schier H (2012) Neuronal Birth Order Identifies a Dimorphic Sensorineural Map. J Neurosci 32:2976–2987.

Rash JE, Curti S, Vanderpool KG, Kamasawa N, Nannapaneni S, Palacios-Prado N, Flores CE, Yasumura T, O'Brien J, Lynn BD, Bukauskas FF, Nagy JI, Pereda AE (2013) Molecular and functional asymmetry at a vertebrate electrical synapse. Neuron 79:957–969.

Satou C, Kimura Y, Hirata H, Suster ML, Kawakami K, Higashijima S-I (2013) Transgenic tools to characterize neuronal properties of discrete populations of zebrafish neurons. Development 140:3927–3931.

Satou C, Kimura Y, Kohashi T, Horikawa K, Takeda H, Oda Y, Higashijima S-I (2009) Functional role of a specialized class of spinal commissural inhibitory neurons during fast escapes in zebrafish. J Neurosci 29:6780–6793.

Scott EK, Baier H (2009) The cellular architecture of the larval zebrafish tectum, as revealed by gal4 enhancer trap lines. Front Neural Circuits 3:13.

Scott JW, Zottoli SJ, Beatty NP, Korn H (1994) Origin and function of spiral fibers projecting to the goldfish Mauthner cell. J Comp Neurol 339:76–90.

Smith M, Pereda AE (2003) Chemical synaptic activity modulates nearby electrical synapses. Proc Natl Acad Sci USA 100:4849–4854.

Stanford TR, Stein BE (2007) Superadditivity in multisensory integration: putting the computation in context. Neuroreport 18:787–792.

Stein BE, Stanford TR (2008) Multisensory integration: current issues from the perspective of the single neuron. Nat Rev Neurosci 9:255–266.

Svoboda KR, Fetcho JR (1996) Interactions between the neural networks for escape and swimming in goldfish. J Neurosci 16:843–852.

Szabo TM, McCormick CA, Faber DS (2007) Otolith endorgan input to the Mauthner neuron in the goldfish. J Comp Neurol 505:511–525.

Szabo TM, Weiss SA, Faber DS, Preuss T (2006) Representation of auditory signals in the M-cell: role of electrical synapses. J Neurophysiol 95:2617–2629.

Takahashi M, Narushima M, Oda Y (2002) In vivo imaging of functional inhibitory networks on the mauthner cell of larval zebrafish. J Neurosci 22:3929–3938.

Thiele TR, Donovan JC, Baier H (2014) Descending Control of Swim Posture by a Midbrain Nucleus in Zebrafish. Neuron 83:679–691.

Tuttle R, Masuko S, Nakajima Y (1986) Freeze-fracture study of the large myelinated club ending synapse on the goldfish Mauthner cell: special reference to the quantitative analysis of gap junctions. J Comp Neurol 246:202–211.

Vogel A, Venugopalan V (2003) Mechanisms of pulsed laser ablation of biological tissues. Chem Rev 103:577–644.

Walker JA, Ghalambor CK, Griset OL, McKenney D, Reznick DN (2005) Do faster starts increase the probability of evading predators? Funct Ecology 19:808–815.

Weiss SA, Preuss T, Faber DS (2008) A role of electrical inhibition in

sensorimotor integration. Proc Natl Acad Sci USA 105:18047–18052.

Weiss SA, Zottoli SJ, Do SC, Faber DS, Preuss T (2006) Correlation of C-start behaviors with neural activity recorded from the hindbrain in free-swimming goldfish (Carassius auratus). J Exp Biol 209:4788–4801.

Whitaker KW, Neumeister H, Huffman LS, Kidd CE, Preuss T, Hofmann HA (2011) Serotonergic modulation of startle-escape plasticity in an African cichlid fish: a single-cell molecular and physiological analysis of a vital neural circuit. J Neurophysiol 106:127–137.

Wolszon LR, Pereda AE, Faber DS (1997) A fast synaptic potential mediated by NMDA and non-NMDA receptors. J Neurophysiol 78:2693–2706.

Yang XD, Korn H, Faber DS (1990) Long-term potentiation of electrotonic coupling at mixed synapses. Nature 348:542–545.

Zhu P (2009) Optogenetic dissection of neuronal circuits in zebrafish using viral gene transfer and the Tet system. Front Neural Circuits 3:1–12.

Zhu P, Fajardo O, Shum J, rer Y-PZSA, Friedrich RW (2012) High-resolution optical control of spatiotemporal neuronal activity patterns in zebrafish using a digital micromirror device. Nat Protoc 7:1410–1425.

Zottoli SJ (1977) Correlation of the startle reflex and Mauthner cell auditory responses in unrestrained goldfish. J Exp Biol 66:243–254.

Zottoli SJ, Bentley AP, Feiner DG, Hering JR, Prendergast BJ, Rieff HI (1994) Spinal cord regeneration in adult goldfish: implications for functional recovery in vertebrates. Prog Brain Res 103:219–228.

Zottoli SJ, Faber DS (1980) An identifiable class of statoacoustic interneurons with bilateral projections in the goldfish medulla. Neuroscience 5:1287–1302.

Zottoli SJ, Faber DS (2000) The Mauthner Cell: What Has it Taught us? The

Neuroscientist 6:26–38.

Zottoli SJ, Hordes AR, Faber DS (1987) Localization of optic tectal input to the ventral dendrite of the goldfish Mauthner cell. Brain Res 401:113–121.

Zucker RS (1972) Crayfish escape behavior and central synapses. I. Neural circuit exciting lateral giant fiber. J Neurophysiol 35:599–620.